Electronic Correlations in Quantum Wires Subjected to Strong Magnetic Fields: Dependence on the Filling Factor

Zhongxi Zhang

A Thesis

in

The Department

of

Physics

Presented in Partial Fulfillment of the Requirements

for the Degree of Doctor of Philosophy at

Concordia University

Montreal, Quebec, Canada

April 2002

Abstract

Electronic Correlations in Quantum Wires Subjected to Strong Magnetic Fields: Dependence on the Filling Factor

Zhongxi Zhang. Ph. D.

Concordia University. 2002

Electron-electron interactions and their effects on Landau levels in quantum wires (QWs). subjected to strong perpendicular and parallel magnetic fields. are discussed. For QWs in strong perpendicular magnetic fields. with integral filling factor ($\nu = 1, 2$. and 3). the screened Coulomb interactions are assessed by solving the integral equations for the screened potential. both analytically and numerically. Correlation energy strongly smoothens the energy dispersion in the vicinity of the Fermi level. The exchange-correlation contribution $v_g^{ec}(k_F)$ to the Fermi-edge group velocity $v_g(k_F)$ is proved to be nonsingular. The energy dispersion. obtained in the local density approximation (LDA). is in line with the observed strong suppression of the spin splitting ($\nu = 1, 3$) and helps in explaining the observed destruction or absence of some quantum Hall states. For QWs in strong parallel magnetic fields. with only the lowest LL occupied, the many-body corrections have a stronger effect on the spin-splitting than in the case of perpendicular magnetic fields.

Acknowledgments

It is my pleasure to express my gratitude to all people who help me in completing the present work.

In particular, I wish to thank **Dr. P. Vasilopoulos**, my Ph.D. supervisor, for his encouragement, patience, academic discussion, and important guidance in my research and thesis revising. The opportunity to work with him in an excellent and pleasant environment will be treasured for my life.

I would also like to thank The School of Graduate Studies and the Physics Department at Concordia University for offering me the Concordia University Graduate Fellowship Award (1997-1999), Concordia University International Tuition Fee Remission Award (1997-1998), and the teaching assitant possitions. Many thanks to all students and professors whom I have met during my studies. Also, the discussion with Dr. O. G. Balev was appreciated.

Finally, great thanks to my parents, my wife, and my daughter for their support, generosity, and understanding.

List of the important abbreviations

2DEG Two-Dimensional Electron Gas

3DEG Three-Dimensional Electron Gas

DFT Density Functional Theory

HA Hartree Approximation

HFA Hartree-Fock Approximation

LDA Local Density Approximation

LFC Local Field Correction

QHE Quantum Hall Effect

QW Quantum Wire

RPA Random Phase Approximation

SCST Self-Consistent Screening Theory

SHFA Screened Hartree-Fock Approximation

Contents

1 Introduction **1**

1.1 Electronic correlations and correlation energies 1

1.2 Coulomb interaction in 3DEG systems 3

1.3 Coulomb interaction in QWs and its effects on the subband structure 5

1.4 The motivation behind this work 10

1.5 Methodology 13

1.6 The organization of this work 15

2 An overview of many-body techniques for correlation energies **18**

2.1 Self-consistent Hartree approximation 18

2.2 Hartree-Fock approximation (HFA) 21

2.2.1 Hartree-Fock equations 21

2.2.2 HFA for 3D free electron gas 23

2.2.3 HFA modified with an equivalent local potential 25

2.3 Linear screening theory 27

2.3.1 Linear screening 27

2.3.2 Coulomb interaction expressed in occupation number representation 28

2.3.3 Linear screening theory of the ground state energy 30

2.3.4 Lindhard or RPA dielectric function 33

2.4 Density functional theory (DFT) 37

3 Screening theories for narrow QWs in strong magnetic fields 41

3.1 Self-consistent screening theories (SCST) 41

3.2 SHFA for QWs in strong magnetic fields 44

3.2.1 General idea 44

3.2.2 Eigenvalues and eigenstates without many-body effects . . . 46

3.2.3 Bare magnetic length and group velocity in Hartree Approximation 50

3.2.4 Edge states, the integral filling factor, and the Fermi wavenumber 51

3.2.5 Two-dimentional Poisson equation 54

3.2.6 Exchange and correlation in QWs: formulation for $\nu = 1$ . . 56

3.2.7 Exchange and correlation in QWs: formulation for $\nu \geq 1$ . . 61

3.3 Screening theories for a 3DEG and for QWs 64

4 Screened fields & correlation energies in QWs : $B_\perp$ (x,y) plane 65

4.1 $\nu = 1$ 65

4.1.1 Approximate analytical solution of the integral equation . . 65

4.1.2 Numerical solutions 75

4.1.3 Exchange and correlation energies, group velocities near the Fermi edge 81

4.1.4 Single-particle energies 85

4.2 $\nu = 2$ 90

4.2.1 Basic formulas 90

4.2.2 Solution of the integral equation for $\nu = 2$ 92

4.2.3 Exchange and correlation energies, group velocities near the Fermi edge 96

4.2.4 Single particle energies for $\nu = 2$ QHE states 98

4.3 $\nu = 3$ 101

4.3.1 Integral equation for $\nu = 3$ 101

4.3.2 Screened fields in QWs ($\nu = 3$) 103

4.3.3 Exchange and correlation corrections 113

4.3.4 v_g^{ec} at Fermi edge: $\nu = 3$ 116

4.3.5 Ground state energies ($\nu = 3$) 120

4.4 Exchange-correlation enhanced g^* factor 120

5 Screen fields & correlation energies in QWs: B ∥ QW 125

5.1 Channel characteristics without many-body effects 125

5.2 Exchange and correlation: formulation 131

5.3 Spin-splitting between filled $(n = 0, \sigma = 1)$ LL and empty $(n = 0, \sigma = -1)$ LL 133

5.3.1 Simplification of the integral equation and its analytic solution 133

5.3.2 Exchange-correlation correction to the lowest LL 136

5.4 Many-body effects on the $(n = 0, \sigma = -1)$ LL 139

5.5 Eigenvalue and eigenstate in a tilted magnetic field 141

6 Summary **143**

List of Figures

3.1 A quantum wire is a qusi-1DEG system where electrons are constrained to move in one direction. It can be realized in a semiconductor device by using the split gate technique. 47

4.1 Solved correlation interactions in QW (Sample 2 of Ref. [50]) with $\nu = 1, \tilde{k}_F = 15$. The dashed curve is the approximate analytic solution and the solid one shows the numerical solution. The two curves are very close and it is hard to notice any difference between them. The confining potential is defined by $\Omega = \omega/45$. In the $\tilde{q} \to 0$ (long wavelength limit) region, correlation interactions tend to diverge. 76

4.2 Solved correlations interactions in QW (Sample 2 of Ref. [50]) with $\nu = 1, \tilde{k}_F = 15$ and $\Omega = \omega/45$. The dashed curve is the approximate analytic solution and the solid one shows the numerical calculation. For $\tilde{q}_x$ 1/15, there are certain differences between the numerical solution and the analytical approximation. 77

4.3 Solved correlation interactions in QW (Sample 2 of Ref. [50])with $\nu = 1, \tilde{k}_F = 15$ and $\Omega = \omega/45$. The dashed curve is the approximate analytic solution and the solid one shows the numerical calculation. For large $\tilde{q}_x$, e.g., $\tilde{q}_x = 2$, there are nearly no differences between the two curves. 78

4.4 Solved correlations interactions in QW (Sample 1 of Ref. [50])with $\nu = 1, \tilde{k}_F = 15, \Omega = \omega/25$ and $\tilde{q}_x = 1/\tilde{k}_F$. Dashed curve represents the approximate analytic solution and the solid one is the numerical calculation. 79

4.5 The exchange-correlation correction $\varepsilon^{ec}_{0,k_x,1}/(\hbar\tilde{\omega})$ vs. $\tilde{k}_x$ curve for sample 1 of Ref.[50] with $\nu = 1$. When $\tilde{k}_x \to \tilde{k}_F = 15$, $\varepsilon^{ec}_{0,k_x,1}$ is very small. 82

4.6 Single particle energies $E/(\hbar\tilde{\omega})$ for sample 1 of Ref. [50], with $\nu = 1$. The parameters are $\hbar\Omega \approx 0.65meV, B \approx 10T, W \approx 0.30\mu m$, $\tilde{k}_F \approx 15$, and $\omega_c/\Omega \approx 25$. Curve 1 shows $E/(\hbar\tilde{\omega}) = \varepsilon_{0,k_x,-1}/(\hbar\tilde{\omega}) - 1/2 = \tilde{k}_x^2(\Omega/\omega_c)^2/2$ for the empty spin down LL. Curve 2 gives total particle energy $E_{0,k_x,1}/(\hbar\tilde{\omega})$ obtained from Eqs. (3.12), (4.32), (4.33), and (4.39). Curve 3 is the quasi-Fermi level. There is no finite gap for a QHE state. 87

4.7 Same as in previous figure with the parameters of sample 2 of Ref. [50], i.e., $\hbar\Omega = (0.46 \pm 0.2)meV, B \approx 7.3T, W \approx 0.33\mu m$, $\tilde{k}_F \approx 15$, and $\omega_c/\Omega \approx 32$. In contrast with Sample 1, when exchange and correlations are taken into account a gap appears between the curves for the $\sigma = -1$ and $\sigma = 1$ LLs and leads to the $\nu = 1$ QHE state. . 88

4.8 Solved correlation interactions in QW (Sample 1 of Ref. [50]) with $\nu = 2, \tilde{k}_{F2} = 10.6$, and $\Omega = \omega/12.5$. Dashed curve is the approximate analytic solution and the solid one shows the numerical calculation. For $\tilde{q}_x \sim 1/\tilde{k}_{F2} = 1/10.6$, there are certain differences between the numerical solution and the analytical one. 94

4.9 Solved correlation interactions in QW (Sample 1 of Ref. [50]) with $\nu = 2$, $\tilde{k}_{F2} = 10.6$, $\tilde{q}_x = 1/\tilde{k}_{F2}$ and $\Omega = \omega/12.5$. Dashed curve is the approximate analytic solution and the solid one shows the numerical calculation. In this figure $\tilde{q}_{y'} < 0$, while in the previous figure, $\tilde{q}_{y'} > 0$. 95

4.10 Single particle energies as functions of $\tilde{k}_x$, for sample 1 of Ref. [50], with $\nu = 2$. The parameters are $\hbar\Omega \approx 0.65meV$, $B \approx 5T$, $W \approx 0.30\mu m$, $\tilde{k}_{F2} \approx 10.6$, and $\omega_c/\Omega \approx 12.5$. Curve 1 shows $E/(\hbar\omega_c) = (\varepsilon_{1,k_x,1}/(\hbar\omega_c) - 1/2 = \tilde{k}_x^2(\Omega/\omega_c)^2/2$ of the empty $(n = 1, \sigma = 1)$ LL. Curve 2, obtained from Eq.(4.60), is the single-particle energy $E_{0,k_x,\pm1}/(\hbar\omega_c) - 1/2$ of the occupied $(n = 0, \sigma = \pm1)$ LL. The Zeeman energy splitting has been neglected. Curve 3 is the Fermi level. There is an obvious energy gap for the $\nu = 2$ QHE state. . . . 99

4.11 Same as in previous figure with the parameters of sample 2 of Ref. [50], i.e., $\hbar\Omega = (0.46 \pm 0.2)meV$, $B \approx 3.65T$, $W \approx 0.33\mu m$, $\tilde{k}_{F2} \approx 10.6$, and $\omega_c/\Omega \approx 16$. The Zeeman splitting between the two lowest LLs is very small $(\Delta E_{Zeeman} \approx 0.013\hbar\omega)$ and has been neglected. Curve 3 is the Fermi level. The finite gap between the empty $(n = 1, \sigma = 1)$ LL and the occupied $(n = 0, \sigma = \pm1)$ LLs means that the $\nu = 2$ QHE state is a thermodynamically allowed equilibrium state. 100

4.12 Solved correlation interactions in QW (Sample 1 of Ref. [50]) with $\nu = 3$, $\tilde{k}_{F3} = 8.66$. Dashed curve is the approximate analytic solution and the solid one shows the numerical calculation. The confinement potential is defined by $\Omega = \omega/(25/3)$. In the long wavelength limit, screened fields tend to diverge and the two curves almost coincide with each other. 110

4.13 Solved correlation interactions in QW (Sample 1 of Ref. [50])with $\nu = 3$. $\tilde{k}_{F3} = 8.66$. $\Omega = \omega/(25/3)$. Dashed curve is the approximate analytic solution and the solid one shows the numerical calculation. For $\tilde{q}_x \sim 1/\tilde{k}_F = 1/8.66$. there are certain differences between the two curves. 111

4.14 Same as Fig.4.12. except for $\tilde{q}_x = 2$. and $\Omega = \omega/(45/3)$. (Sample 2 of Ref. [50]) 112

4.15 The exchange-correlation correction $\varepsilon^{ec}_{1,k_x,1}/(\hbar\tilde{\omega})$ vs. $\tilde{k}_x$ curve for sample 1 of Ref. [50] with $\nu = 3$. For $\tilde{k}_x \to \tilde{k}_F = 8.66$. this curve has negative slope. 115

4.16 Single-particle energies as functions of $\tilde{k}_x$ for sample 1 of Ref. [50]. with $\nu = 3$. The parameters are $\hbar\Omega \approx 0.65meV, B \approx 3.3T, W \approx 0.30\mu m$. $\tilde{k}_{F3} \approx 8.66$. and $\omega_c/\Omega \approx 25/3$. Curve 1 shows $E/(\hbar\tilde{\omega}) = \varepsilon_{1,k_x,-1}/(\hbar\tilde{\omega}) - 3/2 = \tilde{k}_x^2(\Omega/\omega_c)^2/2$ for the empty $(n = 1, \sigma = -1)$ LL. Curve 2. calculated from Eq.(4.112). is the total energy $E_{1,k_x,1}/(\hbar\tilde{\omega})$ of single electron occupying the $(n = 1, \sigma = 1)$ LL. Curve 3 is the quasi-Fermi level. Notice that there is no gap that would lead to the $\nu = 3$ QHE state. 121

4.17 The effective g factor $g^*_{op} = \varepsilon^{ec}_{n,k_x,1}/\mu_B B + g_0$ as a function of $\tilde{k}_x$, in sample 1 and 2 of [50] for filling factor $\nu = 1$. 123

4.18 Same as in Fig. [4.17] in sample 1 for $\nu = 3$. 124

5.1 Electron ditribution in a QW when the magnetic field is perpendicular to the $x - y$ plane. The electrons are displaced by $y_0(k_x) = \hbar k_x \omega_c/(m^* \tilde{\omega}^2)$. 129

5.2 Electron ditribution in a QW when the magnetic field is parallel to the QW. All electrons are located around $y = 0$ and they have different values of k_x. 130

5.3 Energy dependence on the wavenumber when the QW is parallel to the magnetic field and the $(n = 0, \sigma = 1)$ LL is populated. Curve 1 shows the normalized kinetic energy without many-body interactions, i.e., $(\varepsilon_{0,k_x,1} - \hbar\tilde{\omega}/2 - g_0\mu_B s_z B/2)/(\hbar\tilde{\omega}\tilde{k}_F^2)$. Curve 3 is the normalized exchange-correlation energy $\varepsilon^{ec}_{0,k_x,1}/(\hbar\tilde{\omega}\tilde{k}_F^2)$. The x axis is the normalized wavenumber k_x/k_F. 138

Chapter 1

Introduction

1.1 Electronic correlations and correlation energies

In recent decades considerable efforts have been devoted to electronic correlations and correlation energies in quantum wires (QWs) in strong magnetic fields. This is mainly because they are more pronounced than those in two-dimentional or three-dimentional electron gas systems and have potential applications in modern technologies.

Electron correlation means certain kinds of spatial correlations between electrons. These correlations can be expressed through wave functions, electron interactions, or both of them. According to Landau's description [1], there are two kinds of electron correlations: "exchange correlations" and "dynamical correlations".

Exchange correlations, also called Pauli correlations, arise from the antisymmetry of the wave function under permutation of identical fermions. This requirement on the wave functions means their coordinates must be correlated and it results in correlations in the spatial distribution of two electrons whose spins are parallel, even if there were no interaction between them. On the other hand, dynamical correlations come from electron-electron interactions beyond the bare Coulomb force. Such interactions cause the spatial distributions of electrons to be correlated, even if there were no symmetrization requirement on electrons.

Exchange energyis caused by exchange correlations. It can be obtained within the Hartree-Fock approximation (HFA). The correlation energy is the further energy correction beyond that calculated within HFA. Now it is clear that the exchange and correlation corrections in an electronic system are closely related to the screening field in such a system. In fact, the electron energy can be obtained either by calculating exchange and correlation energies respectively or by taking into account the overall screened electron-electron interactions, as discussed in the next section. Hence, the screening theory becomes the central topic when we consider the mutual Coulomb interaction among electrons. (Note that, in this work, although the total screened field in the SHFA is discussed, we still decompose it into bare Coulomb potential and that caused by the induced charges and calculate the exchange energy and the correlation energy separately through. This can help us understand more clearly the effects of each energy correction.)

1.2 Coulomb interaction in 3DEG systems

The Coulomb interaction is one of the essential topics when one considers free electron gas systems. For a 3-dimensional electron gas (3DEG) system, we first consider Hartree equation. This model shows us in a "direct" way how the electrons in the system interact with each other. However, this model is a simplified one because it does not take into account the antisymmetric property of electron wave function. This is done by the Hartree-Fock (HF) model. The exchange energy refers to the energy difference between these two models because it is the energy contributed from the identity of electrons. The HF approximation (HFA) still has a problem: the exchange energy is logarithmically divergent at the Fermi level of the system. To remove this unphysical divergence, we need to take into account the screening effects of other electrons in the system. In reference [11] it was shown that the difference between HF potential and the screened Coulomb potential is the main part of the dynamic correlation. Actually, an efficient approach to consider the electron correlations in QWs is to study the screened interactions between electrons.

With the help of the screening concepts used in classical electrodynamics, screening theories for a 3DEG were developed. They are the Thomas-Fermi model, Lindhard model, Hubbard model, and Singwi-Sjolander approximation. Two of these methodes, the Thomas-Fermi and Lindhard models, are commonly used.

The Thomas-Fermi method is basically a semiclassical approximation requiring a slowly varying screened potential. The Lindhard method is basically an exact Hartree calculation of the charge density in the presence of the self-consistent field of the external charges plus electron gas, except that the Hartree calculation is simplified by the fact that the induced charge density is required to linear order in the screened field. The Thomas-Fermi method has the advantage that it is applicable even when a linear relation between the induced charge and the screened field does not hold. Its disadvantage is that it is reliable only for very slowly varying external potentials.

For the inhomogenous fermion system, the density functional theory (DFT) [10] can be used. Based on this theory, significant efforts have been devoted to the local density approximation (LDA), which is now very useful in studying low-dimensional systems.

1.3 Coulomb interaction in QWs and its effects on the subband structure

Real electrons are three-dimensional but can be made to behave as though they are only free to move in fewer dimensions. This can be achieved by trapping them in a narrow potential well that restricts their motion in one dimension with discrete energy levels. If the separation between these energy levels is large enough, the electrons will appear to be frozen in the ground state and no motion will be possible in this dimension. The result is a two-dimensional electron gas (2DEG). Its practical importance lies in its use as a field effect transistor which goes under a variety of names such as MODFET (MOdulation Doped Field Effect Transistor) or HEMT (High Electron Mobility Transistor). The electron-electron interaction in an exact two-dimensional electron gas at $T = 0$ was discussed in Refs. [12]-[15]. The classic reference on the two-dimensional electron gas is by Ando, Fowler, and Stern (1982) [64]. Its emphasis is on the silicon MOSFET rather than the III-V heterojunctions. Although so much of the material is rather dated, the basic theory remains applicable. As an example, the idea of the screened Hartree-Fock approximation (SHFA), discussed in this reference, is still useful when we consider the many-body effects in QWs.

Since the discovery of the quantum Hall effect by Klitzing *et al* at the be-

gining of the 1980's [4] – [5], both experimentalists and theorists have paid much attention to understanding the behavior of quasi-2D electron systems in strong magnetic fields. People want to study the role of many-body effects in mesoscopic systems (where the behavior of the electrons is determined as much by the structure through which they move as by bulk properties) and see how they alter some of the predictions of single-particle theories.

Quantum wires are usually fabricated by a lateral confinement of a two-dimensional electron gas, e.g., a GaAs/AlGaAs heterostructure. A lateral confinement is realized, for example, by a split-gate technique or shallow or deep mesa etching technique. Various models for the confining potential have been proposed, including an abrupt square well, a parabolic potential, and their combinations. Theoretically, the parabolic one has attracted much attention. This is because, within the harmonic oscillator model, we can calculate the eigenstates and the eigenvalues of an empty system (or when the electron-electron interaction is neglected) and further study the many-body effects in QWs.

It has been shown that the intriguing screening properties in a quasi-2DEG play significant roles for the understanding of many results, such as the capacitance [19] – [22], the specific heat [27], the gate voltage and current [19], [22], [25], [26], the activation energy [19], [22] – [24], [36], and the spin-splitting Lande g^* factor [29] – [35].

Edge states refer to the electron states localized at the edge of the quasi-2D

electron systems, see the discussion in subsection 3.2.4. Magnetotransport along edge states formed in high-mobility quasi-2DEG has attracted significant attention since the 1980's. The concept of such transport allows us to interpret a number of experiments performed in the integeral [40]–[42] and fractional [43]–[44] quantum Hall effect (QHE) regime. In addition, it is also important for us to understand a broad range of the mesoscopic and macroscopic systems.

While most previous theoretical works have developed a noninteracting picture of the edge states in quantum Hall effect regime, the effects of electron-electron interactions on the edge-state properties in a channel [42], [44]–[46], [51] and on the subband structure of quantum wires [46], [48]–[50] have been the subject of intense study in recent years. For example, in Refs. [18], [46], [47], [49], the self-consistent Hartree approach was used to calculate the subband structure of quantum wires in strong magnetic fields. To take into account the exchange interaction, a H-F treatment was used in Ref.[48]. Later, in Refs. [44] and [51] the self-consistent Hartree-Fock approximations were used to study the behavior of flattened edge states.

One consensus of these approaches is that, to study the properties of electron-electron interactions as a function of the width of the interface region, a quantum analysis including electrostatic effects is needed. Usually this is done by combining the Poisson equation with quantum Schroedinger equation and solving them self-consistently. In general, the source part of the Poisson equation comes from the

solution of the Schrodinger equation, while the solution of the Poisson equation contributes to the interaction term in the Schroedinger equation, within either the Hartree or Hartree-Fock Approximation. To solve these coupled equations self-consistently, different approaches have been proposed for various purposes. Actually, most of them considered the cases of very smooth confining potentials, except for Ref.[46] where this problem was solved numerically.

To study the effects of electronic exchange and correlation in narrow (submicrometer) quantum wires in strong magnetic fields, the SHFA suitable for QWs cases was proposed in Ref. [35]. With the help of the random phase approximation (RPA), which agrees very well with experimental measurements for high-density systems[55]-[57], the authors of Ref. [35] first obtained an analytical solution of the Schroedinger equation in the momentum representation. As the Hamiltonian in this equation contains the screened Coulomb interaction, its solution is a function of the screened potential. Then, substituting this solution into the source part of the classical Poisson equation gave a semi-classical integral equation. Therefore, within the RPA, the behavior of electron-electron interactions in quantum wires is basically represented by this semi-classical integral equation. We will refer to this scheme as the Poisson-RPA integral equation.

The remaining problem is how to solve this equation in a proper way. It should be noted that the Schroedinger equation solution, based on the RPA, is just a formal solution, which does not give the explicit expression of the single-particle

energy. To calculate the eigenvalue of the Schrodinger equation self-consistently, the local field correction (LFC) is required.

1.4 The motivation behind this work

As mentioned in the last section, the semi-classical Poisson-RPA integral equation [35] effectively describes the electronic screened potential in QWs. However, some unsolved issues still exist. They are raised below.

1) One important conclusion of Ref. [35] is that correlations caused by screening at the (Fermi) edges strongly suppress the exchange splitting and smoothen the energy dispersion at the (Fermi) edges. This is similar to the case of a 3DEG. As is well known, the unphysical singularity of the Hartree-Fock energy can be traced back to the divergence of the Fourier transform $4\pi e^2/q^2$ at $\mathbf{q}=0$ of the bare Coulomb potential and it can be removed by taking into account the screening effects of other electrons in the system. However, in a quantum wire subject to a strong perpendicular magnetic field, it is not clear how the singularity at the Fermi level caused by exchange is canceled by the screening and what the properties of the screening field are.

2) In Ref. [35] the solution of the Poisson-RPA integral equation was obtained by an incomplete iteration procedure. Actually, it is a first-order iteration solution calculated by replacing the unknown screened Coulomb potential in the integral kernel with the bare Coulomb potential. In principle, one can use a similar approach to get the nth-order (or higher-order) iteration solution by replacing the unknown screened potential in the integral kernel with the (n-1)th-order solution.

If the integral kernel is small enough, a stable solution can be obtained by repeating such a process a sufficient number of times. Otherwise, the result diverges. For QWs, the fact is that in the small q (the long wavelength) region, the screened potential is very large and this leads to divergent result. Therefore, it is impossible to use such an approach to get the solution of the Poisson-RPA integral equation. Similarly, the first-order solution in Ref. [35] is not a reliable one because the bare Coulomb potential ($4\pi^2/q^2$) becomes divergent when q is very small. Though the conclusions of Ref. [35] are reasonable and the final results are in agreement with some experimental results [26], it is still desirable to find out a reasonable iteration procedure so that we can solve the Poisson-RPA self-consistently.

3) Because of the incomplete iteration procedure mentioned in 2), Eq. (33) of Ref. [35] was proposed to reach the conclusion in 1). However, Eq. (33) is based on a nonstandard approximation. Furthermore, mathematically, this formula does NOT show the singularity in the exchange energy is exactly cancelled by the singularity in the correlation energy. The question arises whether we can obtain an expression for the group velocity as explicitly as possible. This is also worth considering because it is not only closely related to the energy dispersion curves but also connected to experimental results[50].

4) In Ref. [35], the strong magnetic field approximation $r_0 = e^2/(\epsilon l_0 \hbar\omega_c) << 1$ plays an important role in simplifying the calculation of many-body effects in QWs. For the typical experimental value $r_0 \sim 1$ ($B = 1 \sim 10T$), some nonstandard as-

sumptions have to be used to get formulas in agreement with the experimental results. It is natural to ask if there is any way, without relying on such approximations, to investigate the screening properties in QWs.

5) The filling factor ν of a LL (Landau Level), discussed in subsection 3.2.4, denotes the fraction of the LL that is occupied for a given magnetic field and electron density. Ref. [35] only dealt with the $\nu = 1$ case, i.e., when the lowest spin-polarized Landau level (LL) is completely occupied. For more complicated cases, say for $\nu = 2, 3$, when more LLs are populated, what would the screened fields be? So far, we haven't seen any progress in this direction.

6) Since we are aware of the importance in understanding the electronic correlations and screening properties in narrow QWs in magnetic fields that are perpendicular to the (x, y) plane, it is natural to ask how the screening properties are modified, for QWs parallel to magnetic fields. Do the electronic correlations still play a significant role in such QWs?

1.5 Methodology

The goal of this work is to find a self-consistent approach to investigate, as clearly as possible, the screening properties of QWs in strong magnetic fields and their impact on the occupied magnetic subbands or LLs. Among the specific objectives described in the previous section, the key one is to find the solution of the Poisson-RPA integral equation in a self-consistent way. To avoid the problems due to the incomplete iteration procedure used in Ref. [35], A different approach is proposed to solve this equation. It consists of the following steps.

1) **Simplification of the Poisson – RPA integral equation**

Actually, the Poisson-RPA integral equation can be simplified by taking into account only the intra-level screening and the adjacent-level screening. Screening from other levels is neglected. This is because for the strong magnetic fields, $B = 1 \sim 10$ T, screening from these LLs involves mainly higher order q, while in the small q region the total screened potential is very strong.

2) **Approximate analytical form of the screened potential**

Based on the mathematical structure of the simplified Poisson-RPA integral equation, the screened field is expressed as a superposition of intra-level and inter-level modes. Furthermore, the intra-level mode consists of two parts: the even parity mode and the odd parity mode. The coefficients of these modes can be obtained by using the generalized "mode-matching technique"[60] as well as some

basic mathematical approximations proposed in this work.

3) **Numerical solution**

To verify the approximate analytical solution obtained in step 2), it is necessary to obtain the numerical solution of the simplified Poisson-RPA integral equation. In principle, an integral equation can be solved numerically by iteration. However, for this integral equation, the traditional iterative method would lead to divergent result, because the integral kernel becomes very large when **q** is small. To avoid this divergence, a new method, called "weighted" iterative method, was proposed. Combined with the proper initial values, which are the approximate analytical solution obtained in step 2), our new iterative method can be used to obtain the numerical solution with any accuracy, provided the iteration times are large enough.

4) **Verification of the proposed approaches**

In general, the above methods are verified in two respects. First, the screened Coulomb potential obtained by our new approach is compared with the numerical solution. Second, the analytic approximation of the screened potential thus obtained is used to calculate the exchange-correlation energies as well as their corrections to single-particle energies. The results are then compared with those of the experiments. In both cases, we obtain satisfactory agreement.

1.6 The organization of this work

This work is organized as follows.

Chapter 1: Introduction

The concepts of electronic correlations and their relations to screening in the 3DEG systems are briefly introduced. Then an overview of recent studies of the many-body effects on the properties of edge states and the subband structure of occupied LLs is presented. Compared with other approaches, the SHFA is a very effective one. It was successfully proposed to study the screened Coulomb interactions in narrow QWs [35]. Of course, as a primary exploration, it has to be improved in several places. The motivations and objectives of this work have been discussed in the later part of this chapter. Then the methodology to reach these objectives have been briefly presented.

Chapter 2: An overview of many-body techniques for correlation energies

Some basic many-body techniques for the 3DEG systems are briefly presented. Although they cannot be applied directly to QWs, their basic ideas and concepts, such as the HA, HFA, RPA, and LDA (Local Density Approximation), are still very useful in finding a suitable approach to study electron-electron interactions

in QWs.

Chapter 3: Screening theories for narrow QWs in strong magnetic fields

Basic theories recently used to study screening in narrow QWs subjected to strong magnetic fields are given. As the SHFA is an effective screening theory for the real QW samples and is the basis of this work, we will extensively discuss the general principle of the SHFA, its formalism and features, assuming that the QWs are perpendicular to the magnetic fields. For QWs parallel to magnetic fields, this SHFA approach needs suitable modifications. The details will be discussed in chapter 5.

Chapter 4: Screened fields in QWs (B $\perp$ x-y plane) and their effects on the QHE states ($\nu = 1, 2, 3$)

The SHFA theory is applied to QWs with integral filling factors ($\nu = 1, 2, 3$). New approaches to find the approximate analytical and the numerical solutions for the screened Coulomb interactions in the QWs are presented. The obtained screened potentials are used to calculate the exchange and correlation corrections. As an important parameter related to the screening properties in QWs, the Fermi edge slopes of the exchange and correlations are proved to be nonsingular. To compare the theoretical results with the experimental ones, we further introduce the LDA approach to calculate the dispersion of the total single-particle energies.

based on which the overall single-particle Fermi edge group velocities as well as the effective g factor are evaluated.

Chapter 5: Screened fields in QWs (B // QW) and their effects on the highest occupied LLs ($n = 0, \sigma = +1, -1$)

Screening properties in QW parallel to the external magnetic field are considered within the SHFA. The discussion includes the screened field, the spin-splitting, and the slope of the exchange-correlation correction near the Fermi level. As a primary exploration, we consider the case of $n = 0$ LL with only one ($\sigma = 1$) or both ($\sigma = \pm 1$) spin sublevels occupied.

Chapter VI Summary and Suggestion

A summary of this work is presented. Suggestions for further work are also given.

Chapter 2

An overview of many-body techniques for correlation energies

2.1 Self-consistent Hartree approximation

When we consider many-body problems, generally the idea is how to approximately replace such problems by single-particle problems. The motivation behind this approximation is that, because there are bound states in nature in which electrons are in energy eigenstates, we should be able to describe a single electron i in state α using a single-particle, bound-state wave function $o_\alpha(\mathbf{r}_i) \equiv o_\alpha(\mathbf{r})$. Correspondingly, there must be an effective, single-particle potential $U_\alpha(\mathbf{r})$. When used in the 1-body Schrodinger equation,

$$[-\frac{\hbar^2\nabla^2}{2m} + U_\alpha(\mathbf{r})]o_\alpha(\mathbf{r}) = \varepsilon_\alpha o_\alpha(\mathbf{r}) \qquad (\alpha = 1, \cdots, N). \tag{2.1}$$

$U_\alpha(\mathbf{r})$ exactly produces $o_\alpha(\mathbf{r})$. Obviously $U_\alpha(\mathbf{r})$ must contain the effect of the other electrons. Hartree hypothesized that the single-particle potential is approximately

$$U_\alpha(\mathbf{r}) \approx \int d\mathbf{r}' \frac{e^2}{|\mathbf{r}-\mathbf{r}'|} \sum_{\beta(\beta\neq\alpha)}^{N} |o_\beta(\mathbf{r}')|^2 - \sum_{\mathbf{R}} \frac{Ze^2}{|\mathbf{r}-\mathbf{R}|} . \tag{2.2}$$

where $\mathbf{R}$ is the position of the ion. The second term on the right hand side of (2.2) is the electron-ion interaction and the first term is the single-particle potential for an ith electron in state α. This potential is the average over the coordinates of all paticles j, with the probability of finding an electron j in state β at $\mathbf{r}_j$ given by $|o_\beta(\mathbf{r}')|^2$. In this approximation the wave function Φ for the complete N-electron system is assumed to be a product of these single-particle states

$$\Phi(1,2,\cdots,N) = o_\alpha(1)o_\beta(2)\cdots o_{\alpha_N}(N). \tag{2.3}$$

where the subscripts on o denote the N different states needed for N electrons. The wave function Φ can be obtained by solving Eqs. (2.1) and (2.2). Analytic solutions are usually impossible for realistic cases but they can be obtained numerically via a self-consistent iteration: a form is guessed for $U_\alpha(\mathbf{r})$ on the basis of which Eq. (2.1) is solved. The improved wave functions o_α are then used to determine an improved $U_\alpha(\mathbf{r})$ by Eq. (2.2), which in turn, determines improved wave functions and so forth. When the wave functions and potentials become self-consistent, i.e., within some level of precision, when the two stop changing, the approximation scheme is considered convergent and successful.

The Hartree approximation is rather a crude aproximation because it does

not take the identity of electrons into consideration and it neglects the details of electron-electron interactions. Therefore, it does not contain any information about electron correlations. However, this can be partly improved by introducing an effective exchange-correlation potential U_{xc} and replacing $U_a(\mathbf{r})$ in Eqs. (2.1) and (2.2) with $U_{eff}(\mathbf{r})$:

$$\left[-\frac{\hbar^2\nabla^2}{2m} + U_{eff}(\mathbf{r})\right]\phi_a(\mathbf{r}) = \varepsilon_a\phi_a(\mathbf{r}) \tag{2.4}$$

$$U_{eff}(\mathbf{r}) = U_a(\mathbf{r}) - U_{xc}(\mathbf{r}). \tag{2.5}$$

This kind of modified Hartree approximation, which is often called H-RPA or HF-RPA [63, 64, 66], is based on the Density Functional Theory. This theory will be discussed in detail in sections 2.4 and 3.1.

2.2 Hartree-Fock approximation (HFA)

2.2.1 Hartree-Fock equations

Since all electrons in a many-body system are identical, the wave function must be antisymmetric under the interchange of the coordinates of any two of them. This is accomplished by using a Slater determinant for the many-electron wave function

$$\Phi = \frac{1}{\sqrt{N!}} \begin{vmatrix} o_\alpha(1) & o_\alpha(2) & \cdots & o_\alpha(N) \\ o_\beta(1) & o_\beta(2) & \cdots & o_\beta(N) \\ \vdots & \vdots & & \vdots \\ o_{\alpha_N}(1) & o_{\alpha_N}(2) & \cdots & o_{\alpha_N}(N) \end{vmatrix}$$

$$= \frac{1}{\sqrt{N!}} \sum_P (-1)^P \prod_{i=1}^{N} o_{P\alpha_i}(i) = \frac{1}{\sqrt{N!}} \sum_P (-1)^P \prod_{i=1}^{N} o_{\alpha_i}(Pi). \qquad (2.6)$$

Here, the subscripts on the o's (the rows) indicate orbitals (which can contain spin wave functions), the arguments (the columns) indicate the particles, and the sum is over all possible permutations P of orbitals (particles) with the sign depending on P.

Replacing Eq. (2.3) with Eq. (2.6) and with the help of the Rayleigh-Ritz variational principle, which states that the correct ground-state wave function minimizes the ground-state energy E, we can obtain, with orthogonal single elec-

tron wave functions $o_1, \ldots, o_N$, the total expectation energy of the many-electron system

$$\begin{aligned}\langle H\rangle = & \sum_i \int d\mathbf{r} o_i^*(\mathbf{r})(-\frac{\hbar^2}{2m}\nabla^2 - \sum_R \frac{Ze^2}{|\mathbf{r}-\mathbf{R}|})o_i(\mathbf{r}) \\ & + \frac{1}{2}\sum_{i,j}\int d\mathbf{r}d\mathbf{r}' \frac{e^2}{|\mathbf{r}-\mathbf{r}'|}|o_i(\mathbf{r})|^2 |o_j(\mathbf{r}')|^2 \\ & - \frac{1}{2}\sum_{i,j}\int d\mathbf{r}d\mathbf{r}' \frac{e^2}{|\mathbf{r}-\mathbf{r}'|}\delta_{s_i,s_j} o_i^*(\mathbf{r})o_i(\mathbf{r}')o_j^*(\mathbf{r}')o_j(\mathbf{r}) \qquad (2.7)\end{aligned}$$

and the nonlinear integro-differential equation for the single-particle wave function known as the Hartree-Fock equation

$$(-\frac{\hbar^2}{2m}\nabla^2 + U^{ion} + U^{el})o_i(\mathbf{r}) + \int d\mathbf{r}' U^x(\mathbf{r},\mathbf{r}')o_i(\mathbf{r}') = \varepsilon_i o_i(\mathbf{r}). \qquad (2.8)$$

where $U^{ion} = -\sum_{\mathbf{R}} Ze^2/|\mathbf{r}-\mathbf{R}|$ and $U^{el} = \sum_j \int d\mathbf{r}' e^2/|\mathbf{r}-\mathbf{r}'| |o_j(\mathbf{r}')|^2$ are the ion-potential and electron-electron potential, respectively. The exchange potential $U^x(\mathbf{r},\mathbf{r}')$

$$U^x(\mathbf{r},\mathbf{r}') = -\sum_j \frac{e^2}{|\mathbf{r}-\mathbf{r}'|}\delta_{s_i,s_j} o_j^*(\mathbf{r}')o_j(\mathbf{r}) \qquad (2.9)$$

connects only states of parallel spin. The negative sign on the right of above equation is required by the antisymmetry of the Fermion wave function. Equation (2.8) can also be expressed in Dirac notation:

$$[\frac{\mathbf{p}^2}{2m} + U^{ion}(\mathbf{r}) + U^{el}(\mathbf{r})]|i\rangle - \sum_{k,j}\langle k|\langle j|\frac{e^2}{|\mathbf{r}-\mathbf{r}'|}|i\rangle|j\rangle|k\rangle = \varepsilon_i|i\rangle. \qquad (2.10)$$

2.2.2 HFA for 3D free electron gas

Eq. (2.8) differs from the Hartree equation (2.1) by an additional term known as exchange term. The complexity introduced by the exchange term is considerable. Unlike the direct term, which has the form $U(\mathbf{r})\phi_a(\mathbf{r})$, it has the structure $\int d\mathbf{r}' U(\mathbf{r}, \mathbf{r}')\phi(\mathbf{r}')$, i.e., it is an integral operator. As a result, the Hartee-Fock equations are in general quite intractable. The one exception is the free electron gas (jellium model), for which the ion potential is constant

$$U^{ion}(\mathbf{r}) \approx \int d\mathbf{r}' \frac{e\rho(\mathbf{r}')}{|\mathbf{r} - \mathbf{r}'|} \ . \tag{2.11}$$

with $\rho(\mathbf{r}') = -eN/V$ $(e < 0)$ and V the volume. Then Hartree-Fock equations can be solved by choosing ϕ to be a set of orthogonal plane waves

$$\phi_i(\mathbf{r}) = (\frac{e^{i\mathbf{k}_i \cdot \mathbf{r}}}{\sqrt{V}}) \times (spin\ function). \tag{2.12}$$

which satisfy the periodic boundary condition. This can be shown by taking into account the fact that the electronic charge in this case will be uniform

$$U^{ion} + U^{el} = 0. \tag{2.13}$$

and the exchange term will be reduced to

$$\begin{aligned} & - \sum_j \int d\mathbf{r}' \phi_j^*(\mathbf{r}') \frac{e^2}{|\mathbf{r} - \mathbf{r}'|} \phi_j(\mathbf{r}) \phi_i(\mathbf{r}') \\ = & -[\sum_j \int d\mathbf{r}\, d\mathbf{r}' \phi_i^*(\mathbf{r}) \phi_j^*(\mathbf{r}') \frac{e^2}{|\mathbf{r} - \mathbf{r}'|} \phi_j(\mathbf{r}) \phi_i(\mathbf{r}')]\, \phi_i(\mathbf{r}) \end{aligned}$$

$$
\begin{aligned}
&= -[\sum_j \langle i|\langle j|\frac{e^2}{|\mathbf{r}-\mathbf{r}'|}|i\rangle|j\rangle]\ \langle \mathbf{r}|i\rangle \\
&= -\frac{1}{V}\sum_{|\mathbf{k}_j|<k_F}\frac{4\pi e^2}{|\mathbf{k}_i-\mathbf{k}_j|^2}\ o_i(\mathbf{r}) = -\frac{2e^2k_F}{\pi}F(\frac{k_i}{k_F})\ o_i(\mathbf{r}). \qquad (2.14)
\end{aligned}
$$

where $F(x) = 1/2+[(1-x^2)/4x]\log|(1+x)/(1-x)|$ and the relations $\langle o_i|o_j\rangle = \delta_{ij}$, $e^2/r = \sum_q(4e^2\pi/V)e^{i\mathbf{q}\cdot\mathbf{r}}/q^2$, $\sum_{\mathbf{k}} \to \int_0^{k_F} d\mathbf{k}V/(2\pi)^3$ are used.

The energy factors in Eq. (2.14) are known as exchange self-energies, for they arise merely from the symmetry requirement of the state functions under permutation. Since the energy factors in the direct term in the Hartree (or HF) equations do not take the symmetry of the wave function into consideration, the energy factors in the above expressions are actually a kind of Coulomb energy corrections. These energy corrections are merely caused by the Pauli correlation. That is why we call these energy corrections as exchange energies and classify this kind of correlation as "exchange correlation". In addition to this exchange correction, there is another self-energy correction associated with the screened potential. The corresponding electron correlation belongs to dynamical correlations[11]. In section 2.3 it will be discussed in the second quantization formalism.

With the help of Eq. (2.14), the eigenvalues of the HF equations (2.8) are

$$
\varepsilon_i = \frac{\hbar^2k_i^2}{2m} - \frac{2e^2k_F}{\pi}F(\frac{k_i}{k_F}). \qquad (2.15)
$$

Then the average ground-state energy for electon gas can be calculated as

$$
E_g^0 = \frac{2}{N}\sum_{|\mathbf{k}|<k_F}[\ \frac{\hbar^2k^2}{2m} - \frac{1}{2}\frac{2e^2k_F}{\pi}F(\frac{k}{k_F})\ ]
$$

$$= \frac{V}{N}\left[\int_{|\mathbf{k}|<k_F} d\mathbf{k}\frac{2}{(2\pi)^3}\frac{\hbar^2 k^2}{2m} - \left(\frac{e^2 k_F}{\pi}\right)\frac{k_F^3}{2\pi^2}\int_0^1 x^2 dx\left(1 + \frac{1-x^2}{2x}\log\left|\frac{1+x}{1-x}\right|\right)\right]$$

$$= \frac{3}{5}\frac{\hbar^2 k_F^2}{2m} - \frac{3}{4}\frac{e^2 k_F}{\pi}$$

$$= \left[\frac{2.21}{(r_s/a_0)^2} - \frac{0.916}{r_s/a_0}\right]Ry. \tag{2.16}$$

where $n_0 = N/V = k_F^3/3\pi^2 = [\frac{4\pi}{3}(a_0 r_s)^3]^{-1}$, $a_0 = \hbar^2/me^2$ and $1Ry = e^2/2a_0 = \hbar^2/2ma_0^2$. The second term in Eq. (2.16) is called exchange energy (E_{ex}). The correlation energy is defined as the difference between the actual energy and the sum of kinetic energy and exchange energy ($3/5E_F + E_{ex}$).

2.2.3 HFA modified with an equivalent local potential

For the homogeneous electron gas model, the exchange term in the HF equations can be written in the form $E_{ex}o_i(\mathbf{r})$, since the bare Coulomb potential can be expanded as the superposition of a series of momentum functions. However, in general, this is not necessarily true that the exchange term in Eq.(2.8) can be factorized into such a form, mainly because of the nonlocality of the exchange potential

$$U(\mathbf{r},\mathbf{r}') = -\sum_j \frac{e^2}{|\mathbf{r}-\mathbf{r}'|}\delta_{s_i,s_j}o_j^*(\mathbf{r}')o_j(\mathbf{r}). \tag{2.17}$$

which arises from the correlation nature of the electron's wave function. Determining $o_i(\mathbf{r})$ from the HF equations thus requires knowledge of the wave functions in all other orbitals as well as other positions $\mathbf{r}'$. This is reasonable, because in an interacting system the electrons respond if the state of an electron at one point is modified. Thus the effective potential is nonlocal. One approximation technique to process this is to assume that the range of the nonlocality is small, so that $o_i(\mathbf{r}') \approx o_i(\mathbf{r})$ inside the integral in the HF equations. This leaves an approximate equivalent local potential [2]:

$$\begin{aligned} \int d\mathbf{r}' U(\mathbf{r}, \mathbf{r}') o_i(\mathbf{r}') &\approx \int d\mathbf{r}' U(\mathbf{r}, \mathbf{r}') o_i(\mathbf{r}) \\ &\equiv U^{eq}(\mathbf{r}) o_i(\mathbf{r}) \end{aligned} \tag{2.18}$$

and the HF equations are modified as

$$[-\frac{\hbar^2}{2m}\nabla^2 + U^{ion}(\mathbf{r}) + U^{el}(\mathbf{r}) - U^{eq}(\mathbf{r})] o_i(\mathbf{r}) = \varepsilon_i o_i(\mathbf{r}) \ . \tag{2.19}$$

We thus obtain a one-electron wave equation. There are other forms of approximate equivalent local potentials [2], but the basic ideas is the same, that is, to find an equivalent local potential to replace the nonlocal potential. In fact the equivalent local potential in (2.19) is similar to the exchange-correlation potential $U_{xc}(\mathbf{r})$ in Eq. (2.5).

2.3 Linear screening theory

2.3.1 Linear screening

Screening is one of the most important concepts in many-body problems. Charges will move in response to an electric field. This charge movement will stabilize into a new distribution of charge around the electric field. Otherwise more charge will still be attracted until it is sufficient for cancellation. If the electric field is caused by an impurity charge distribution $\varrho_i(\mathbf{r})$, with net charge $Q_i = \int d\mathbf{r}\varrho_i(\mathbf{r})$, the amount of mobile charge attracted to the surroundings is exactly $-Q_i$. The name screening charge ϱ_s is applied to the mobile charge attracted by the impurity field or an external field. According to the classical macroscopic theory, the screened potential from the impurity charge $\varrho_i(\mathbf{r})$ and the screening charge $\varrho_s(\mathbf{r})$ is given by

$$o(\mathbf{r}) = \int d\mathbf{r}' \frac{\varrho_i(\mathbf{r}') + \varrho_s(\mathbf{r}')}{|\mathbf{r} - \mathbf{r}'|}. \tag{2.20}$$

where $\varrho_i(\mathbf{r})$ and $\varrho_s(\mathbf{r})$ satisfy Gauss's Law:

$$\nabla \cdot \mathbf{D}(\mathbf{r}) = 4\pi\varrho_i(\mathbf{r}) \tag{2.21}$$

$$or \qquad \nabla \cdot \mathbf{E}(\mathbf{r}) = 4\pi[\varrho_i(\mathbf{r}) + \varrho_s(\mathbf{r})]. \tag{2.22}$$

Their Fourier components are

$$i\mathbf{q} \cdot \mathbf{D}(\mathbf{q}) = 4\pi\varrho_i(\mathbf{q}) \tag{2.23}$$

$$i\mathbf{q}\cdot\mathbf{E}(\mathbf{q}) = 4\pi[\varrho_t(\mathbf{q}) + \varrho_s(\mathbf{q})] \tag{2.24}$$

or

$$\mathbf{D}_l(\mathbf{q}) = \frac{4\pi}{iq}\varrho_t(\mathbf{q}) \tag{2.25}$$

$$\mathbf{E}_l(\mathbf{q}) = \frac{4\pi}{iq}[\varrho_t(\mathbf{q}) + \varrho_s(\mathbf{q})] \tag{2.26}$$

$$\phi(\mathbf{q}) = \frac{4\pi}{q^2}[\varrho_t(\mathbf{q}) + \varrho_s(\mathbf{q})]. \tag{2.27}$$

The dielectric response function $\epsilon(\mathbf{q})$ is defined as

$$\epsilon(\mathbf{q}) = \lim_{\varrho_t\to 0}\frac{\mathbf{D}_l(\mathbf{q})}{\mathbf{E}_l(\mathbf{q})} = \lim_{\varrho_t\to 0}\frac{\varrho_t(\mathbf{q})}{\varrho_t(\mathbf{q}) + \varrho_s(\mathbf{q})}. \tag{2.28}$$

In the limit $\varrho_t \to 0$, $\epsilon(\mathbf{q})$ becomes a property of the material and is independent of the charge distribution. The linear screening model assumes this definition is true for finite ϱ_t.

$$\epsilon(\mathbf{q}) = \frac{\varrho_t(\mathbf{q})}{\varrho_t(\mathbf{q}) + \varrho_s(\mathbf{q})} \tag{2.29}$$

and the total potential becomes

$$\phi(\mathbf{q}) = \frac{4\pi}{q^2}\frac{\varrho_t(\mathbf{q})}{\epsilon(\mathbf{q})} \quad . \tag{2.30}$$

or

$$\phi(\mathbf{r}) = \int \frac{d\mathbf{q}}{(2\pi)^3}\frac{4\pi}{q^2}\frac{\varrho_t(\mathbf{q})}{\epsilon(\mathbf{q})}e^{i\mathbf{q}\cdot\mathbf{r}} \quad . \tag{2.31}$$

2.3.2 Coulomb interaction expressed in occupation number representation

Since electrons in a many-body system cannot be distinguished from each other by any experimental means, it should be much more convenient to discuss many-body problems in the second quantization representation, which takes into account the indistinguishability of identical particles. Another advantage of this formalism is that the observables are defined referring only to the single-particle state.[8] Thus we can describe the many-body system (except for the internal degrees of freedom) in three-dimensional space, in contrast to the case of the Schrodinger formalism, in which the multi-particle space of dimension 3N (N being the number of particles) must be considered.

The Hamiltonian for a many-electron system can be written as

$$H = \sum_i \left[\frac{\mathbf{p}_i^2}{2m} + U(\mathbf{r}_i)\right] + \frac{1}{2}\sum_{i\neq j} V(\mathbf{r}_i - \mathbf{r}_j). \tag{2.32}$$

where $U(\mathbf{r})$ is $U^{ion}(\mathbf{r})$ in Eq. (2.8) and $V(\mathbf{r}_i - \mathbf{r}_j) = e^2/|\mathbf{r}_i - \mathbf{r}_j|$. This can be written in terms of creation and destruction operators as[6]

$$H = \sum_{ij} H_{ij} c_i^\dagger c_j + \frac{1}{2}\sum_{ijlm} c_j^\dagger c_m^\dagger V_{ijlm} c_l c_i \quad . \tag{2.33}$$

where $H_{ij} = \langle i|[\frac{\mathbf{p}^2}{2m} + U(\mathbf{r})]|j\rangle$ and $V_{ijlm} = \langle j|\langle m|V(\mathbf{r} - \mathbf{r}')|l\rangle|i\rangle$. For the study of homogenous electrons in 3D solids, a popular basis set is plane waves. The Hamiltonian then has the form

$$H = \sum_{\mathbf{k},\sigma} \varepsilon_{\mathbf{k}} c_{\mathbf{k},\sigma}^\dagger c_{\mathbf{k},\sigma} + \frac{1}{2V}\sum_{\mathbf{k}\mathbf{k}'\sigma\sigma'\mathbf{q}\neq 0} c_{\mathbf{k}+\mathbf{q},\sigma}^\dagger c_{\mathbf{k}'-\mathbf{q},\sigma'}^\dagger v_{\mathbf{q}} c_{\mathbf{k}'\sigma'} c_{\mathbf{k}\sigma} \quad , \tag{2.34}$$

where $v_{\mathbf{q}} = \int d\mathbf{r} V(\mathbf{r}) e^{-i\mathbf{q}\cdot\mathbf{r}} = e^2/q^2$ and $\varepsilon_{\mathbf{k}} = \hbar^2\mathbf{k}^2/2m$. The ground state energy,

in the first order approximation, can be written as

$$E_g^0 = \frac{2}{N} \sum_{|\mathbf{k}|<k_F} \frac{\hbar^2 \mathbf{k}^2}{2m} + \frac{1}{2N} \sum_{\mathbf{k},\sigma} n_{\mathbf{k}} [- \sum_{\mathbf{q}} \frac{v_{\mathbf{q}}}{V} n_{\mathbf{k}+\mathbf{q}}], \tag{2.35}$$

which is actually the same as Eq. (2.16).

2.3.3 Linear screening theory of the ground state energy

Numerical results from Eq. (2.35) or Eq. (2.16) differ from the experimental data by about 10% or more. The reason is that the actual Coulomb interaction is not as strong as the one leading to Eq. (2.35) or Eq. (2.16). Better results can be obtained by taking the screening effect of electrons into consideration.

According to the linear screening theory, two impurity charges $Z_1 e$ and $Z_2 e$ at $\mathbf{r}_1$ and $\mathbf{r}_2$ respectively, will cause a screened Coulomb interaction of the form

$$V'(\mathbf{r}_1, \mathbf{r}_2) = Z_1 Z_2 \int \frac{d\mathbf{q}}{(2\pi)^3} \frac{v_{\mathbf{q}}}{\epsilon_{\mathbf{q}}} e^{i\mathbf{q}\cdot(\mathbf{r}_2 - \mathbf{r}_1)} , \tag{2.36}$$

if the solution of Poisson's equation $\phi(\mathbf{r}) = \int \frac{d\mathbf{q}}{(2\pi)^3} (4\pi/q^2)[\varrho_i(\mathbf{q})/\epsilon_{\mathbf{q}}] e^{i\mathbf{q}\cdot\mathbf{r}}$, with $\varrho_i(\mathbf{q}) = Z_i e e^{-i\mathbf{q}\cdot\mathbf{r}_i} (i = 1, 2)$ and $v_{\mathbf{q}} = 4\pi e^2/q^2$. On the other hand, based on the Green's function theory, one has [6]

$$\begin{aligned} V'(\mathbf{r}_1 - \mathbf{r}_2) &= Z_1 Z_2 \int \frac{d\mathbf{q}}{(2\pi)^3} v_{\mathbf{q}} e^{i\mathbf{q}\cdot(\mathbf{r}_1 - \mathbf{r}_2)} \\ &\times [1 - \frac{v_{\mathbf{q}}}{V\beta} \int_0^\beta d\tau_1 \int_0^\beta d\tau_2 \langle T_\tau \rho(\mathbf{q}, \tau_1) \rho(-\mathbf{q}, \tau_2) \rangle], \end{aligned} \tag{2.37}$$

where T_τ is the τ ordering operator. Comparing (2.36) with (2.37) leads to

$$\begin{aligned}\frac{1}{\epsilon_{\mathbf{q}}} &= 1 - \frac{v_{\mathbf{q}}}{V\beta}\int_0^\beta d\tau_1 \int_0^\beta d\tau_2 \langle T_\tau \rho(\mathbf{q},\tau_1)\rho(-\mathbf{q},\tau_2)\rangle \\ &= 1 - \frac{v_{\mathbf{q}}}{V}\int_0^\beta d\tau \langle T_\tau \rho(\mathbf{q},\tau)\rho(-\mathbf{q},0)\rangle. \end{aligned} \tag{2.38}$$

Generalizing Eq. (2.38) to finite frequencies, we have

$$\frac{1}{\epsilon(\mathbf{q},\omega)} = 1 - \frac{v_{\mathbf{q}}}{V}\int_0^\beta d\tau e^{i\omega\tau}\langle T_\tau \rho(\mathbf{q},\tau)\rho(-\mathbf{q},0)\rangle. \tag{2.39}$$

At zero temperature, Eq. (2.39) leads to

$$-\frac{v_{\mathbf{q}}}{V}\langle \rho(\mathbf{q})\rho(-\mathbf{q})\rangle = \int \frac{d\omega}{\pi} Im[\frac{1}{\epsilon(\mathbf{q},\omega)}]. \tag{2.40}$$

if the mathematical formula $\lim_{y\to 0}\frac{1}{x+iy} = P(\frac{1}{x}) - i\pi\delta(x)$ is used.

Formula (2.40) can be used to derive the correlation energies of the homogenous electron gas. To see this, we rewrite the Coulomb interaction term in Eq. (2.34) in the form

$$H' \equiv \frac{1}{2V}\sum_{\mathbf{k}\mathbf{k}'\sigma\sigma'\mathbf{q}\neq 0} c^\dagger_{\mathbf{k}+\mathbf{q},\sigma} c^\dagger_{\mathbf{k}'-\mathbf{q},\sigma'} v_{\mathbf{q}} c_{\mathbf{k}'\sigma'} c_{\mathbf{k}\sigma} = \frac{1}{2V}\sum_{\mathbf{q}} v_{\mathbf{q}}[\rho(\mathbf{q})\rho(-\mathbf{q}) - N]. \tag{2.41}$$

The strict ground state $|0\rangle$ average of $\rho(\mathbf{q})\rho(-\mathbf{q})$ in the electron gas is

$$\frac{v_{\mathbf{q}}}{2V}\langle 0|\rho(\mathbf{q})\rho(-\mathbf{q})|0\rangle = -\frac{1}{2}\int \frac{d\omega}{\pi} Im[\frac{1}{\epsilon(\mathbf{q},\omega)}]. \tag{2.42}$$

Thus the interaction energy E_{int} of the electron gas, per electron, can be written in the form

$$\begin{aligned} E_{int}(e^2) &= \langle 0|H'|0\rangle = \sum_{\mathbf{q}}[-\frac{1}{2}\int \frac{d\omega}{\pi} Im(\frac{1}{\epsilon(\mathbf{q},\omega)}) - \frac{N}{2V}v_{\mathbf{q}}]/N \\ &= 2\pi e^2 \int \frac{d\mathbf{q}}{(2\pi)^3}\frac{1}{q^2}[S(q) - 1] = \frac{e^2}{\pi}\int_0^\infty dq[S(q) - 1], \end{aligned} \tag{2.43}$$

where

$$S(\mathbf{q}) = -\frac{1}{n_0 v_{\mathbf{q}}} \int_0^\infty \frac{d\omega}{\pi} Im(\frac{1}{\epsilon(\mathbf{q}, \omega)}) \tag{2.44}$$

is the state structure factor or static form factor.

The quantity $E_{int}(e^2)$ is not the Coulomb contribution to the ground-state energy. To obtain the ground-state energy per particle E_g, one must do a coupling constant integration based on the Feyman Principle

$$\frac{\partial E_n}{\partial \lambda} = \langle n, \lambda | \frac{\partial h(\lambda)}{\partial \lambda} | n, \lambda \rangle. \tag{2.45}$$

The result is

$$E_g = \frac{3}{5} E_F + \int_0^{e^2} \frac{d\lambda}{\lambda} E_{int}(\lambda). \tag{2.46}$$

which is different from E_g^0 given by Eq. (2.16). It is conventional to introduce a dimensionless function

$$\gamma \equiv \frac{-1}{2k_F} \int dq [S(q) - 1]. \tag{2.47}$$

Then, the interaction energy per electron may be written as

$$E_{int} = -\frac{2}{\pi} e^2 k_F \gamma = -\frac{4}{\pi r_s} (\frac{9\pi}{4})^{\frac{1}{3}} \gamma (Ry). \tag{2.48}$$

If we change e^2 to λe^2 and $v_{\mathbf{q}}$ in $\epsilon(\mathbf{q}, \omega)$ to $\lambda v_{\mathbf{q}}$, where $0 \leq \lambda \leq 1$, we have

$$E_{int} = -\lambda \frac{4}{\pi r_s} (\frac{9\pi}{4})^{\frac{1}{3}} \gamma (\lambda r_s), \tag{2.49}$$

and[6]:

$$E_g = \frac{3}{5}E_F - \frac{4}{\pi r_s}(\frac{9\pi}{4})^{\frac{1}{3}} \int_0^1 d\lambda \gamma(\lambda r_s). \tag{2.50}$$

The first term in above expression is equal to $2.21/(r_s/a_0)^2$. The correlation energy E_c consists of all contributions to the (strict) ground-state energy E_g except kinetic and exchange. Thus, with the help of Eq. (2.16), E_c is given by

$$E_c = \frac{0.916}{r_s} - \frac{4}{\pi r_s}(\frac{9\pi}{4})^{\frac{1}{3}} \int_0^1 d\lambda \gamma(\lambda r_s). \tag{2.51}$$

which is formula (5.6.5) in Ref. [6]. This is a rigorous formula connecting the correlation energy and $\gamma(\lambda r_s)$ [or $\epsilon(\mathbf{q}, \omega)$] and it can be used for different linear screening models. Some of them, which are often used, will be discussed in the following subsections.

One can verify that E_c given by Eq.(2.51) vanishes when $\gamma(r_s)$ is calculated in the Hartree-Fock approximation [6]. This is in agreement with the fact that one cannot find any correlation information from the HF equations (2.8) .

2.3.4 Lindhard or RPA dielectric function

The idea used to deal with the many-body interaction in the Lindhard model or random phase approximation (RPA) is actually the same as the one used in the modified HFA, where the electron-electron interaction is equivalent to an effective local potential $U^{eq}(\mathbf{r})$ of Eq. (2.19). Now, when we consider the screening

effect, this local potential becomes the time-dependent total potential $V(\mathbf{r}, t)$, or self-consistent field, to which the electrons respond. In other words, in RPA, the electron gas responds as if it were non-interacting and only perturbed by an effective mean field. Based on this, we can view the Eq. (2.34) as the form below

$$H = \sum_{\mathbf{k},\sigma} \varepsilon_{\mathbf{k}} c^{\dagger}_{\mathbf{k},\sigma} c_{\mathbf{k},\sigma} + \frac{1}{V} \sum_{\mathbf{q}=0} V(\mathbf{q}, t)\rho(\mathbf{q}), \tag{2.52}$$

where

$$\rho(\mathbf{q}) = \sum_{\mathbf{p},\sigma} c^{\dagger}_{\mathbf{p}-\mathbf{q},\sigma} c_{\mathbf{p},\sigma} = \sum_{\mathbf{p},\sigma} \rho^{\dagger}_{pq} \tag{2.53}$$

is the particle density operator and $V(\mathbf{q}, t)$ is the qth Fourier component of $V(\mathbf{r}, t)$. Obviously, $V(\mathbf{q}, t)$ should be approximately proportional to the density $\rho(\mathbf{q}, \mathbf{t})$. To find the relationship between them, let's consider the operator in (2.53). Physically, this operator represents a type of electron-hole pair excitation having total momentum $\mathbf{q}$: an electron at state $|\mathbf{p}\rangle$ (e.g., within the Fermi sphere) is excited (or scatted) by the mean field V, to the state $|\mathbf{p}+\mathbf{q}\rangle$ (e.g., outside the Fermi sphere). In the Heisenberg picture, this operator has the equation

$$i\hbar \frac{d}{dt} c^{\dagger}_{\mathbf{p}+\mathbf{q},\sigma} c_{\mathbf{p},\sigma} = [H, c^{\dagger}_{\mathbf{p}-\mathbf{q},\sigma} c_{\mathbf{p},\sigma}]. \tag{2.54}$$

With the help of the Eq. (2.52) and the commutator relations

$$\sum_{\mathbf{k},s} \varepsilon_{\mathbf{k}} [c^{\dagger}_{\mathbf{k},s} c_{\mathbf{k},s}\ ,\ c^{\dagger}_{\mathbf{p}+\mathbf{q},\sigma} c_{\mathbf{p},\sigma}] = (\varepsilon_{\mathbf{p}-\mathbf{q}} - \varepsilon_{\mathbf{p}}) c^{\dagger}_{\mathbf{p}+\mathbf{q},\sigma} c_{\mathbf{p},\sigma}\ . \tag{2.55}$$

$$\sum_{\mathbf{k},\mathbf{q}',s} V(\mathbf{q}', t)[c^{\dagger}_{\mathbf{k}+\mathbf{q}',s} c_{\mathbf{k},s}, c^{\dagger}_{\mathbf{p}+\mathbf{q},\sigma} c_{\mathbf{p},\sigma}] = \sum_{\mathbf{q}'} V(\mathbf{q}', t)(c^{\dagger}_{\mathbf{p}+\mathbf{q}+\mathbf{q}',\sigma} c_{\mathbf{p},\sigma}, -c^{\dagger}_{\mathbf{p}+\mathbf{q},\sigma} c_{\mathbf{p}-\mathbf{q}',\sigma}), \tag{2.56}$$

we obtain

$$(\varepsilon_{\mathbf{p}} - \varepsilon_{\mathbf{p}+\mathbf{q}} + \hbar\omega)c^{\dagger}_{\mathbf{p}+\mathbf{q},\sigma}c_{\mathbf{p},\sigma} = \frac{1}{V}\sum_{\mathbf{q}'} V(\mathbf{q}',t)(c^{\dagger}_{\mathbf{p}+\mathbf{q}+\mathbf{q}',\sigma}c_{\mathbf{p},\sigma} - c^{\dagger}_{\mathbf{p}+\mathbf{q},\sigma}c_{\mathbf{p}-\mathbf{q}',\sigma}). \tag{2.57}$$

This gives

$$\begin{aligned} \rho(\mathbf{q},t) &= \sum_{\mathbf{p},\sigma} c^{\dagger}_{\mathbf{p}+\mathbf{q},\sigma}c_{\mathbf{p},\sigma} \\ &= \sum_{\mathbf{p},\sigma}\sum_{\mathbf{q}'} \frac{V(\mathbf{q}',t)}{V}\frac{(c^{\dagger}_{\mathbf{p}+\mathbf{q}+\mathbf{q}',\sigma}c_{\mathbf{p},\sigma} - c^{\dagger}_{\mathbf{p}+\mathbf{q},\sigma}c_{\mathbf{p}-\mathbf{q}',\sigma})}{\varepsilon_{\mathbf{p}} - \varepsilon_{\mathbf{p}+\mathbf{q}} + \hbar\omega} \end{aligned} \tag{2.58}$$

To simplify the right side of Eq. (2.58), we take only terms having $\mathbf{q}' = -\mathbf{q}$ in the summation. The terms with other values of $\mathbf{q}'$ are neglected. Physically, this means that we only take into account the electron-hole pair excitations with total momentum zero. (Note that they are connected with the effective mean field of momentum $\mathbf{q}$.) Those pairs with non-zero momenta are neglected. This is because the phase between them are randomly distributed and the expected values of these excitations cancel each other. This is what is meant by the RPA (**Random Phase Approximation**). Its classical correspondence is the approximation

$$\rho_{\mathbf{p}} = \sum_{i} e^{i\mathbf{p}\cdot\mathbf{r}_i} \approx 0. \tag{2.59}$$

because for $\mathbf{p} \neq 0$, $\rho_{\mathbf{p}}$ is the sum of exponential terms with randomly varying phase [9]. Therefore, the RPA reduce Eq.(2.58) to

$$\rho(\mathbf{q},t) \approx \frac{V(\mathbf{q},t)}{V}\sum_{\mathbf{p},\sigma}\frac{c^{\dagger}_{\mathbf{p},\sigma}c_{\mathbf{p},\sigma} - c^{\dagger}_{\mathbf{p}+\mathbf{q},\sigma}c_{\mathbf{p}-\mathbf{q},\sigma}}{\varepsilon_{\mathbf{p}} - \varepsilon_{\mathbf{p}-\mathbf{q}} + \hbar\omega}. \tag{2.60}$$

To linearize the nonlinear parts in the above expression, we need to take the approximation:

$$\langle c^{\dagger}_{\mathbf{p},\sigma} c_{\mathbf{p},\sigma} \rangle - \langle c^{\dagger}_{\mathbf{p}+\mathbf{q},\sigma} c_{\mathbf{p}+\mathbf{q},\sigma} \rangle = n_F(\varepsilon_{\mathbf{p}}) - n_F(\varepsilon_{\mathbf{p}+\mathbf{q}}) \tag{2.61}$$

Also, if the impurity is assumed to oscillate at a single frequency, then $\langle \rho(\mathbf{q}, t) \rangle$ and $\langle V(\mathbf{q}, t) \rangle$ are replaced by $\langle \rho(\mathbf{q}, t) \rangle = \rho(\mathbf{q}, \omega) e^{-i\omega t}$ and $\langle V(\mathbf{q}, t) \rangle = V(\mathbf{q}, \omega) e^{-i\omega t}$, respectively.

Thus, one obtains

$$\rho(\mathbf{q}, \omega) = \frac{V(\mathbf{q}, \omega)}{V} \sum_{\mathbf{p},\sigma} \frac{n_F(\varepsilon_{\mathbf{p}}) - n_F(\varepsilon_{\mathbf{p}+\mathbf{q}})}{\varepsilon_{\mathbf{p}} - \varepsilon_{\mathbf{p}+\mathbf{q}} + \omega} \equiv V(\mathbf{q}, \omega) P^{(1)}(\mathbf{q}, \omega). \tag{2.62}$$

The Lindhard dielectric function $\epsilon_{RPA}(\mathbf{q}, \omega)$ can be obtained from Eq. (2.62) and the relations

$$\epsilon(\mathbf{q}, \omega) = \frac{V_i(\mathbf{q}, \omega)}{V(\mathbf{q}, \omega)}. \tag{2.63}$$

$$V(\mathbf{q}, \omega) = V_i(\mathbf{q}, \omega) + V_s(\mathbf{q}, \omega). \tag{2.64}$$

$$V_s(\mathbf{q}, \omega) = \frac{4\pi e^2}{q^2} \rho_s(\mathbf{q}, \omega). \tag{2.65}$$

$$\langle \rho_s(\mathbf{q}, t) \rangle = \langle \rho(\mathbf{q}, t) \rangle = \langle \sum_{\mathbf{p}} c^{\dagger}_{\mathbf{p}+\mathbf{q},\sigma} c_{\mathbf{p},\sigma} \rangle = \rho(\mathbf{q}, \omega) e^{-i\omega t}. \tag{2.66}$$

where the subscript "s" denotes the screening and "i" the impurity. The result is

$$\begin{aligned} \epsilon_{RPA} &= 1 - v_{\mathbf{q}} P^{(1)}(\mathbf{q}, \omega), \\ P^{(1)}(\mathbf{q}, \omega) &= \frac{1}{V} \sum_{\mathbf{p},\sigma} \frac{n_F(\varepsilon_{\mathbf{p}}) - n_F(\varepsilon_{\mathbf{p}+\mathbf{q}})}{\varepsilon_{\mathbf{p}} - \varepsilon_{\mathbf{p}+\mathbf{q}} + \omega}. \end{aligned} \tag{2.67}$$

2.4 Density functional theory (DFT)

The density functional theory (DFT) is a kind of generalized Thomas-Fermi method. As in the Thomas-Fermi theory, the basic dynamical quantity is a single-particle density, yet whereas Thomas-Fermi theory is for a locally homogenous gas of electrons (fermions), the DFT is for an inhomogenous gas.

In Ref. [10] it has been demonstrated that all aspects of the electronic structure of a system in a nondegenerate ground state are completely determined by its density $\rho(\mathbf{r})$. In the simplest form of DFT, the energy of a system is viewed as a functional of the density $\rho(\mathbf{r})$ with the constraint

$$\int d\mathbf{r}\rho(\mathbf{r}) = N . \tag{2.68}$$

The energy is separated as

$$E[\rho] = K[\rho] + \int d\mathbf{r}\Phi(\mathbf{r})\rho(\mathbf{r}) + \frac{1}{2}\int d\mathbf{r}d\mathbf{r}'\frac{e^2\rho(\mathbf{r})\rho(\mathbf{r}')}{|\mathbf{r}-\mathbf{r}'|} + E_{xc}[\rho], \tag{2.69}$$

i.e., a kinetic energy for the electrons K, an interaction Φ of the electrons with the nucleus, an electron-electron potential interaction, and the exchange correlation energy E_{xc}. If we demand that the energy E be an extremum for variations of the density,

$$\delta E[\rho] = 0. \tag{2.70}$$

the DFT dynamical equations result. These equations are single-particle equations:

$$[-\frac{\hbar^2}{2m}\nabla^2 + U_{eff}(\mathbf{r})]\phi_a(\mathbf{r}) = \varepsilon_a\phi_a(\mathbf{r}). \tag{2.71}$$

which can be solved self-consistently together with

$$U_{eff}(\mathbf{r}) = U(\mathbf{r}) - U_{xc}(\mathbf{r}) \tag{2.72}$$

and

$$\rho(\mathbf{r}) = \sum_{a=1}^{N} |\phi_a(\mathbf{r})|^2 . \tag{2.73}$$

Here the sum is over the N lowest occupied eigenstates. U is the total classical potential energy

$$U(\mathbf{r}) = \Phi(\mathbf{r}) + \int d\mathbf{r}' \frac{e^2\rho(\mathbf{r}')}{|\mathbf{r} - \mathbf{r}'|}. \tag{2.74}$$

and $U_{xc}(\mathbf{r})$ is the exchange correlation potential. which can be calculated by a functional derivative of the exchange correlation energy

$$U_{xc}(\mathbf{r}) = \frac{\delta E_{xc}[\rho(\mathbf{r})]}{\delta\rho(\mathbf{r})}. \tag{2.75}$$

The functional E_{xc} is expressed in terms of another (unknown) functional g

$$E_{xc}[\rho] = \int d\mathbf{r}\{g[\rho(\mathbf{r})] - K[\rho(\mathbf{r})]\}. \tag{2.76}$$

where g contains the kinetic, exchange, and correlation energy parts.

Sometimes the unknown functional $g[\rho]$ or $E_{xc}[\rho]$ can be approximated in the following ways [10].

(a) Approximations for the functional $g[\rho]$. If the density is slightly inhomogeneous

$$\rho(\mathbf{r}) \approx \rho_0 + \Delta\rho(\mathbf{r}). \tag{2.77}$$

then g is given by a power series in the inhomogeneity

$$g[\rho] \approx g[\rho_0] + \int d\mathbf{r}'\kappa(|\mathbf{r} - \mathbf{r}'|)\Delta\rho(\mathbf{r})\Delta\rho(\mathbf{r}'). \tag{2.78}$$

The kernel κ is expanded as a Fourier series in the momentum transfer dependence of the dielectric constant ϵ of a homogeneous electron gas

$$\kappa(\mathbf{r} - \mathbf{r}') = \frac{1}{V}\sum_{\mathbf{q}} \frac{2\pi e^{-i\mathbf{q}\cdot(\mathbf{r}-\mathbf{r}')}}{q^2[\epsilon(\mathbf{q}) - 1]}. \tag{2.79}$$

(b) Approximation for the Exchange-Correlation Energy $E_{xc}[\rho]$.

(a) The local density approximation (LDA): For a system with slowly varying density, we make the LDA

$$E_{xc}[\rho] = \int d\mathbf{r}\rho(\mathbf{r})\varepsilon_{xc}(\rho(\mathbf{r})). \tag{2.80}$$

where ε_{xc} is the exchange and correlation energy per particle of an electron gas of density $\rho(\mathbf{r})$. In the LDA,

$$U_{xc}(\mathbf{r}) = \frac{d}{d\rho}[\rho(\mathbf{r})\varepsilon_{xc}] \equiv \mu_{xc}(\rho(\mathbf{r})). \tag{2.81}$$

where $\mu_{xc}(\rho(\mathbf{r}))$ is the exchange and correlation contribution to the chemical potential of a uniform system.

(3) Gradient Correction to $E_{xc}[\rho]$: Including the lowest-order gradient correction. $E_{xc}[\rho]$ has the form

$$E_{xc}[\rho] = \int d\mathbf{r}\rho(\mathbf{r})\varepsilon_{xc}(\rho(\mathbf{r})) + \int d\mathbf{r}B_{xc}(\rho(\mathbf{r}))|\nabla\rho(\mathbf{r})|^2 \ .$$

The function $B_{xc}(\rho)$ has been calculated in the RPA[61,62].

(4) Approach to E_{xc} via the Exchange-Correlation Hole: It can be shown [63] that the exchange-correlation energy is given exactly by the expression

$$E_{xc}[\rho] = \frac{1}{2}\int d\mathbf{r}_1 d\mathbf{r}_2 \frac{1}{|\mathbf{r}_1 - \mathbf{r}_2|}\rho(\mathbf{r}_1)H(\mathbf{r}_1, \mathbf{r}_2)\rho(\mathbf{r}_2) \ . \tag{2.82}$$

or

$$E_{xc}[\rho] = \frac{1}{2}\int d\mathbf{r}_1 d\mathbf{r}_2 \frac{1}{|\mathbf{r}_1 - \mathbf{r}_2|}\rho(\mathbf{r}_1)N_{xc}(\mathbf{r}_1, \mathbf{r}_2) \ . \tag{2.83}$$

where $N_{xc}(\mathbf{r}_1, \mathbf{r}_2) = H(\mathbf{r}_1, \mathbf{r}_2)\rho(\mathbf{r}_2)$ is the average exchange-correlation hole density satisfying the perfect screening sum rule

$$\int d\mathbf{r}_2 N_{xc}(\mathbf{r}_1, \mathbf{r}_2) = -1$$

and

$$H(\mathbf{r}_1, \mathbf{r}_2) \equiv \int_0^1 d\lambda h_\lambda(\mathbf{r}_1, \mathbf{r}_2), \quad h_\lambda(\mathbf{r}_1, \mathbf{r}_2) \equiv g_\lambda(\mathbf{r}_1, \mathbf{r}_2) - 1 \ .$$

The pair correlation function $g(\mathbf{r}_1, \mathbf{r}_2)$ is the probability of finding a pair of electrons at points $\mathbf{r}_1$ and $\mathbf{r}_2$ and $g_\lambda(\mathbf{r}_1, \mathbf{r}_2)$ is defined as

$$\rho(\mathbf{r}_1)g_\lambda(\mathbf{r}_1, \mathbf{r}_2)\rho(\mathbf{r}_2) = \{\langle\hat{\rho}(\mathbf{r}_1)\hat{\rho}(\mathbf{r}_2)\rangle_\lambda - \delta(\mathbf{r}_1 - \mathbf{r}_2)\rho(\mathbf{r}_1)\}. \tag{2.84}$$

with $\hat{\rho}(\mathbf{r})$ being the density operator.

Chapter 3

Screening theories for narrow QWs in strong magnetic fields

The above many-body techniques, except for local density approximation, cannot be used directly to QWs because the electrons there are not homogeneous in the transverse direction. However the basic ideas, such as single-electron approximation, linear screening theory, RPA, ect., still can be used. The following approaches are examples and are very useful in recent studies of electronic correlations.

3.1 Self-consistent screening theories (SCST)

SCST obtain the $U_{xc}(\mathbf{r})$ by replacing $U_{eff}(\mathbf{r})$ in Eqs. (2.71) and (2.72) with the

screened potential $V = V_b + V_s$ (b: background)[47,48], while V is the solution of Poisson's equation

$$\Delta V = -\frac{4\pi e^2}{\epsilon}(\rho_b + \rho_s); \tag{3.1}$$

Then Eq. (2.71) becomes

$$[\frac{\mathbf{p}^2}{2m} + V(\mathbf{r})]\phi_a(\mathbf{r}) = \varepsilon_a \phi_a(\mathbf{r}). \tag{3.2}$$

with $\rho_s(\mathbf{r})$ obtained from the eigenfunction and the occupation function $f(\varepsilon_a - \mu)$ by [18]

$$\rho_s(\mathbf{r}) = g\sum_a f(\varepsilon_a - \mu)|\phi_a(\mathbf{r})|^2 \ . \tag{3.3}$$

where μ is the chemical potential and g the degeneracy factor. For the given ρ_b, Eqs. (3.1)-(3.3) should be solved self-consistently.

Consider a 2DEG in the (x, y) plane with a perpendicular magnetic field $\mathbf{B} = B\mathbf{e}_z$. In the Landau gauge $\mathbf{A} = (0, Bx, 0)$, $\mathbf{p}$ in Eq. (3.2) is simply changed to ($e < 0$ for electron)

$$\mathbf{p} \Rightarrow (\mathbf{p} - \frac{e}{c}\mathbf{A}) = -i\hbar\nabla - \frac{e}{c}Bx\mathbf{e}_y.$$

With periodic boundary conditions in the y direction the normalized eigenfunction can be written as $\phi_a(x, y, z) = \phi_a(x, z)e^{ik_y y}$, leading to the reduced Hamiltonian

$$H = -\frac{\hbar^2}{2m}\frac{\partial^2}{\partial x^2} - -\frac{\hbar^2}{2m_z}\frac{\partial^2}{\partial z^2} + \frac{1}{2}m\omega_c^2(x - x_0)^2 + V(\mathbf{r}) \qquad (m_x = m_y = m). \tag{3.4}$$

with $x_0 = -l^2 k_y$ and $\omega_c = |e|B/(mc)$.

SCST is also known as Screened Hartree Approximation-RPA (SHA-RPA) [65],[66] because the screened potential in Eq. (3.2) is just the equivalent local potential in the modified Hartree equation (2.4) and that the electron-electron interaction is averaged with a screened potential is the main idea used in the RPA.

Note that in the Eq. (3.2), the equivalent local potential should effectively represent the many-body effects. Therefore, before we use this equation we need to know if the electron-electron interactions in the system can be properly factorized into the form of $V(\mathbf{r})\rho(\mathbf{r})$. As mentioned in 2.2.3, this is not always guaranteed. There are many attempts at finding an equivalent local potential for the lower dimensional electronic systems. The recently developed SHFA for QWs is one of them. It will be discussed extensively in the following sections.

3.2 SHFA for QWs in strong magnetic fields

3.2.1 General idea

The general idea of the SHFA is to replace the Coulomb interaction $e^2/|\mathbf{r}-\mathbf{r}'|$ in the exchange potential $U^{-}(\mathbf{r},\mathbf{r}')$ of Eq. (2.10) with the screened potential $V^{-}(\mathbf{r},\mathbf{r}')$

$$\frac{\mathbf{p}^2}{2m}|i\rangle + \sum_{j,k}\langle k|\langle j|V^{-}(\mathbf{r},\mathbf{r}')|i\rangle|j\rangle|k\rangle = \varepsilon_i|i\rangle. \tag{3.5}$$

It should be noted that now the state $|\alpha\rangle(\alpha = i,j,k)$ does not have the pure plane wave form. To factorize the exchange term, we can neglect the end effects of the QW and assume that the screening in QW does not change the electron homogeneity in the longitudinal (x) direction. Therefore, all electron states in this direction still have the plane wave form. This property guarantees that the exchange term in Eq. (3.5) can be written in the form of $V^{-}|i\rangle$ and Eq. (3.5) can be reduced to

$$\frac{\mathbf{p}^2}{2m}|i\rangle + \sum_{j}\langle i|\langle j|V^{-}(\mathbf{r},\mathbf{r}')|i\rangle|j\rangle|i\rangle = \varepsilon_i|i\rangle. \tag{3.6}$$

The screened potential can be obtained with the help of the Poisson equation.

$$\Delta V^{-}(\mathbf{r},\mathbf{r}') = -\frac{4\pi e^2}{\epsilon}\rho(\mathbf{r},\mathbf{r}'). \tag{3.7}$$

If we neglect the screening of the Coulomb interaction between two electrons, at $\mathbf{r}$ and $\mathbf{r}'$ respectively, then from Eq.(3.7) we have $\rho(\mathbf{r},\mathbf{r}') = \delta(\mathbf{r}-\mathbf{r}')$ and $V^{-}(\mathbf{r},\mathbf{r}') = e^2/|\mathbf{r}-\mathbf{r}'|$.

In the SHFA-RPA, $\rho(\mathbf{r}, \mathbf{r}')$ is obtained within the random phase approximation. For example, the Fourier component of $\rho(\mathbf{r})$ for a 3D homogeneous electron gas is given by Eq. (2.62).

$$\rho(\mathbf{q}, \omega) = \frac{V^{s}(\mathbf{q}, \omega)}{V^{s}} \sum_{\mathbf{p}, \sigma} \frac{n_F(\varepsilon_{\mathbf{p}}) - n_F(\varepsilon_{\mathbf{p}-\mathbf{q}})}{\varepsilon_{\mathbf{p}} - \varepsilon_{\mathbf{p}-\mathbf{q}} + \omega} . \tag{3.8}$$

where $V^{s}(\mathbf{q}, \omega)$ satisfies

$$V^{s}(\mathbf{r}, t) = \sum_{\mathbf{q}} V^{s}(\mathbf{q}, \omega) e^{-i\omega t} e^{i\mathbf{q}\cdot\mathbf{r}} \tag{3.9}$$

and $V^{s}(\mathbf{r}, t)$ is the total screened field. For QWs that are perpendicular to magnetic fields, detailed discussions are given below.

3.2.2 Eigenvalues and eigenstates without many-body effects

To better understand the screened Coulomb interaction in QWs, we first consider the basic QW characteristics without many-body effects, or within Hartree approximation. Suppose a 2DEG is confined in a narrow channel, in the (x, y) plane of width $L_y = W$ and of length $L_x = L$. For simplicity we will neglect its thickness d ($d \to 0$). Within Hartree approximation, the bare confining potential for $y \leq W$ can be written in the form of $V_y = m^*\Omega^2 y^2/2$,[67]-[69] where m^* is the effective mass. In the $y > W$ region, the confining potential increases sharply. For narrow QWs, we can approximately take $V_y = V_0 \gg m^*\Omega^2 W^2/8$.[46]. Here V_0 depends on the bias voltage of the split gate technique[49],[70]-[71], or the surface charge distribution of the mesa etching technique[72]-[85]. When a strong magnetic field is applied along the z direction in the Landau gauge for the vector potential $\mathbf{A} = (-By, 0, 0)$ the one-electron Hamiltonian h^0 is given by

$$h^0 = [(p_x + \frac{eBy}{c})^2 + p_y^2]/(2m^*) + V_y + g_0\mu_B s_z B/2 \tag{3.10}$$

where $\mathbf{p}$ is the momentum operator, $e(< 0)$ the electron, g_0 the bare Lande g-factor and μ_B the Bohr magneton. s_z is the z-component of spin operator with eigenvalues $\sigma = 1$ and $\sigma = -1$ for spin up and down, respectively.

For the system that is homogenous in x direction, we can take the eigenfunction of Eq. (3.10) in the form $\langle x, y|\alpha\rangle = e^{ik_x x}\chi_\alpha(y)|\sigma\rangle$. Setting $\omega_c = |e|B/(cm^*)$, $\xi =$

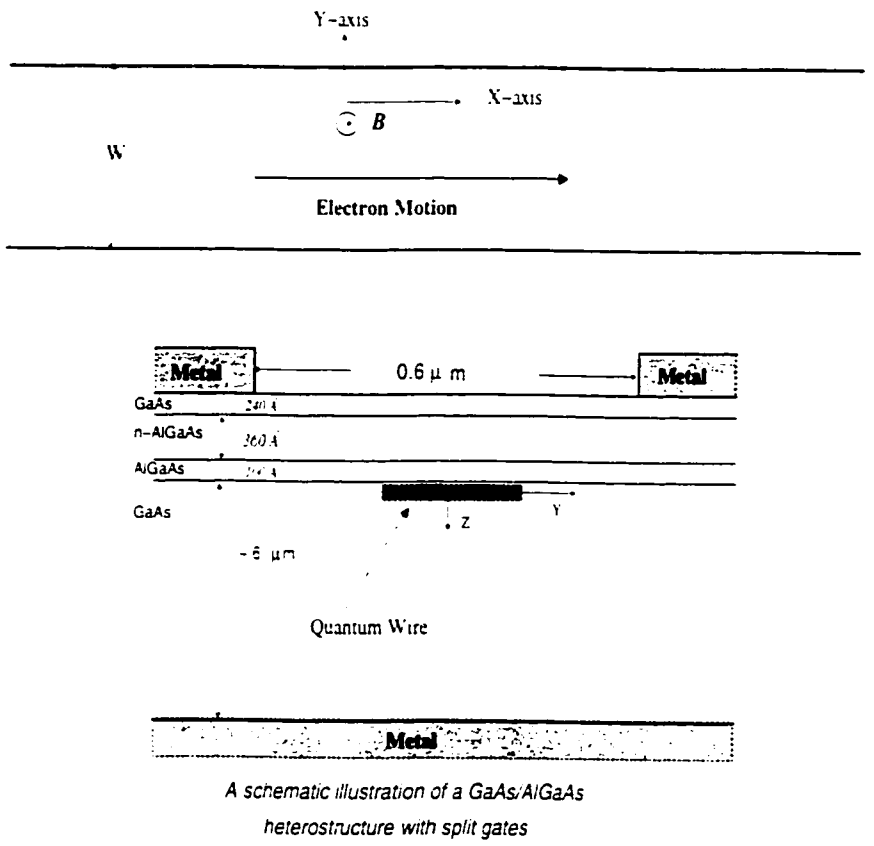

Figure 3.1: A quantum wire is a qusi-1DEG system where electrons are constrained to move in one direction. It can be realized in a semi-conductor device by using the split gate technique.

$(\omega_c^2 + \Omega^2)^{\frac{1}{2}}$, $\tilde{m} = m^*\tilde{\omega}^2/\Omega^2$, $y_0(k_x) = \hbar k_x \omega_c/(m^*\tilde{\omega}^2)$, one can rewrite Eq. (3.10) as

$$\begin{aligned} h^0 &= \frac{(\hbar k_x - m^*\omega_c y)^2}{2m^*} + \frac{p_y^2}{2m^*} - \frac{1}{2}m^*\Omega^2 y^2 + g_0\mu_B s_z B/2 \\ &= \frac{p_y^2}{2m^*} + \frac{1}{2}m^*\tilde{\omega}^2[y - y_0(k_x)]^2 + \frac{\hbar^2 k_x^2}{2\tilde{m}} - g_0\mu_B s_z B/2 . \end{aligned} \tag{3.11}$$

This form of the Hamiltonian gives basic channel properties of QW, i.e., the electron moves freely in the longitudinal direction and behaves like a harmonic oscillator centered at the position $y = y_0$, with frequency $\tilde{\omega}$. Note that the oscillation center y_0 is proportional to the wavenumber in the x direction (k_x). Therefore, electrons centered near the middle of the channel always have small k_x and those near the edge of the QW always have larger k_x . The eigenvalues are

$$\varepsilon_\alpha \equiv \varepsilon_{n,k_x,\sigma} = \hbar\tilde{\omega}(n + 1/2) + \hbar^2 k_x^2/(2\tilde{m}) + g_0\mu_B\sigma B/2. \tag{3.12}$$

with n the index of the magnetic subband (or Landau level). The normalized eigenstates in the position representation are

$$\langle x, y|\alpha\rangle \equiv \langle x, y|nk_x\rangle|\sigma\rangle = e^{ik_z z}\Phi_n(y - y_0(k_x))|\sigma\rangle/\sqrt{L}. \tag{3.13}$$

Here $\Phi_n(y)$ is a harmonic oscillator function and $|\sigma\rangle$ is the spin state vector satisfying $\langle\sigma_1|\sigma_2\rangle = \delta_{\sigma_1\sigma_2}$. For the calculation that follows we need the matrix elements[48], [35], [52]

$$\begin{aligned} \langle n'k_x'|e^{i\mathbf{q}\cdot\mathbf{r}}|nk_x\rangle &= \int d\mathbf{r} e^{-ik_z' z}\Phi_{n'}^*(y, k_x')\Phi_n(y, k_x)e^{ik_z z}e^{i\mathbf{q}\cdot\mathbf{r}}/L \\ &= \delta_{q_z - k_z - k_z', 0}\int dy \Phi_{n'}^*(y, k_x')\Phi_n(y, k_x)e^{iq_y y} \quad (L \to \infty) \end{aligned}$$

$$
\begin{aligned}
&\equiv \delta_{q_x+k_-,0}\langle n'k'_x|e^{iq_y y}|nk_x\rangle \\
&= \left(\frac{n'!}{n!}\right)^{1/2}\left(\frac{a(k'_x-k_x)+iq_y}{\sqrt{2}/\tilde{l}}\right)^{n-n'} e^{\frac{-u}{2}} L_{n'}^{n-n'}(u) e^{\frac{iaq_y k_- \tilde{l}^2}{2}}. \ (n > n') \\
&= \left(\frac{n!}{n'!}\right)^{1/2}\left(\frac{a(k_x-k'_x)+iq_y}{\sqrt{2}/\tilde{l}}\right)^{n'-n} e^{\frac{-u}{2}} L_{n}^{n'-n}(u) e^{\frac{iaq_y k_- \tilde{l}^2}{2}}. \ (n' > n)
\end{aligned}
\tag{3.14}
$$

with $u = [a^2(k'_x - k_x)^2 + q_y^2]\tilde{l}^2/2$ and $k_- = k'_x + k_x$. The magnetic length $\tilde{l}$ is independent of the specific material. cf. Eqs.(3.17). For the Laguerre polynomials $L_n^m(x)$. which can be calculated by $L_n^m(x) = (1/n!)e^x x^{-m}(d^n/dx^n)[e^{-x}x^{n-m}]$. we have relation $L_0^m(x) = 1$. Physically. the above matrix element refers to the transition in which the electron in state $|n, k_x\rangle$ are scattered into state $|n', k'_x\rangle$ by the potential $e^{i\mathbf{q}\cdot\mathbf{r}}$. Due to the plane wave form of the eigenfunction in the x direction. k_x and k'_x should have relation

$$
q_x + k_- = 0 \tag{3.15}
$$

which means the electron with initial momentum $k_x\hbar$ in the x direction absorbs q_x from the Coulomb field and change its moment to $k'_x\hbar = (k_x + q_x)\hbar$. In the other words. the transition in the x direction should satisfy the momentum conservation given by Eq.(3.15). In the y direction. the factor $e^{-u/2}$ means that the transition mainly happens within the region of $u < 1$. Beyond this region. the probability of transition is very small. This makes it possible for us to simplify the study of screened field $V^s(q_x, q_y, q'_y)$ by paying more attention to its behavior in the region within $\tilde{q} < 1$ and $\tilde{q}' < 1$ $[\tilde{q}^2 = (q_x^2 + q_y^2)\tilde{l}^2,\ \tilde{q}'^2 = (q_x^2 + q_y'^2)\tilde{l}^2]$. The phase shift

factor in Eq. (3.14) is caused by the overlap between a displaced Fock state and an excited coherent state[38]. It leads to the oscillation of the screened fields in their momentum space.

3.2.3 Bare magnetic length and group velocity in Hartree Approximation

To have a pictorial description of the bare magnetic length l_0, the eigenvalue and eigenfunctions given in the previous section, let us follow the semiclassical approach. At first, we consider the case of a free electron in a magnetic field. Classically, it goes round in a circular orbit due to the Lorentz force. The electron can have any speed $|\mathbf{v}|$ and moves in a circular path of any radius r_0. Quantum mechanically, however, the circumference must be an integer number (n) of de Broglie wavelengths ($\lambda = h/p$):

$$2\pi r_c = n\hbar/(m^* v), \tag{3.16}$$

with different n corresponding to different electron energy levels given by Eq.(3.12). Eq. (3.16) can also be written as

$$r_c = \sqrt{\frac{n\hbar}{m^*\omega_c}} = \sqrt{\frac{n\hbar c}{|e|B}} = \sqrt{n} l_0, \tag{3.17}$$

which means that l_0 represent the minimum radius of the electron orbit. (For $B \approx 10T$, $l_0 \approx 80nm$.) In other words, the area occupied by an electron in ground

state is around πl_0^2. Next, we consider a QW, with a parabolic confining potential, in the same magnetic field. Within the Landau gauge, the electron will behave as if there is only an equivalent magnetic field, with $B_{eq} > B$, except that the center of the electron should be located at certain place (y_0). Assuming that this electron has momentum $p = k_x\hbar$ in the x direction, we can imagine that the electron moves back and forth in the y direction with frequency $\tilde{\omega} = \sqrt{\omega_c^2 + \Omega^2}$. Such harmonic movement center is related to k_x by $y_0 = l_0^2 k_x$. At the same time, this electron has a group velocity in the x direction.

$$\begin{aligned} v_g^{HA}(k_x) &= \hbar^{-1}\frac{\partial \epsilon_{n,k_x,\sigma}}{\partial k_x} \\ &= \frac{\hbar k_x}{\tilde{m}} \approx \frac{\hbar k_x}{m^*}(\frac{\Omega}{\omega})^2 = \tilde{l}^2\Omega^2 k_x/\omega_c \quad (\omega_c >> \Omega) \end{aligned} \tag{3.18}$$

Here, v_g^{HA} refers to the group velocity in the Hartree approximation because $\epsilon_{n,k_x,\sigma}$ used in (3.18) is the Landau level energy given by (3.12), which neglects the many-body effects. Note that the group velocity, $\hbar k_x/\tilde{m}$, is much smaller than that of the free electron having the same k_x. This is because of the transverse effects due to the magnetic field and the confining potential.

3.2.4 Edge states, the integral filling factor, and the Fermi wavenumber

Edge states are the electronic states centered near the edges of the qusi-2D electronic system. Note that, such edges are not necessarily located at the boundary

of the QW. Strictly speaking, the distance between them depends on the magnetic field B, the gate voltage (of the split gate technique) or the surface charge distributions (of the mesa etching technique), the overall electron distribution in the QW, and so on. For a QW with fixed gate voltage (or the surface charge distribution), we only concern ourselves with the cases where the external magnetic fields B are adjusted so that some Landau levels, e.g., $n = 0, 1$, are fully occupied. Therefore the outermost edge of each occupied subband is almost located at the boundary of the QW. Here we neglect the effect of the overall electron distribution on the location of edges, for it has been shown that[49], [35] such electron distribution is primarily determined by the large electrostatic energy. Also, for the submicron width QWs having rather steep confining potentials, the dispersion of edge states corresponding to lower subbands does not[49] exhibit the flattening suggeted by ref. [42]. To simplify the following calculation, we neglect such flattening of the edge state due to the dipolar distribution in the vicinity of the Fermi level[42], [51]. (We will confirm this in sections discussing the Fermi edge group velocities v_g^{ec}.) Therefore, in our models, the filling factor ν is approximated as a constant integral in the whole $|y| \leq W/2$ region and the center of each harmonic state is equidistant in the y direction.

To see the meaning of the filling factor, we consider a QW with fixed width W. As discussed in the previous section, the center of the harmonic oscillator

$y_0 = \hbar k_x/(m^* \tilde{\omega}^2) \approx \tilde{l}^2 k_x$ ($\tilde{l} = \sqrt{\hbar/(m * \tilde{\omega})}$, $\omega_c >> \Omega$) satisfies

$$0 \leq y_0 \leq W. \tag{3.19}$$

which is equivalent to

$$0 \leq k_x \leq \frac{W}{\tilde{l}^2} \tag{3.20}$$

Using periodic boundary condition along x gives $k_x = 2\pi p/L$, where p is the integral. We can rewrite Eq.(3.20) as

$$0 \leq p \leq \frac{WL}{2\pi\tilde{l}^2} = \frac{S}{2\pi\tilde{l}^2}. \tag{3.21}$$

where S is the area of the channel. The above equation means that the maximum number of k_x states (or occupied electrons) is $N = S/2\pi\tilde{l}^2$ with spin up or down. Therefore, for a given magnetic subband, or LL, the the maximum electron density is $N/S = 1/(2\pi\tilde{l}^2)$, or the area occupied by each electron is the order of $2\pi\tilde{l}^2$. The integral quantum Hall effect states refers to the case where the total electron state density in the channel is the integral ν times $1/(2\pi\tilde{l}^2)$:

$$n_s = \nu\frac{1}{2\pi l_0^2} = \nu\frac{|e|B}{2\pi\hbar c}. \tag{3.22}$$

where ν is named as the filling factor. For example, in the $\nu = 1$ QHE regime, there is only one electron in each area of $2\pi\tilde{l}^2$ and all states at the lowest LL ($n = 1$, spin up) are occupied. Similarly, $\nu = 2$ means that there are two electrons in each area of $2\pi\tilde{l}^2$ and the $n = 1$ LL is fully occupied by the spin up and down electrons.

For a given QW, the total electron number or the total electron density should be fixed. Thus Eq.(3.22) leads to

$$\nu B = constant. \tag{3.23}$$

which means that, the stronger the magnetic field B, the lower ν the QHE state.

When a LL is fully occupied, its Fermi wavelength can be obtained from Eq.(3.20)

$$k_F = \frac{W}{2\tilde{l}^2}.$$

or

$$\tilde{k}_F = \frac{W}{2\tilde{l}} = \frac{W\sqrt{|e|B}}{2\sqrt{\hbar c}}. \tag{3.24}$$

which depends on the width of the QW and the intensity of the B field. Therefore, if we have $\nu = 1$ with field $B = B_1$ and $\tilde{k}_{F1} \equiv \tilde{k}_F = 15$, then we have $B_2 = B_1/2$, $B_3 = B_1/3$, cf. Eq.(3.22) and $\tilde{k}_{F2} = 15/\sqrt{2}$, $\tilde{k}_{F3} = 15/\sqrt{3}$ for $\nu = 2, 3$.

3.2.5 Two-dimentional Poisson equation

In previous sections, the electron properties are discussed within the Hartree approximation. To investigate the screened Coulomb interactions in QWs, we need to use the SHFA which consists of the 2D-Poisson equation. Actually, it can be obtained from the 3D cases. In real QW samples, the 3D solution

$$\phi(\mathbf{r}) = \mathbf{e}\int \mathbf{dr}' \frac{\rho(\mathbf{x}', \mathbf{y}')\delta(\mathbf{z}')}{\epsilon|\mathbf{r} - \mathbf{r}'|} \tag{3.25}$$

of the Poisson equation in a medium with the background dielectric constant ϵ (around 12.5 in GaAs) determines the potential energy $V(x, y) = eo(x, y, 0)$ of the 2D electrons

$$V(\mathbf{R}) = \mathbf{e}^2 \int \mathbf{dR}' \frac{\rho(\mathbf{x}', \mathbf{y}')}{\epsilon|\mathbf{R} - \mathbf{R}'|} \tag{3.26}$$

Taking 2D Fourier transformations, we have

$$V(\mathbf{q}) = \frac{\mathbf{2\pi e^2}}{\mathbf{q}\epsilon}\rho_{\mathbf{q}}. \tag{3.27}$$

where ρ_q is the Fourier component of $\rho(R)$. Its classical form is given in subsection 2.3.3. To get the above equation we need to notice that the 3D Fourier spectrum of the Coulomb potential is $4\pi/q^2$, but the 2D one is $2\pi/q$ or

$$\frac{1}{|\mathbf{R} - \mathbf{R}'|} = \int d\mathbf{q} \frac{\mathbf{2\pi}}{\mathbf{q}} \mathbf{e}^{\mathbf{iq}(\mathbf{R}-\mathbf{R}')}. \tag{3.28}$$

where the following relations are used [74].

$$\int_0^\pi \sin(z\cos x)dx = 0, \quad \int_0^\pi \cos(z\cos x)dx = \pi J_0(z).$$
$$\int_0^\infty e^{-\alpha x}\cosh \beta x J_0(\gamma x)dx = (\alpha\beta)^{1/2}\frac{1}{r_1 r_2}\sqrt{\frac{r_2 + r_1}{r_2 - r_1}}. \tag{3.29}$$

with $r_1^2 = \gamma^2 + (\beta - \alpha)^2$ and $r_2^2 = \gamma^2 + (\beta + \alpha)^2$.

3.2.6 Exchange and correlation in QWs: formulation for $\nu = 1$

Now we consider the exchange contribution in the HF equation (3.6). Using the first order perturbation theory, when the $(n = 0, \sigma = -1)$ LL is empty, one can approximately obtain the exchange term (Note: $\mathbf{R} = (x, y)$; $\mathbf{r} = (x, y, z)$)

$$exchange\ term \approx \sum_{jl} \langle 0, k_l | \langle 0, k_j | V^s(\mathbf{R}, \mathbf{R}') | 0, k_l \rangle | 0, k_j \rangle \langle \mathbf{R} | 0, k_l \rangle \tag{3.30}$$

and the exchange-correlation contribution $\epsilon^{ec}_{0,k_x,1}$ to the single-particle energy

$$\varepsilon^{ec}_{0,k_x,1} \approx -\sum_{k'_x} \langle 0k_x | \langle 0k'_x | V^s(\mathbf{R}, \mathbf{R}') | 0k_x \rangle | 0k'_x \rangle \ . \tag{3.31}$$

Formula (3.31) is similar to the exchange energy expressed in Eq. (2.14), which is an exact expression for a 3D homogeneous electron gas. Note that screened Coulomb interaction $V^s(\mathbf{R}, \mathbf{R}')$ in Eq. (3.31) cannot be simply written in the form $V^s(|\mathbf{R} - \mathbf{R}'|)$ because of the edges of the wire. But, as it has the translational invariance in the x direction, we still have

$$V^s(x - x'; y, y') = \frac{1}{(2\pi)^3} \int_{-\infty}^{\infty} dq_x dq_y dq'_y e^{iq_x(x-x') + iq_y y + iq'_y y'} V^s(q_x, q_y, q'_y) \tag{3.32}$$

Substituting Eq. (3.32) into Eq. (3.31) leads to

$$\begin{aligned} \varepsilon^{ec}_{0,k_x,1} &\approx -\frac{1}{(2\pi)^3} \int_{-\infty}^{\infty} dq_x dq_y dq'_y V^s(q_x, q_y, q'_y) \sum_{k'_x} \langle 0k_x | \langle 0k'_x | e^{i\mathbf{q}\cdot\mathbf{r} + i\mathbf{q}'\cdot\mathbf{r}'} | 0k_x \rangle | 0k'_x \rangle |_{q'_x = -q_x} \\ &= -\frac{1}{(2\pi)^3} \int dk'_x dq_y dq'_y V^s(k_x - k'_x, q_y, q'_y) (0k_x | e^{iq_y y} | 0k'_x) (0k'_x | e^{iq'_y y} | 0k_x) \end{aligned} \tag{3.33}$$

In the above expression. $V^s(k_x - k'_x, q_y, q'_y)$ is the screened Coulomb interaction between the charge distribution having Fourier index (q_x, q_y) and (q'_x, q'_y). The momentum conservation in the x direction requires that $q_x = -q'_x = k_x - k'_x$. where k_x and k'_x are the state index of the related electrons. The expression of $V^s(k_x - k'_x, q_y, q'_y)(0, k_x|e^{iq_y y}|0, k'_x)(0, k'_x|e^{iq'_y y}|0, k_x)$ represents the exchange-correlation energy due to screened Coulomb interaction. The integration over q_y and q'_y ($\int dq_y dq'_y ...$) means the exchange-correlation energy between electrons with (k_x, y) and (k'_x, y'). If we neglect the screening of the Coulomb interaction between two electrons. located at (x, y) and (x', y') by all other electrons in the QW. then Eq. (3.31) will give the exchange energy of the ground state $\varepsilon^{ex}_{0,k_x,1}$.

The screened Coulomb interaction $V^s(q_x, q_y, q'_y) = e\phi(q_x, q_y, q'_y)$ can be replaced by the Fourier transform of the solution of Poisson's equation

$$\phi(\mathbf{R}) = \frac{e}{\epsilon}\int d\mathbf{R}'\frac{1}{|\mathbf{R}-\mathbf{R}'|}\rho(\mathbf{R}'). \tag{3.34}$$

To do this, let us consider the statistical screened potential $\phi(x, y; x', y')$ of an electron charge at (x', y') with $\omega = 0$. $e\delta(\mathbf{R}-\mathbf{R}') = e\sum_{\mathbf{q}} e^{i\mathbf{q}\cdot\mathbf{R}-\mathbf{R}'}$. The 2D-Fourier transform $\phi(q_x, q_y; x', y')$ of $\phi(x, y; x', y')$ obeys Poisson's equation[18]

$$\phi(q_x, q_y; x_0, y_0) = \frac{2\pi e}{q\epsilon}[(\rho_i)_q + (\rho_s)_q], \tag{3.35}$$

where $e(\rho_i)_q = ee^{-i\mathbf{q}\cdot\mathbf{R}'}$ is the Fourier transform of the external charge density. The qth Fourier component of the screening charge density, $e(\rho_s)_{\mathbf{q}}$, can be related to

$e\rho_s$ with formula [2]:

$$(\rho_s)_{\mathbf{q}} = Tr\{\rho_s e^{-i\mathbf{q}\cdot\mathbf{R}}\}$$
$$= \sum_{n_\alpha, n_\beta, k_{x\alpha}, k_{x\beta}} \langle n_\alpha, k_{x_\alpha}|e^{-i\mathbf{q}\cdot\mathbf{R}}|n_\beta, k_{x_\beta}\rangle\langle n_\beta, k_{x_\beta}|\rho_s|n_\alpha, k_{x_\alpha}\rangle. \tag{3.36}$$

The matrix elements $\langle n_\beta, k_{x_\beta}|\rho_s|n_\alpha, k_{x_\alpha}\rangle$ can be related to $V^s = e\phi(q_x, q_y; x', y')$ within the RPA as follows: in the static limit ($\omega = 0$), the density matrix, $\rho = \rho_0 + \rho_s$, which obeys

$$i\hbar\dot{\rho}_0 = [h^0, \rho_0], \quad i\hbar\dot{\rho} = [H, \rho] \quad (H = h^0 + V^s). \tag{3.37}$$

satisfies

$$[h^0, \rho_s]|n_\alpha, k_{x_\alpha}\rangle + [V^s, \rho_0]|n_\alpha, k_{x_\alpha}\rangle \approx 0 \tag{3.38}$$

where $\rho_0|n, k_x\rangle = f^0(n, k_x)|n, k_x\rangle$ ($f^0(n, k_x) \equiv f_{n,k_x} = 1/[1 + e^{(\epsilon_{n,k_x} - E_F)/kT}]$), and the approximation $[V^s, \rho_s] \approx 0$ is used. Then, from Eq. (3.38), one can find the matrix elements between two states $|n_\alpha, k_{x_\alpha}\rangle$ and $|n_\beta, k_{x_\beta}\rangle$:

$$(\varepsilon_{n_\beta,k_{x_\beta},1} - \varepsilon_{n_\alpha,k_{x_\alpha},1})\langle n_\beta, k_{x_\beta}|\rho_s|n_\alpha, k_{x_\alpha}\rangle = (f_{n_\beta,k_{x_\beta}} - f_{n_\alpha,k_{x_\alpha}})\langle n_\beta, k_{x_\beta}|V^s|n_\alpha, k_{x_\alpha}\rangle \tag{3.39}$$

or

$$\langle n_\beta, k_{x_\beta}|\rho_s|n_\alpha, k_{x_\alpha}\rangle = \frac{f_{n_\beta,k_{x_\beta}} - f_{n_\alpha,k_{x_\alpha}}}{\varepsilon_{n_\beta,k_{x_\beta},1} - \varepsilon_{n_\alpha,k_{x_\alpha},1}}\langle n_\beta, k_{x_\beta}|V^s|n_\alpha, k_{x_\alpha}\rangle$$

$$
\begin{aligned}
&\equiv \frac{f_\beta - f_\alpha}{\varepsilon_\beta - \varepsilon_\alpha}\langle n_\beta, k_{x\beta}|V^{rs}|n_\alpha, k_{x\alpha}\rangle \\
&= F_{\beta,\alpha}\int \frac{dq_{1y}}{2\pi L} V^{rs}(k_{x\beta} - k_{x\alpha}, q_{1y}, x', y')(n_\beta k_{x\beta}|e^{iq_{1y}y}|n_\alpha k_{x\alpha}) .
\end{aligned}
\tag{3.40}
$$

where $F_{\beta,\alpha} = (f_\beta - f_\alpha)/(\varepsilon_\beta - \varepsilon_\alpha)$ and the Fourier transform of $V^{rs}(\mathbf{R}, \mathbf{R}')$

$$
V^{rs}(\mathbf{R}, \mathbf{R}') = \int \frac{dq_{1y}dq_{1x}}{(2\pi)^2} V^{rs}(q_{1x}, q_{1y}, x', y')e^{iq_{1x}x - iq_{1y}y} \tag{3.41}
$$

has been used. Substituting Eqs. (3.40) and (3.36) into Eq. (3.35), we get the integral equation:

$$
\begin{aligned}
o(q_x, q_y, x', y') &= \frac{2\pi e}{q\epsilon}\{e^{-i\mathbf{q}\cdot\mathbf{R}'} + \frac{e}{2\pi L}\sum_{n_\alpha, n_\beta}\sum_{k_{x\alpha}} F_{\alpha,\beta}\int_{-\infty}^{\infty} dq_{1y}\ \ o(q_x, q_{1y}, x', y') \\
&\times (n_\beta, k_{x\beta}|e^{iq_{1y}y}|n_\alpha, k_{x\alpha})(n_\alpha, k_{x\alpha}|e^{-iq_y y}|n_\beta, k_{x\beta})\}_{k_{x\beta}=k_{x\alpha}-q_x}
\end{aligned}
\tag{3.42}
$$

which is the same as the integral equation (11) in Ref. [35] if we make replacement $(n_\alpha, k_{x\alpha}) \leftrightarrow (n_\beta, k_{x\beta})$. Due to the spatial homogeneity of the system along the x axis, we look for solutions of Eq.(3.42) in the form $o(q_x, q_y, x', y') = o(q_x, q_y, y')e^{iq_x x'}$. Then $o(q_x, q_y, y')$ obeys Eq.(3.42) if we change $o(q_x, q_y, x', y')$ to $o(q_x, q_y, y')$ and $e^{-i\mathbf{q}\cdot\mathbf{R}'}$ to $e^{-iq_y y'}$. Taking the Fourier transform with respect to y' of this equation for $o(q_x, q_y, y')$, we finally get the Poisson-RPA integral equation

$$
\begin{aligned}
o(q_x, q_y, q_y') &= \frac{2\pi e}{q\epsilon}\{2\pi\delta(q_y + q_y') + \frac{e}{2\pi L}\sum_{n_\alpha, n_\beta}\sum_{k_{x\alpha}} F_{\alpha,\beta}\int_{-\infty}^{\infty} dq_{1y} o(q_x, q_{1y}, q_y') \\
&\times (n_\alpha, k_{x\alpha}|e^{iq_{1y}y}|n_\beta, k_{x\beta})(n_\beta, k_{x\beta}|e^{-iq_y y}|n_\alpha, k_{x\alpha})\}|_{k_{x\beta}=k_{x\alpha}-q_x}.
\end{aligned}
\tag{3.43}
$$

[Note, the replacement $(n_\alpha, k_{x\alpha}) \leftrightarrow (n_\beta, k_{x\beta})$ has been used.] Equivalently, we may write

$$V^{xc}(q_x, q_y, q_y') = \frac{v_0\,\delta(q_y + q_y')}{q} + \frac{v_0}{8\pi^3 q}\int_{-\infty}^{\infty} dq_{y1}\, V^{xc}(q_x, q_{y1}, q_y')$$
$$\times \sum_{n_\alpha, n_\beta} \int dk_{x\alpha} F_{\alpha,\beta}(n_\alpha, k_{x\alpha}|e^{iq_{y1}y}|n_\beta, k_{x\alpha} - q_x)(n_\beta, k_{x\alpha} - q_x|e^{-iq_{y1}y}|n_\alpha, k_{x\alpha}). \tag{3.44}$$

where $v_0 = 4\pi^2 e^2/\epsilon$, $F_{\alpha,\beta} \equiv (f_{n_\alpha,k_{x\alpha}} - f_{n_\beta,k_{x\beta}})/(\varepsilon_{n_\alpha,k_{x\alpha}} - \varepsilon_{n_\beta,k_{x\beta}})$, and $q = \sqrt{q_x^2 + q_y^2}$.

Substituting the solution of Eq. (3.44) into Eq. (3.33), one can, in principle, calculate the exchange-correlation energies $\varepsilon^{ec}_{0,k_x,1}$ (in the ground state). Furthermore, the effective exchange-correlation potential V_{xc} can be related to the exchange-correlation energies by formula

$$V_{xc}(y) = \varepsilon^{ec}_{0,y\pm(l_0^2\omega_c),1} \tag{3.45}$$

with $l_0 = (\hbar/m^*\omega_c)$ being the bare magnetic length.

3.2.7 Exchange and correlation in QWs: formulation for $\nu \geq 1$

In the last subsection, we considered the simplest case $\nu = 1$, when only the lowest spin-polarized LL (n=0, $\sigma = 1$) is occupied and all other LLs are empty. For more complicated cases, e.g., for $\nu = 2$ (n=0, $\sigma = +1$ and -1), $\nu = 3$ (n=1, $\sigma = 1$), obtaining the form of the Poisson-RPA integral equation and the general expressions of exchange and correlation energies are more involved in this subsection. We proceed as follows.

Following the idea of Eq. (2.10) it is not difficult to see that the general expression of exchange and correlation energy can be written as

$$\varepsilon^{ec}_{n,k_x,\sigma_i} \approx - \sum_{n',k'_x,\sigma_j} \langle n, k_x, \sigma_i | \langle n', k'_x, \sigma_j | V^{rs}(\mathbf{R}, \mathbf{R}') | n, k_x, \sigma_i \rangle | n', k'_x, \sigma_j \rangle \tag{3.46}$$

Within the first-order perturbation theory, we can neglect the difference between real eigenstate $|0, k'_x, \sigma\rangle$ and the free electron eigenstate $|0, k'_x\rangle|\sigma\rangle$, and reduce the above formula to

$$\varepsilon^{ec}_{n,k_x,\sigma_i} \approx - \sum_{n',k'_x,\sigma_j} \langle n, k_x | \langle n', k'_x | V^{rs}(\mathbf{R}, \mathbf{R}') | n, k_x \rangle | n', k'_x \rangle \delta_{\sigma_i,\sigma_j}. \tag{3.47}$$

Eq. (3.47) can also be rewritten as

$$\varepsilon^{ec}_{n,k_x,\sigma} \approx \frac{-1}{8\pi^3} \sum_{n'} \int dk'_x dq_y dq'_y V^{rs}(k_x - k'_x, q_y, q'_y)(n, k_x | e^{iq_y y} | n', k'_x)(n', k'_x | e^{iq'_y y} | n, k_x), \tag{3.48}$$

where $V^s(k_-, q_y, q_y')$ obeys an equation similar to Eq. (3.44), except that the number $F_{\alpha,\beta}$ need to be changed to $F^{\sigma}_{\alpha,\beta}$ and the sum over σ is necessary:

$$V^s(q_x, q_y, q_y') = \frac{v_0\,\delta(q_y + q_y')}{q} + \frac{v_0}{8\pi^3 q}\int_{-\infty}^{\infty} dq_{y1} V^s(q_x, q_{y1}, q_y')$$
$$\times \sum_{n_\alpha, n_\beta}\sum_{\sigma=\pm 1}\int dk_{x\alpha} F^{\sigma}_{\alpha,\beta}(n_\alpha, k_{x\alpha}|e^{iq_y y}|n_\beta, k_{x\alpha} - q_x)(n_\beta, k_{x\alpha} - q_x|e^{-iq_y y}|n_\alpha, k_{x\alpha}). \tag{3.49}$$

with

$$F^{\sigma}_{\alpha,\beta} = \frac{f_{n_\beta, k_{x\beta}, \sigma} - f_{n_\alpha, k_{x\alpha}, \sigma}}{\varepsilon_{n_\beta, k_{x\beta}, \sigma} - \varepsilon_{n_\alpha, k_{x\alpha}, \sigma}}. \tag{3.50}$$

Note that, in the general case, the total screened charge in Eq. (3.36) consists of two parts:

$$(\rho_s)^{\sigma}_{\mathbf{q}} = \sum_{n_\alpha, n_\beta, k_{x\alpha}, k_{x\beta}} \langle n_\alpha, k_{x_\alpha}, \sigma|e^{-i\mathbf{q}\cdot\mathbf{R}}|n_\beta, k_{x_\beta}, \sigma\rangle\langle n_\beta, k_{x_\beta}, \sigma|\rho_s|n_\alpha, k_{x_\alpha}, \sigma\rangle$$
$$(\sigma = 1, 2) \tag{3.51}$$

The screened charge contributions from "cross" term due to different spin states is zero. We can see this either from Eq.(3.36) or Eq.(3.40), because in both formulas, no matrix element contains the spin operator.

When $\nu = 1$, Eq.(3.49) reduced to Eq.(3.44), because the linear response coefficients $F^{\sigma}_{\alpha,\beta}$ are all zero, except $F^{1}_{(0,n)}$ and $F^{1}_{(n,0)}$ (n=0,1,2,3...). For $\nu = 2$, all $F^{\sigma}_{\alpha,\beta}$ are zero, except $F^{\pm 1}_{(0,n)}$ and $F^{\pm 1}_{(n,0)}$ (n=0,1,2,3...). Similarly, for $\nu = 3$, we have $F^{\sigma}_{\alpha,\beta} = 0$, except $F^{\pm 1}_{(0,n)}, F^{\pm 1}_{(n,0)}, F^{1}_{(1,n)}$, and $F^{1}_{(n,1)}$ (n=0,1,2,3...).

If $F^{\uparrow}_{\alpha,\beta}F^{\downarrow}_{\alpha,\beta} \neq 0$, e.g., in the case of $\nu \geq 2$, we can neglect the energy difference due to Zeeman effect and simplify Eq.(3.49) using

$$F^{\uparrow}_{\alpha,\beta} \approx F^{\downarrow}_{\alpha,\beta} \approx F_{\alpha,\beta} \tag{3.52}$$

3.3 Screening theories for a 3DEG and for QWs

Generally, there are two kinds of approaches to calculate the exchange-correlation energies. One is based on approach using formula (2.51), which requires the knowledge of the dielectric functions of the systems. The other one is to solve the Hartree-Fock equations or similar approach such as the DFT, where the effective exchange and correlation potential need to be obtained from other methods, e.g., Poisson-RPA equations. The advantage of the first one is that formula (2.51) is a rigorous one and we can get more accurate results by improving the expressions of dielectric functions $\epsilon(\mathbf{q}, \omega)$, from the Lindhard model to the Hubbard model and to the Singwi-Sjolander model. However, such approaches can be applied only to homogeneous electron gases. When we deal with bounded inhomogeneous systems, because the relationships between $V^s(\mathbf{q}, \omega)$ and $\rho_{\mathbf{q}}$ are much more complicated, we usually resort to the second kind of approaches. To study the many-body interactions in bounded inhomogeneous systems, such as quantum wires, considerable efforts have been devoted[56] – [58]. Compared with other theories dealing with inhomogeneous electron systems, the screened Hartree-Fock approximation-RPA (SHF-RPA) is very efficient one. However, this approach is exact only in the high-density limit. For QWs with $r_s = 1/2Na^* > 3$, other approaches should be used[57]. The QWs discussed in this work have the effective Bohr radii $a^* \sim 10^{-6}$cm[58], with linear charge densities $N \sim 5 \times 10^6$ cm^{-1}. Therefore, for these QWs, we have $r_s \sim 0.1$.

Chapter 4

Screened fields & correlation energies in QWs : B⊥ (x,y) plane

4.1 $\nu = 1$

4.1.1 Approximate analytical solution of the integral equation

The exchange and correlation contribution to the single-particle energy, when only the lowest spin $\uparrow$ of the $n = 0$ LL is occupied, can be calculated according to formula (3.31)

$$\varepsilon^{ec}_{0,k_x,1} \approx -\frac{1}{(2\pi)^3}\int dk'_x dq_y dq'_y V^{\uparrow s}_1(k_x - k'_x, q_y, q'_y)(0k_x|e^{iq_y y}|0k'_x)(0k'_x|e^{iq'_y y}|0k_x)$$

(4.1)

and formula (3.44)

$$V_1^s(q_x, q_y, q_y') = \frac{v_0\,\delta(q_y + q_y')}{q} + \frac{v_0}{8\pi^3 q}\int_{-\infty}^{\infty} dq_{y1} V_1^s(q_x, q_{y1}, q_y')$$
$$\times \sum_{n_\alpha, n_\beta} \int dk_{x\alpha} F_{\alpha,\beta}(n_\alpha, k_{x\alpha}|e^{iq_{y1}y}|n_\beta, k_{x\alpha} - q_x)(n_\beta, k_{x\alpha} - q_x|e^{-iq_y y}|n_\alpha, k_{x\alpha}).$$

(4.2)

The first term on the right-hand side of Eq. (4.2) is the bare Coulomb potential: the other terms are caused by screening in the QW. The $F_{0,0}$ term involves transitions and screening within the lowest occupied LL, whereas the $F_{0,n}$ and $F_{n,0}$ (n = 1, 2, 3...) terms involve inter-level transitions and screening. In strong magnetic fields, the total screening contribution is determined mainly by the $F_{0,0}$ term and it is sufficient to replace the sum $\sum_{n_\alpha, n_\beta}^{\infty}$ in Eq. (4.2) by only three terms [28], [35], $F_{0,0}$, $F_{0,1}$, and $F_{1,0}$. This means that we take into account only the intra-level and adjacent-level screening. Therefore, Eq. (4.2) can be simplified as follows.

We first split V_1^s as $V_1^s(q_x, q_y, q_y') = v_0\delta(q_y - q_y')/q + V_{c1}^s(q_x, q_y, q_y')$, $q = \sqrt{q_x^2 - q_y^2}$. This leads to the integral equation:

$$V_{c1}^s(q_x, q_y, q_y')$$
$$= \frac{v_0^2}{8\pi^3 q q'} \sum_{n_\alpha, n_\beta} \int dk_{x\alpha} F_{\alpha,\beta}(n_\alpha, k_{x\alpha}|e^{-iq_y' y}|n_\beta, k_{x\alpha} - q_x)(n_\beta, k_{x\alpha} - q_x|e^{-iq_y y}|n_\alpha, k_{x\alpha})$$

$$+ \frac{v_0}{8\pi^3 q}\int_{-\infty}^{\infty} dq_{y1} V_{c1}^s(q_x, q_{y1}, q_y')$$

$$\times \sum_{n_\alpha, n_\beta} \int dk_{x\alpha} F_{\alpha,\beta}(n_\alpha, k_{x\alpha}|e^{iq_{y1}y}|n_\beta, k_{x\alpha} - q_x)(n_\beta, k_{x\alpha} - q_x|e^{-iq_y y}|n_\alpha, k_{x\alpha}). \tag{4.3}$$

with $q' = \sqrt{q_x^2 + q_y'^2}$. Then using the relations $q_i \tilde{l} \equiv \tilde{q}_i$ $(i : x, y, \ldots)$ $\tilde{l}^2 = \hbar/(m^* \tilde{\omega})$, $\tilde{\omega} = \sqrt{\omega_c^2 + \Omega^2}$, $\tilde{q}_a = a\tilde{q}_x + i\tilde{q}_y$, $\tilde{q}_a^* = a\tilde{q}_x - i\tilde{q}_y$, $\tilde{q}_a^2 = a^2\tilde{q}_x^2 + \tilde{q}_y^2$, $\tilde{q}_a' = a\tilde{q}_x + i\tilde{q}_y'$, $\tilde{q}_a'^* = a\tilde{q}_x - i\tilde{q}_y'$, $\tilde{q}_a'^2 = a^2\tilde{q}_x^2 + \tilde{q}_y'^2$, ...

$$\begin{aligned}
(n, k_{x\alpha} - q_x|e^{iq_y y}|0, k_{x\alpha}) &= (0, k_{x\alpha}|e^{iq_y y}|n, k_{x\alpha} - q_x) \\
&= \frac{1}{\sqrt{n!}}\left(\frac{\tilde{q}_a}{\sqrt{2}}\right)^n e^{i\tilde{q}_y a(\tilde{k}_{x\alpha} - \tilde{q}_x/2)} e^{-\tilde{q}_a^2/4}. \\
(n, k_{x\alpha}|e^{iq_y y}|0, k_{x\alpha} - q_x) &= (0, k_{x\alpha} - q_x|e^{iq_y y}|n, k_{x\alpha}) \\
&= \frac{1}{\sqrt{n!}}\left(\frac{-\tilde{q}_a^*}{\sqrt{2}}\right)^n e^{i\tilde{q}_y a(\tilde{k}_{x\alpha} - \tilde{q}_x/2)} e^{-\tilde{q}_a^2/4}.
\end{aligned} \tag{4.4}$$

$$\varepsilon_{n_\alpha} - \varepsilon_{n_\beta} \approx (n_\alpha - n_\beta)\hbar\tilde{\omega}. \tag{4.5}$$

and

$$\sum_{n_\alpha, n_\beta} F_{\alpha,\beta} \to \sum_{n_\alpha, n_\beta = 0}^{n_\alpha, n_\beta = 1} F_{\alpha,\beta}. \tag{4.6}$$

we can, when $T = 0^o K$, reduce Eq.(4.3) to

$$\begin{aligned}
V_1^c(q_x, q_y, q_y') &\approx \frac{v_0^2}{8\pi^3}\frac{1}{qq'}\int_{-\infty}^{\infty} dk_{x\alpha} e^{-ia(\tilde{q}_y - \tilde{q}_y')(\tilde{k}_{x\alpha} - \tilde{q}_x/2) - \tilde{q}_a^2/4 - (\tilde{q}_a'^2)/4} \\
&\times \left\{F_{0,0} - \frac{f_{0,k_{x\alpha} - q_x}}{\hbar\tilde{\omega}}\frac{\tilde{q}_a}{\sqrt{2}}\frac{\tilde{q}_a'}{\sqrt{2}} - \frac{f_{0,k_{x\alpha}}}{\hbar\tilde{\omega}}\frac{\tilde{q}_a^*}{\sqrt{2}}\frac{\tilde{q}_a'^*}{\sqrt{2}}\right\} \\
&+ \frac{v_0}{8\pi^3}\frac{1}{q}\int_{-\infty}^{\infty} dq_{y1} V_1^c(q_x, q_{y1}, q_y')\int_{-\infty}^{\infty} dk_{x\alpha} e^{ia(\tilde{q}_{y1} - \tilde{q}_y)(\tilde{k}_{x\alpha} - \tilde{q}_x/2) - \tilde{q}_a^2/4 - \tilde{q}_{a1}^2/4} \\
&\times \left\{F_{0,0} - \frac{f_{0,k_{x\alpha} - q_x}}{\hbar\tilde{\omega}}\frac{\tilde{q}_a}{\sqrt{2}}\frac{\tilde{q}_{a1}^*}{\sqrt{2}} - \frac{f_{0,k_{x\alpha}}}{\hbar\tilde{\omega}}\frac{\tilde{q}_a^*}{\sqrt{2}}\frac{\tilde{q}_{a1}}{\sqrt{2}}\right\}.
\end{aligned} \tag{4.7}$$

where the second and third terms in the first braces come from the $F_{0,1}$ and $F_{1,0}$ ones of Eq.(4.3).

Integrating over $k_{x\alpha}$, the $F_{0,0} = (f_{0,k_{x\alpha}-q_x} - f_{0,k_{x\alpha}})/(\varepsilon_{0,k_{x\alpha}-q_x} - \varepsilon_{0,k_{x\alpha}})$ term leads to

$$\int_{-\infty}^{\infty} dk_{x\alpha} F_{0,0} e^{-ia(\tilde{q}_y+\tilde{q}'_y)(\tilde{k}_{x\alpha}-\tilde{q}_x/2)}$$
$$= (-\int_{-k_F}^{-k_F-q_x} + \int_{k_F}^{k_F-q_x}) \frac{dk_{x\alpha} e^{-ia(\tilde{q}_y+\tilde{q}'_y)(\tilde{k}_{x\alpha}-\tilde{q}_x/2)}}{\frac{\hbar^2}{2\tilde{m}^2}[(k_{x\alpha}-q_x)^2 - k_{x\alpha}^2]} = 2v_1 \cos \tilde{k}_F a(\tilde{q}_y + \tilde{q}'_y). \tag{4.8}$$

where $v_1 = -\tilde{m}/(\hbar^2 k_F) = -1/[v_g^{HA}(k_F)\hbar] = -(\frac{\tilde{\omega}}{\tilde{\Omega}})^2/(\hbar\tilde{\omega}\tilde{l}\tilde{k}_F)$ and the approximation

$$\int_{-k_F}^{-k_F-q_x} dk_{x\alpha} e^{-ia(\tilde{q}_y+\tilde{q}'_y)(\tilde{k}_{x\alpha}-\tilde{q}_x/2)} \frac{-1}{\frac{\hbar^2}{2\tilde{m}}[(k_{x\alpha}-q_x)^2 - k_{x\alpha}^2]}$$
$$= e^{ia(\tilde{q}_y+\tilde{q}'_y)(\tilde{q}_x/2)} \int_{-k_F}^{-k_F-q_x} dk_{x\alpha} \frac{e^{-ia(\tilde{q}_y+\tilde{q}'_y)\tilde{k}_{x\alpha}}}{\frac{\hbar^2}{2\tilde{m}} 2(k_{x\alpha} - \frac{q_x}{2})q_x}$$
$$= v_1 \frac{\tilde{k}_F}{\tilde{q}_x} \{E_i[i(\tilde{q}_y + \tilde{q}'_y)(\tilde{k}_F + \tilde{q}_x/2)] - E_i[i(\tilde{q}_y + \tilde{q}'_y)(\tilde{k}_F - \tilde{q}_x/2)]\}$$
$$\approx v_1 e^{ia(\tilde{q}_y+\tilde{q}'_y)\tilde{k}_F} \tag{4.9}$$

has been used. E_i is the exponential integral[74]. In Eq. (4.9) we can neglect the change in amplitude because it has a very small effect on the screened field described by Eq. (4.7) and on the exchange and correlation energy given by Eq. (4.6). However, as will be seen later, the variation in phase caused by different $\tilde{q}_x$ plays a much more important role in Eq.(4.6). To simplify the results, we make the approximation (4.9).

Note that in Ref. [35] the intra-level Coulomb interaction was treated by only considering the Fermi edge case: $F_{0,0} \approx -2\bar{m}\delta(k_{x\alpha}^2 - k_F^2)/\hbar^2$. Using this approximation to calculate the $F_{0,0}$ term will lead to

$$\int_{-\infty}^{\infty} dk_{x\alpha} F_{0,0} e^{-ia(\tilde{q}_y+\tilde{q}'_y)(\tilde{k}_{x\alpha}-\tilde{q}_x/2)} = 2v_1 \cos \tilde{k}_F a(\tilde{q}_y + \tilde{q}'_y) e^{ia(\tilde{q}_y-\tilde{q}'_y)\tilde{q}_x/2}. \tag{4.10}$$

which is different from Eq.(4.8) by an important phase factor $e^{ia(\tilde{q}_y-\tilde{q}'_y)\tilde{q}_x/2}$. This is because the intra-level transition mainly happens NEAR the Fermi edge, rather than AT the Fermi edge. Such difference will cause very small change on the amplitude of the screened field. But it brings considerable change in the phase of the screened field.

With the help of Eq.(4.8) and the note

$$sinc(x) = \frac{\sin(\tilde{k}_F x)}{x} \tag{4.11}$$

we can rewrite above equation as

$$\begin{aligned} V_{c1}^{s}(q_x, q_y, q'_y) &= \frac{2v_0^2 v_1 \bar{l}^2}{8\pi^3} \frac{1}{\tilde{q}\tilde{q}'} e^{-\tilde{q}_\alpha^2/4 - \tilde{q}_\alpha'^2/4} \\ &\times \left[\cos \tilde{k}_F a(\tilde{q}_y + \tilde{q}'_y) - \frac{1}{2\hbar \bar{l} a v_1}(a^2 \tilde{q}_x^2 - \tilde{q}_y \tilde{q}'_y) sinc(\tilde{q}_y + \tilde{q}'_y)\right] \\ &+ \frac{2v_0 v_1}{8\pi^3} \frac{1}{\tilde{q}} \int d\tilde{q}_{y1} V_1^c(q_x, q_{y1}, q'_y) e^{-\tilde{q}_\alpha^2/4 - \tilde{q}_{\alpha 1}^2/4} \\ &\times \left[\cos \tilde{k}_F a(\tilde{q}_y - \tilde{q}_{y1}) - \frac{1}{2\hbar \bar{l} a v_1}(a^2 \tilde{q}_x^2 + \tilde{q}_y \tilde{q}_{y1}) sinc(\tilde{q}_y - \tilde{q}_{y1})\right] \end{aligned} \tag{4.12}$$

The solution of the Eq. (4.12) can be sought in the form

$$V_{c1}^{s}(q_x, q_y, q'_y) = v_0 \Phi(\tilde{q}_x, \tilde{q}_y) \Phi(\tilde{q}_x, \tilde{q}'_y)$$

$$\times \quad [\tilde{k}_{c1}\cos\tilde{k}_F a\tilde{q}_y \cos\tilde{k}_F a\tilde{q}'_y + \tilde{k}_{s1}\sin\tilde{k}_F a\tilde{q}_y \sin\tilde{k}_F a\tilde{q}'_y$$

$$+\tilde{k}_{sc1}(a^2\tilde{q}_x^2 - \tilde{q}_y\tilde{q}'_y)sinc(\tilde{q}_y + \tilde{q}'_y)]. \tag{4.13}$$

where

$$\Phi(\tilde{q}_x, \tilde{q}_y) = \tilde{l}e^{-\tilde{q}_a^2/4}/\tilde{q}.$$

$$\tilde{k}_i \equiv \tilde{k}_i(\tilde{q}_x, \tilde{q}_y, \tilde{q}'_y) \quad (i = c1, s1, sc1). \tag{4.14}$$

and $\tilde{k}_{c1}, \tilde{k}_{s1}$, and $\tilde{k}_{sc1}$ are to be determined. In Eq. (4.13), the first and the second terms correspond to the intra-level Coulomb interactions. One has even parity and the other has odd parity. The third term comes from the inter-level transition. Substituting the trial solution (4.13) into Eq.(4.12) and setting $a = 1$, we have

$$\begin{aligned}
&\tilde{k}_{c1}\cos\tilde{k}_F\tilde{q}_y\cos\tilde{k}_F\tilde{q}'_y - \tilde{k}_{s1}\sin\tilde{k}_F\tilde{q}_y\sin\tilde{k}_F\tilde{q}'_y - \tilde{k}_{sc1}(\tilde{q}_x^2 - \tilde{q}_y\tilde{q}'_y)sinc(\tilde{q}_y - \tilde{q}'_y) \\
= \quad & -\alpha_0[\cos\tilde{k}_F\tilde{q}_y\cos\tilde{k}_F\tilde{q}'_y - \sin\tilde{k}_F\tilde{q}_y\sin\tilde{k}_F\tilde{q}'_y + (\frac{\Omega}{\tilde{\omega}})^2\tilde{k}_F(\tilde{q}_x^2 - \tilde{q}_y\tilde{q}'_y)sinc(\tilde{q}_y + \tilde{q}'_y)] \\
& -\alpha_0\int d\tilde{q}_{y1}\frac{e^{-\tilde{q}_{1x}^2}}{\tilde{q}_1} \\
& \times[\tilde{k}_{c1}\cos\tilde{k}_F\tilde{q}_{y1}\cos\tilde{k}_F\tilde{q}'_y + \tilde{k}_{s1}\sin\tilde{k}_F\tilde{q}_{y1}\sin\tilde{k}_F\tilde{q}'_y + \tilde{k}_{sc1}(\tilde{q}_x^2 - \tilde{q}'_y\tilde{q}_{y1})sinc(\tilde{q}_{y1} + \tilde{q}'_y)] \\
& \times[\cos\tilde{k}_F\tilde{q}_y\cos\tilde{k}_F\tilde{q}_{y1} + \sin\tilde{k}_F\tilde{q}_y\sin\tilde{k}_F\tilde{q}_{y1} + (\frac{\Omega}{\tilde{\omega}})^2\tilde{k}_F(\tilde{q}_x^2 - \tilde{q}_y\tilde{q}_{y1})sinc(\tilde{q}_y - \tilde{q}_{y1})].
\end{aligned} \tag{4.15}$$

Here, relations

$$v_1 \equiv \frac{-\tilde{m}}{\hbar^2 k_F} = \frac{-(\frac{\tilde{\omega}}{\Omega})^2}{\hbar\tilde{k}_F\tilde{\omega}\tilde{l}} = \frac{-1}{v_g^{HA}(k_F)\hbar}, \tag{4.16}$$

$$\frac{2}{8\pi^3}v_0 v_1 = \frac{-r_0}{\pi\tilde{k}_F}(\frac{\tilde{\omega}}{\Omega})^2 \equiv -\alpha_0; \tag{4.17}$$

have been used. Further, with the help of $sinc(x) \sim \delta(x)$ and the neglect of small oscillatory terms, we can make the following approximations

$$\int d\tilde{q}_{y1} \frac{e^{-\tilde{q}_1^2/2}}{\tilde{q}_1} \tilde{k}_{sc1}(\tilde{q}_x, \tilde{q}_{y1}, \tilde{q'}_y) \cos \tilde{k}_F \tilde{q}_{y1} (q_x^2 - \tilde{q'}_y \tilde{q}_{y1}) sinc(\tilde{q'}_y + \tilde{q}_{y1})$$
$$\approx \frac{1}{2}\pi \tilde{k}_3(\tilde{q}_x, -\tilde{q'}_y, \tilde{q'}_y) \cos \tilde{k}_F \tilde{q'}_y e^{-\tilde{q'}^2/2} \tilde{q'}. \tag{4.18}$$

$$\int d\tilde{q}_{y1} \frac{e^{-\tilde{q}_1^2/2}}{\tilde{q}_1} \tilde{k}_{sc1}(\tilde{q}_x, \tilde{q}_{y1}, \tilde{q'}_y) \sin \tilde{k}_F \tilde{q}_{y1} (q_x^2 - \tilde{q'}_y \tilde{q}_{y1}) sinc(\tilde{q'}_y + \tilde{q}_{y1})$$
$$\approx -\frac{1}{2}\pi \tilde{k}_3(\tilde{q}_x, -\tilde{q'}_y, \tilde{q'}_y) \sin \tilde{k}_F \tilde{q'}_y e^{-\tilde{q'}^2/2} \tilde{q'}. \tag{4.19}$$

$$\int d\tilde{q}_{y1} \frac{e^{-\tilde{q}_1^2/2}}{\tilde{q}_1} \tilde{k}_{sc1}(\tilde{q}_x, \tilde{q}_{y1}, \tilde{q'}_y)(q_x^2 - \tilde{q'}_y \tilde{q}_{y1}) sinc(\tilde{q'}_y + \tilde{q}_{y1})(q_x^2 - \tilde{q}_y \tilde{q}_{y1}) sinc(\tilde{q}_y - \tilde{q}_{y1})$$
$$\approx \pi(q_x^2 - \tilde{q'}_y \tilde{q}_y) sinc(\tilde{q'}_y - \tilde{q}_y) \tilde{k}_{sc1}(\tilde{q}_x, \tilde{q}_y, \tilde{q'}_y) e^{-\tilde{q'}^2/2} \tilde{q'}$$
$$\approx \pi(q_x^2 - \tilde{q'}_y \tilde{q}_y) sinc(\tilde{q'}_y - \tilde{q}_y) \tilde{k}_{sc1}(\tilde{q}_x, \tilde{q}_y, \tilde{q'}_y) e^{-\tilde{q}^2/2} \tilde{q} \tag{4.20}$$

in (4.15). Similar to the "mode-matching" technique [60], we equate the coefficients of $\cos \tilde{k}_F \tilde{q}_y \cos \tilde{k}_F \tilde{q}'_y$, $\sin \tilde{k}_F \tilde{q}_y \sin \tilde{k}_F \tilde{q}'_y$, and $sinc(\tilde{q}_y - \tilde{q}'_y)$ terms on both side of equation (4.15) respectively, and obtain three equations:

$$\tilde{k}_{sc1}(\tilde{q}_x, \tilde{q}_y, \tilde{q}'_y) = -\alpha_0 (\frac{\Omega}{\tilde{\omega}})^2 \tilde{k}_F - \alpha_0 (\frac{\Omega}{\tilde{\omega}})^2 \tilde{k}_F \pi e^{-\tilde{q}'^2/2} \tilde{q}' \tilde{k}_{sc1}(\tilde{q}_x, \tilde{q}_y, \tilde{q}'_y)$$

$$\tilde{k}_1(\tilde{q}_x, \tilde{q}_y, \tilde{q}'_y) = -\alpha_0 - \alpha_0 \tilde{K}_- \tilde{k}_1(\tilde{q}_x, \tilde{q}'_y) - \frac{1}{2}\alpha_0 \pi e^{-\tilde{q}'^2/2} \tilde{q}' \tilde{k}_{sc1}(\tilde{q}_x, -\tilde{q'}_y, \tilde{q'}_y)$$
$$-\frac{1}{2}\alpha_0 (\frac{\Omega}{\tilde{\omega}})^2 \tilde{k}_F \pi e^{-\tilde{q}^2/2} \tilde{q} \tilde{k}_1(\tilde{q}_x, \tilde{q}_y, \tilde{q}'_y)$$

$$\tilde{k}_2(\tilde{q}_x, \tilde{q}_y, \tilde{q}'_y) = \alpha_0 - \alpha_0 \tilde{K}_- \tilde{k}_2(\tilde{q}_x, \tilde{q}'_y) + \frac{1}{2}\alpha_0 \pi e^{-\tilde{q}'^2/2} \tilde{q}' \tilde{k}_{sc1}(\tilde{q}_x, -\tilde{q'}_y, \tilde{q'}_y)$$
$$-\frac{1}{2}\alpha_0 (\frac{\Omega}{\tilde{\omega}})^2 \tilde{k}_F \pi e^{-\tilde{q}^2/2} \tilde{q} \tilde{k}_2(\tilde{q}_x, \tilde{q}_y, \tilde{q}'_y) \tag{4.21}$$

So we first get

$$\tilde{k}_{sc1}(\tilde{q}_x, \tilde{q}_y, \tilde{q}'_y) = \frac{-r_0}{\pi} - \frac{r_0}{\pi}\frac{\pi}{2}\tilde{q}e^{-\tilde{q}^2/2}\tilde{k}_{sc1}(\tilde{q}_x, \tilde{q}_y, \tilde{q}'_y) = \frac{-r_0/\pi}{1 + r_0\tilde{q}e^{-\tilde{q}^2/2}}. \tag{4.22}$$

The expression of $\tilde{K}_{\pm}$ in Eq. (4.21) will be given at the end of this subsection. Eq. (4.22) can be rewritten as

$$\tilde{k}_{sc1}(\tilde{q}_x, \tilde{q}_y, \tilde{q}'_y) = \frac{-X r_0/\pi}{1 + r_0\tilde{q}e^{-\tilde{q}^2/2}}. \tag{4.23}$$

with $X = 1$. This value of X leads to a potential expression that agrees with the numerical solution of Eq. (4.12), depending on the value of $\tilde{q}_x$, to within $80 \sim 90\%$. A much better agreement can be obtained if we modify X as

$$X = 1 - e^{-200\tilde{q}_x^4}. \tag{4.24}$$

As for $\tilde{k}_i (i = c1, s1)$, we assume that they can be factorized as $\tilde{k}_i(\tilde{q}_x, \tilde{q}_y, \tilde{q}'_y) = \tilde{k}_{iqx}(\tilde{q}_x)\tilde{k}_{iqxy}(\tilde{q}_x, \tilde{q}_y)\tilde{k}_{iqxy'}(\tilde{q}_x, \tilde{q}'_y)$. With equation (4.23), we obtain

$$\begin{aligned}\tilde{k}_{c1}(\tilde{q}_x, \tilde{q}_y, \tilde{q}'_y) = \quad & -\alpha_0 - \alpha_0\tilde{K}_-\tilde{k}_{c1qx}\tilde{k}_{1qxy'} - \alpha_0\pi\tilde{q}'e^{-\tilde{q}'^2/2}\frac{-\frac{1}{2}X r_0/\pi}{1 + r_0\tilde{q}'e^{-\tilde{q}'^2/2}} \\ & -\frac{1}{2}r_0\tilde{q}e^{-\tilde{q}^2/2}\tilde{k}_{c1}(\tilde{q}_x, \tilde{q}_y, \tilde{q}'_y)\end{aligned} \tag{4.25}$$

or

$$\begin{aligned}\tilde{k}_{c1qx}\tilde{k}_{c1qxy}\tilde{k}_{c1qxy'}(1 + \frac{1}{2}r_0\tilde{q}e^{-\tilde{q}^2/2}) = \quad & -\alpha_0\left[1 - \frac{r_0\frac{1}{2}X\tilde{q}'e^{-\tilde{q}'^2/2}}{1 + r_0\tilde{q}'e^{-\tilde{q}'^2/2}}\right] \\ & -\alpha_0\tilde{k}_{c1qx}\tilde{k}_{c1qxy'}\tilde{K}_-\end{aligned} \tag{4.26}$$

The final solutions for $\tilde{k}_i(i = c1, s1)$ are

$$\begin{aligned}\tilde{k}_i(\tilde{q}_x, \tilde{q}_y, \tilde{q}'_y) &= -\frac{\pm\alpha_0}{1+\alpha_0\tilde{K}_\pm}\frac{1}{1+r_0\frac{1}{2}\tilde{q}e^{-\tilde{q}^2/2}}\left[1-\frac{r_0\frac{1}{2}X\tilde{q}'e^{-\tilde{q}'^2/2}}{1+r_0\tilde{q}'e^{-\tilde{q}'^2/2}}\right] \\ &\equiv -\frac{\pm\alpha_0}{1+\alpha_0\tilde{K}_\pm}C_1(\tilde{q}_x, \tilde{q}_y)C_2(X, \tilde{q}_x, \tilde{q}'_y). \\ &\qquad (+: i = c1; \ -: i = s1;) \end{aligned} \tag{4.27}$$

with

$$\tilde{K}_\pm(\tilde{q}_x) = \int \frac{d\tilde{q}_y e^{-\tilde{q}^2/2}(1 \pm \cos 2\tilde{k}_F\tilde{q}_y)/2}{\tilde{q}(1+r_0\frac{1}{2}\tilde{q}e^{-\tilde{q}^2/2})} \tag{4.28}$$

In Eq. (4.27) C_1 and C_2 have different forms because of inhomogeneous screening in the transverse direction of the QW. However, this does not mean that the many-body energy correction will be unsymmetric with respect to k_x, see the discussion in subsection 4.1.3.

Functions $\tilde{K}_\pm$ and $K_\pm$ introduced before can be considered as special cases of the general form defined as

$$\tilde{K}_{\pm,\nu}(\tilde{q}_x) = \int_{-\infty}^{\infty} \frac{d\tilde{q}_y e^{-\tilde{q}^2/2}(1 \pm \cos 2\tilde{k}_F\tilde{q}_y)/2}{\tilde{q}(1+r_0\frac{\nu}{2}\tilde{q}e^{-\tilde{q}^2/2})} \tag{4.29}$$

When $\nu = 1$, we have $\tilde{K}_{\pm,1}(\tilde{q}_x) = \tilde{K}_\pm(\tilde{q}_x)$. Setting $\nu = 0$ leads to

$$\tilde{K}_{\pm,0}(\tilde{q}_x, 0) \equiv K_\pm(\tilde{q}_x) \approx [\frac{1}{2}K_0(\tilde{q}_x^2/4)e^{\tilde{q}_x^2/4} \pm K_0(2\tilde{k}_F\tilde{q}_x)]e^{-\tilde{q}_x^2/2}, \tag{4.30}$$

which is the main part of $\tilde{K}_\pm(\tilde{q}_x)$. For small $\tilde{q}_x$, we have the approximation

$$\begin{aligned}\tilde{K}_{\pm,\nu}(\tilde{q}_x) &= \int_{-\infty}^{\infty} d\tilde{q}_y \frac{e^{-\tilde{q}^2/2}}{\tilde{q}}\frac{(1 \pm \cos 2\tilde{k}_F\tilde{q}_y)/2}{1+\frac{\nu r_0}{2}\tilde{q}e^{-\tilde{q}^2/2}} \\ &= \int_{-\infty}^{\infty} d\tilde{q}_y \frac{e^{-\tilde{q}^2/2}}{\tilde{q}}\frac{1 \pm \cos 2\tilde{k}_F\tilde{q}_y}{2}\sum_{n=0}(-\frac{\nu r_0}{2}\tilde{q}e^{-\tilde{q}^2/2})^n \\ &= K_\pm(\tilde{q}_x) - \frac{\nu r_0}{2}\int_{-\infty}^{\infty} \frac{d\tilde{q}_y e^{-\tilde{q}^2}(1 \pm \cos 2\tilde{k}_F\tilde{q}_y)/2}{1+\frac{\nu r_0}{2}\tilde{q}e^{-\tilde{q}^2/2}}. \end{aligned} \tag{4.31}$$

which will be used later.

4.1.2 Numerical solutions

In principle, Eq. (4.12) can be solved by iterations. However, as the integral kernel on the right-hand side (RHS) of the equation becomes very large when q_x ($q_x = k_x - k'_x$) is very small, any small deviation in the trial values would cause a very large deviation on the RHS and lead to either divergent results or an extremely long procedure. We avoided these problems by taking the approximate analytic solution Eq. (4.13) as the initial value and applying a "weighted" iterative method. The details are as follows.

Suppose V_l^i is the LHS value obtained by substituting the trial value of the ith iteration V^i into the RHS of the Eq. (4.12). Then the trial value of the $(i+1)$th iteration is taken as $V^{i+1} = V^i + x(V_l^i - V^i)$, where $0 \leq x \leq 1$ is the "weighting" factor. If we take $x = 0$ we have $V^{i+1} = V^i$, which means there is no change between successive iterations. On the other hand, if we take $x = 1$ we have $V^{i+1} = V_l^i$, as in the traditional iterative method, which can be used only when the integral kernel is smaller than one. Otherwise, the "DIRECT" correction ($x = 1$) to the trial value ($V_l^i - V^i$) is too large, and finally results in a divergence problem. This can be solved by using the "WEIGHTED" correction approach, at the expense of increasing the iteration times. For example, in Eq. (4.12) we take small x, say 0.5% for $q_x = 1/150$, to avoid divergent results between iterations. In this way one can obtain the numerical solution with any accuracy, provided the iteration times are large enough.

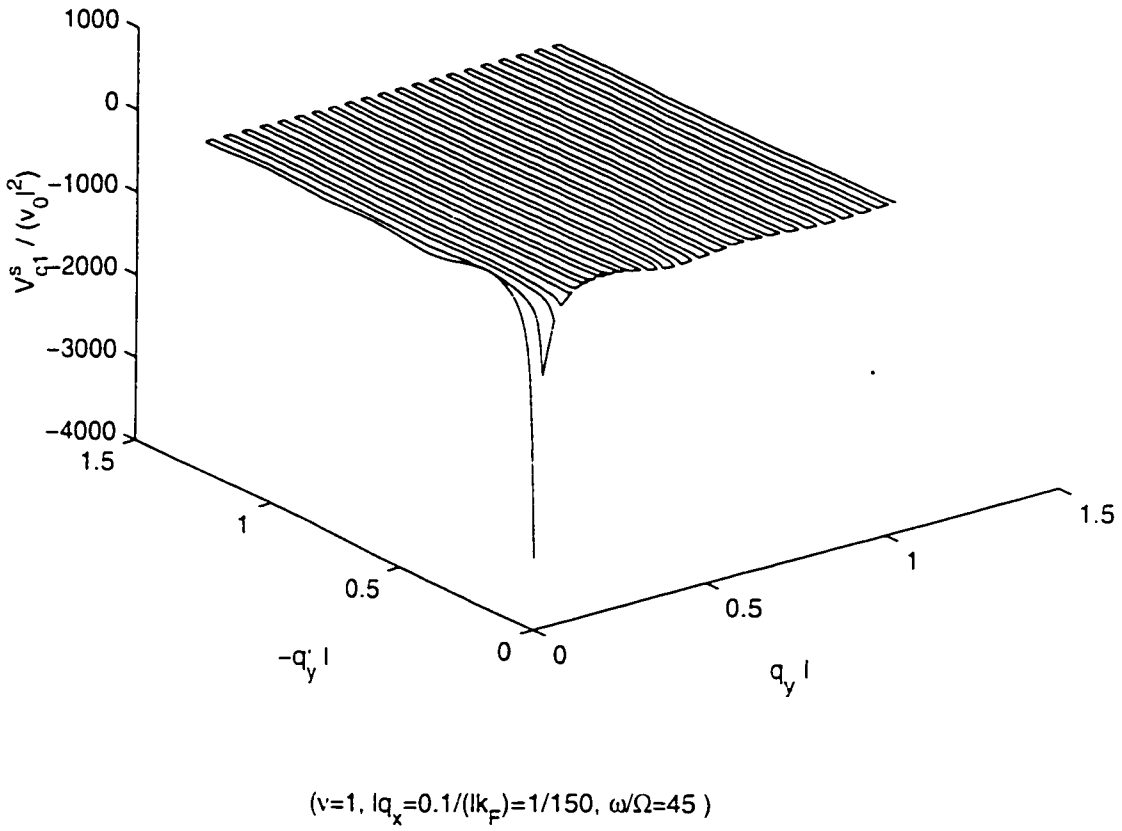

Figure 4.1: Solved correlation interactions in QW (Sample 2 of Ref. [50]) with $\nu = 1, \tilde{k}_F = 15$. The dashed curve is the approximate analytic solution and the solid one shows the numerical solution. The two curves are very close and it is hard to notice any difference between them. The confining potential is defined by $\Omega = \omega/45$. In the $\bar{q} \to 0$ (long wavelength limit) region, correlation interactions tend to diverge.

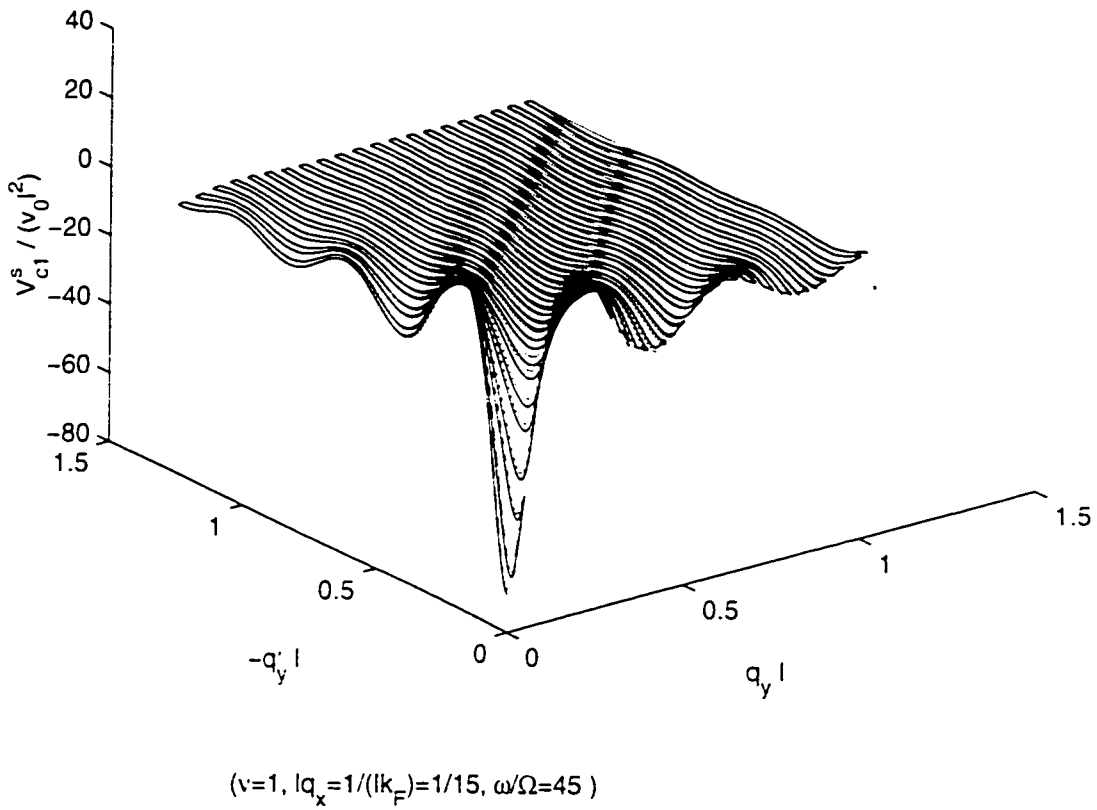

Figure 4.2: Solved correlations interactions in QW (Sample 2 of Ref. [50]) with $\nu = 1, \tilde{k}_F = 15$ and $\Omega = \omega/45$. The dashed curve is the approximate analytic solution and the solid one shows the numerical calculation. For $\tilde{q}_x$ 1/15, there are certain differences between the numerical solution and the analytical approximation.

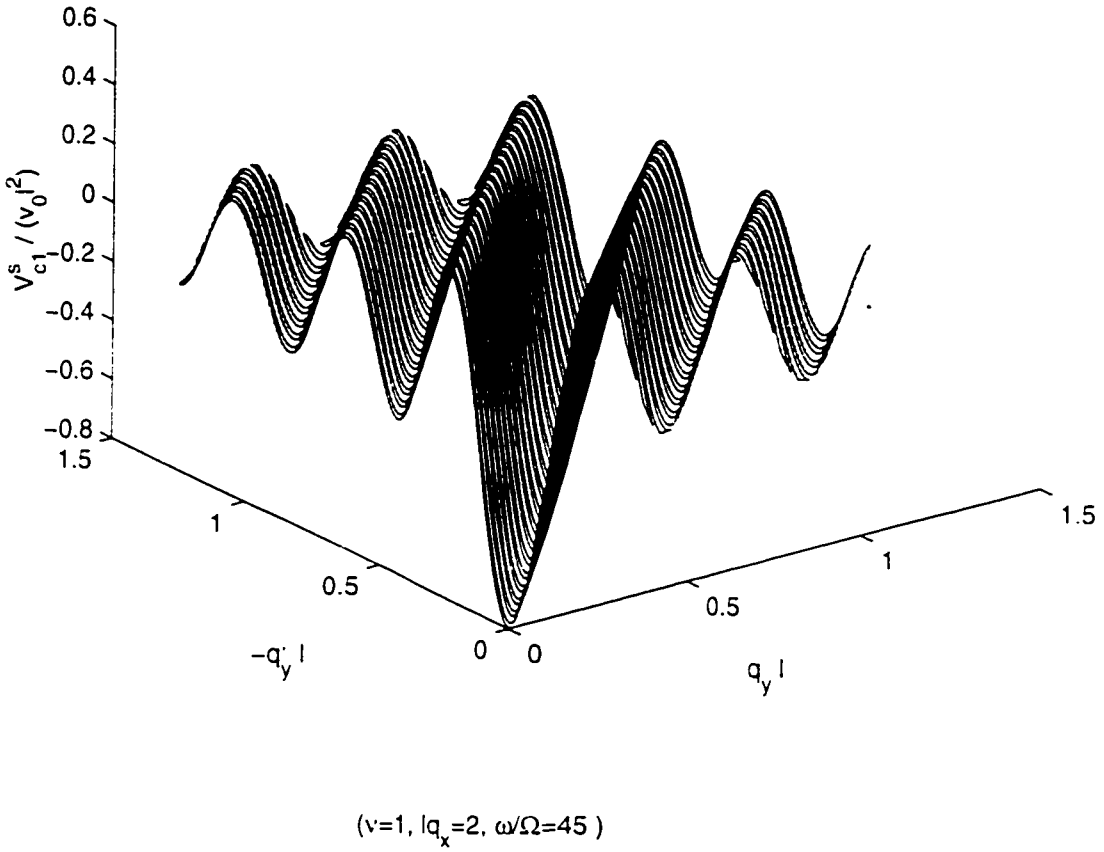

Figure 4.3: Solved correlation interactions in QW (Sample 2 of Ref. [50])with $\nu = 1, \tilde{k}_F = 15$ and $\Omega = \omega/45$. The dashed curve is the approximate analytic solution and the solid one shows the numerical calculation. For large $\tilde{q}_x$, e.g., $\tilde{q}_x = 2$, there are nearly no differences between the two curves.

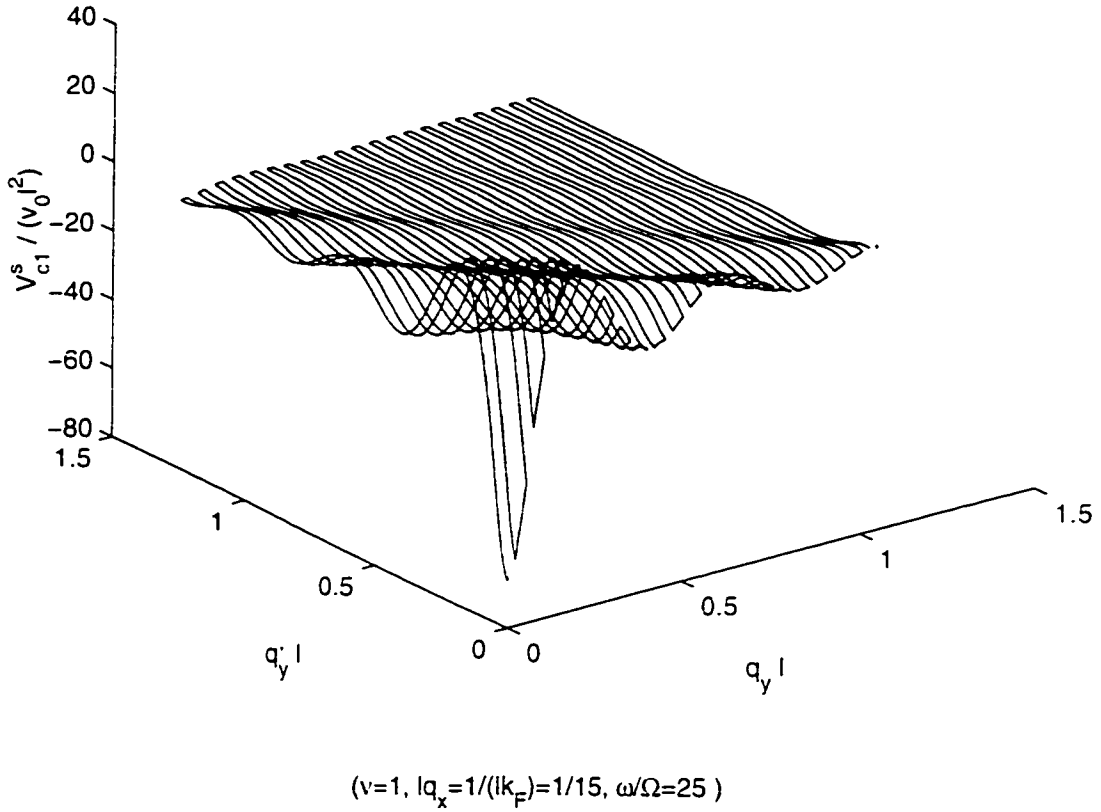

Figure 4.4: Solved correlations interactions in QW (Sample 1 of Ref. [50])with $\nu = 1, \tilde{k}_F = 15$, $\Omega = \omega/25$ and $\tilde{q}_x = 1/\tilde{k}_F$. Dashed curve represents the approximate analytic solution and the solid one is the numerical calculation.

The results of the numerical solution of Eq. (4.12) are plotted in Figs. 4.1 to 4.4 for some special values of q_x and ω_c/Ω. For comparison the results of the approximate analytical solution, expressed by Eqs. (4.13), (4.23), and (4.27) are shown by the dotted curves. As can be seen, the two results agree very well and this holds for large ranges of the parameters. For example, the value of ω_c/Ω can be changed, at least from 25 to 45, and that of $\tilde{q}_x = lq_x$ from the very small value $0.1/\tilde{k}_F$ to the very large one e.g., $\tilde{k}_F$.

Figs. 4.1 to 4.3 show that for small or large $\tilde{q}_x$ (ω_c/Ω=45), the numerical and analytic results are almost the same. There are some small differences between them when when $\tilde{q}_x$ near $1/\tilde{k}_F = 1/15$. Fig. 4.2 shows the worst case ($\tilde{q}_x = 1/\tilde{k}_F$). For ($\omega_c/\Omega$=25), we have similar results. Fig. 4.4 shows the field distributions for $\tilde{q}_x = 1/\tilde{k}_F$, which is the worst case for ω_c/Ω=25.

4.1.3 Exchange and correlation energies, group velocities near the Fermi edge

With the help of Eqs.(4.1), (4.13), (4.23), and (4.27), we get the correlation energy

$$\begin{aligned}
\varepsilon^{co}_{0,k_x,1} &\approx -\frac{1}{(2\pi)^3}\int_{-k_F}^{k_F} dk'_x \int_{-\infty}^{\infty} dq_y dq'_y V^{-s}_{c1}(k_x - k'_x, q_y, q'_y)(0k_x|e^{iq_y y}|0k'_x)(0k'_x|e^{iq'_y y}|0k_x) \\
&= -\frac{1}{(2\pi)^3}\left(\int_0^{\tilde{k}_F+\tilde{k}_x} + \int_{\tilde{k}_x-\tilde{k}_F}^{0}\right)\frac{d\tilde{k}_-}{\tilde{l}}\int_{-\infty}^{\infty} dq_y dq'_y v_0 \tilde{l}^2 \frac{e^{-\tilde{q}_-^2/4}}{\tilde{q}_-}\frac{e^{-\tilde{q}'^2_-/4}}{\tilde{q}'_-} \\
&\quad \times[\tilde{k}_{c1}\cos\tilde{k}_F\tilde{q}_y\cos\tilde{k}_F\tilde{q}'_y + \tilde{k}_{s1}\sin\tilde{k}_F\tilde{q}_y\sin\tilde{k}_F\tilde{q}'_y \\
&\quad +\tilde{k}_{sc1}(\tilde{k}_-^2 - \tilde{q}_y\tilde{q}'_y)sinc(\tilde{q}_y - \tilde{q}'_y)] \times e^{i\tilde{q}_y\tilde{k}_-/2-\tilde{q}_-^2/4}e^{i\tilde{q}'_y\tilde{k}_-/2-\tilde{q}'^2_-/4}.
\end{aligned} \tag{4.32}$$

with $\tilde{q}_-^2 = \tilde{k}_-^2 + \tilde{q}_y^2$, $\tilde{q}'^2_- = \tilde{k}_-^2 + \tilde{q}'^2_y$, and $\tilde{k}_\pm = \tilde{k}_x \pm \tilde{k}'_x$. The exchange correction is

$$\varepsilon^{ex}_{0,k_x,1} = -\frac{v_0}{(2\pi)^3}\left(\int_0^{\tilde{k}_F+\tilde{k}_x} + \int_0^{\tilde{k}_F-\tilde{k}_x}\right)\frac{d\tilde{k}_-}{\tilde{l}}\int_{-\infty}^{\infty} d\tilde{q}_y \frac{e^{-(\tilde{k}_-^2+\tilde{q}_y^2)/2}}{\sqrt{\tilde{k}_-^2+\tilde{q}_y^2}} \tag{4.33}$$

The last term in the square brackets of Eq. (4.32) is the correlation contributed from the neighboring level. The other two terms can be separated in two parts. One is the contribution from one side of the channel ($\int_0^{\tilde{k}_F-\tilde{k}_x} d\tilde{k}_-...$) and the other is that from the other side of the channel ($\int_{\tilde{k}_x-\tilde{k}_F}^{0} d\tilde{k}_-...$). [Note that the displaced center of the free electron is determined uniquely by the plane wave vector of this electron, cf. subsection 3.2.2.] The exchange-correlation correction $\varepsilon^{ec}_{0,k_x,1}$ is the sum of the contributions from Eqs. (4.32) and (4.33). Fig. 4.5 shows the dependence of the exchange-correlation correction on $\tilde{k}_x$. It is symmetric with respect to $k_x = 0$ (or

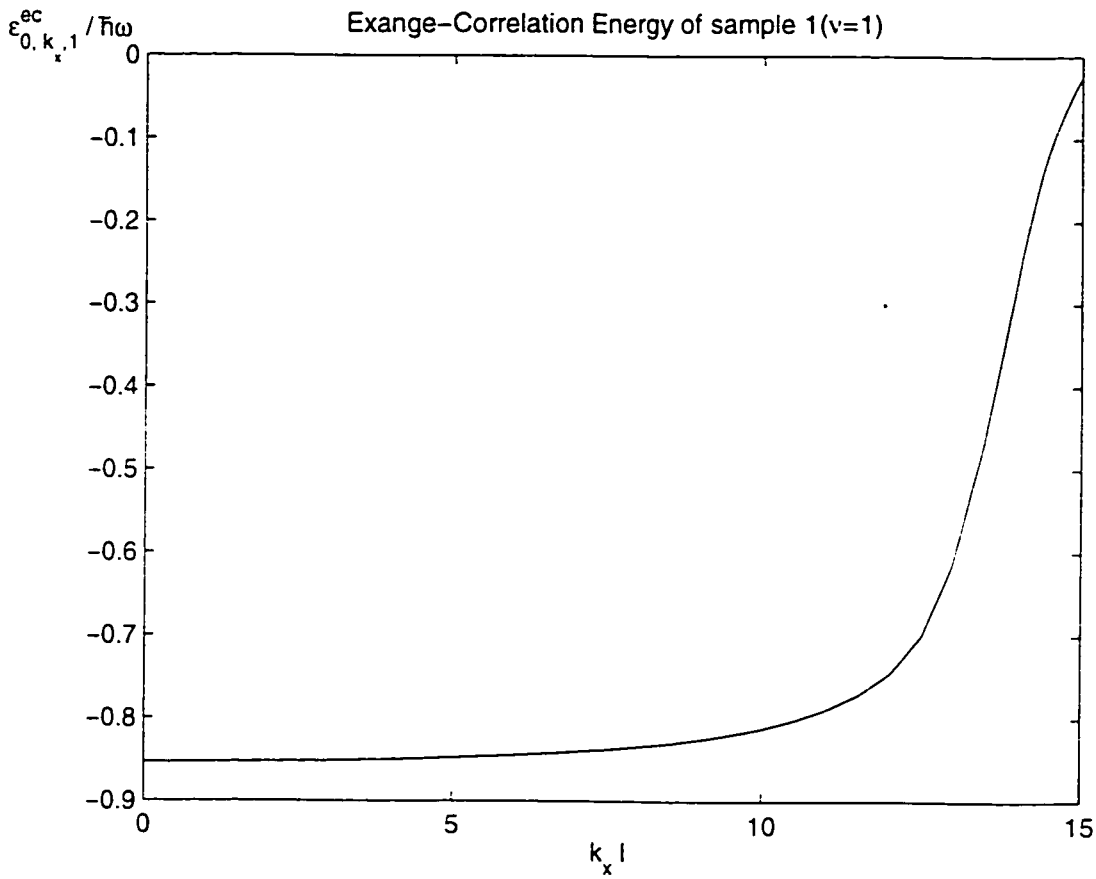

Figure 4.5: The exchange-correlation correction $\varepsilon^{ec}_{0,k_x,1}/(\hbar\tilde{\omega})$ vs. $\tilde{k}_x$ curve for sample 1 of Ref.[50] with $\nu = 1$. When $\tilde{k}_x \to \tilde{k}_F = 15$, $|\varepsilon^{ec}_{0,k_x,1}|$ is very small.

$y = 0$) axis, because $\tilde{K}_{\pm}(\tilde{k}_-)$ and $C_i(\tilde{k}_-)$ ($i = 1, 2$) introduced in Eq. (4.28) and Eq. (4.27) have properties $\tilde{K}_{\pm}(-\tilde{k}_-) = \tilde{K}_{\pm}(\tilde{k}_-)$ and $C_i(-\tilde{k}_-) = C_i(\tilde{k}_-)$, which give us $\tilde{k}_i(-\tilde{k}_-) = \tilde{k}_i(\tilde{k}_-)$ and $\varepsilon^{co}_{0,k_x,1} = \varepsilon^{co}_{0,-k_x,1}$. This is a reasonable conclusion, considering that the QW geometry is symmetric with respect to the $y = 0$ axis.

For electrons in edge states, the exchange-correlation correction reaches to the maximum value, with non zero slope. To study the behavior of exchange and correlation near the Fermi edge we consider the derivative

$$\begin{aligned} v_g^{ec}(k_F) &= \frac{\tilde{l}}{\hbar}\frac{\partial}{\partial \tilde{k}_x}\varepsilon^{ec}_{0,k_x,1}|_{k_x \to k_F} \\ &= \frac{\tilde{l}\tilde{\omega}r_0}{2\pi}\left[K_0(\frac{\tilde{k}_0^2}{4}) - \frac{\alpha_0 \tilde{K}_-(\tilde{k}_0)\tilde{K}_-(\tilde{k}_0)}{1+\alpha_0\tilde{K}_-(\tilde{k}_0)} - \frac{\alpha_0 \tilde{K}_-(\tilde{k}_0)\tilde{K}_-(\tilde{k}_0)}{1+\alpha_0\tilde{K}_-(\tilde{k}_0)}\right]|_{\tilde{k}_0 \to 0}. \end{aligned} \tag{4.34}$$

where $\tilde{k}_0 = \tilde{k}_F - \tilde{k}_x$. In deriving Eq. (4.34), we neglect the contributions from the other side of the channel ($\int_0^{\tilde{k}_F - \tilde{k}_x} d\tilde{k}_- ...$). When $\tilde{k}_0 \to 0$, the first term in (4.34) , which is caused by the exchange interaction, is positive and logarithmically divergent. On the other hand, the second term in Eq. (4.34), corresponding to an even-parity mode of the screened potential, also has a logarithmic singularity. But it is a negative one. Each singularity is caused by the Coulomb interactions between edge states. To show that the total effect is nonsingular, we need to prove that these two singularities cancel each other exactly. This is shown below.

Making the approximations $\alpha_0\tilde{K}_{\pm}/(1 + \alpha_0\tilde{K}_{\pm}) \approx 1 - 1/\alpha_0\tilde{K}_{\pm}$, for $\alpha_0\tilde{K}_{\pm} > 1$

and $K_0(x)|_{x\to 0}$, and using Eq. (4.31), we can simplify Eq.(4.34) further and obtain

$$
\begin{aligned}
v_g^{ec}|_{\tilde{k}_0\to 0} &= \frac{\tilde{l}\tilde{\omega} r_0}{2\pi}\left[K_0(\frac{\tilde{k}_0^2}{4}) - (1-\frac{1}{1+\alpha_0\tilde{K}_+})K_+ - (1-\frac{1}{1+\alpha_0\tilde{K}_-}K_-\right]|_{\tilde{k}_0\to 0} \\
&\approx \tilde{l}\Omega(\frac{\Omega}{\tilde{\omega}}\tilde{k}_F)\left[\frac{K_+}{\tilde{K}_+} + \frac{K_-}{\tilde{K}_-} - \frac{K_-}{\alpha_0\tilde{K}_-^2}\right]/2|_{\tilde{k}_0=0} \qquad (4.35)
\end{aligned}
$$

From Eq. (4.35) we can see clearly that the first logarithmic divergence resulting from exchange is exactly canceled by the sigularities in correlations contributed from the intra-level screening. This conclusion is also true even when the condition $\alpha_0\tilde{K}_- > 1$ is not satisfied. [Note that $K_0(x)|_{x\to 0} \approx \ln(2/x)$ and $K_0(\tilde{k}_0)|_{\tilde{k}_0\to 0} = K_-(0.5\tilde{k}_0^2/4)e^{-\tilde{k}_0^2/4} - K_0(2\tilde{k}_0\tilde{k}_F)e^{-\tilde{k}_0^2/2}|_{\tilde{k}_0\to 0} \approx 0.5\ln(8\tilde{k}_F^2)$.] Also, in Eq. (4.34), there is no adjacent-level contribution because near the Fermi edge the integral kernel ($\tilde{k}_3$) in Eq. (4.32) tends to zero very quickly. Therefore, the nonsingular part of the total derivative only comes from intra-level screening. For strong magnetic fields, $v_g^{ec}(k_F)$ given by Eq. (4.35) tends to be a constant.

$$
v_g^{ec}(k_F) = v_g^H\left[1 + \frac{1}{\tilde{K}_-}\frac{r_0}{4}\int_{-\infty}^{\infty}\frac{d\tilde{q}_y e^{-\tilde{q}_y^2}(1-\cos 2\tilde{k}_F\tilde{q}_y)}{2 + r_0\tilde{q}_y e^{-\tilde{q}_y^2/2}}\right] \approx v_g^H(k_F). \qquad (4.36)
$$

where $v_g^H(k_F) = \tilde{l}\Omega(\Omega\tilde{k}_F/\tilde{\omega})$. This conclusion is reached because the second term in the square brackets is less than 4% of the first term, e.g., for $r_0 = 1$, and is consistent with the value proposed in Ref. [35].

4.1.4 Single-particle energies

In previous sections, we obtained, within the SHFA, the exchange-correlation energy $\varepsilon^{ec}_{0,k_z,1}$ and its contribution to the Fermi-edge group velocity. Our derivation is based on the approximate solution of the integral equation for the screened potential. As shown above, this approximate solution, which served as a very good first step for the iteration procedure, agrees very well with the numerical one. Another important point is that, in contrast with standard perturbative calculations, the value of r_0 did not have to be too small.

As for the single-particle energy $E_{n,k_z,\sigma}$, similar to Ref. [35], we can describe it in the framework of the local-density approximation (LDA)[10]. This is because it is not sufficient to consider only the exchange and correlation correction to the free electron energy. To be self consistent, the single-particle energy should be the eigenvalue of the the single-particle Schrodinger equation ($T = 0$)

$$[h^0 + V_{xc}(y)]|\varphi\rangle = E_{n,k_z,\sigma}|\varphi\rangle, \tag{4.37}$$

where $V_{XC}(y)$ is the effective potential. Now as in Ref. [35] we take

$$V_{XC}(y) \approx \varepsilon^{ec}_{0,y/l^2,1} = \varepsilon^{ec}_{0,k_z,1} \qquad |y| \leq y_0(k_F). \tag{4.38}$$

As for the region $|y| > y_0(k_F)$, we take $V_{XC}(y) = 0$. Considering that the effective potential is much smaller than the free electron energy [From (3.11), we can

estimate that, for the electron centered at $y_0 = k_{x0}\tilde{l}^2$, the harmonic potential in y direction $\hbar\tilde{\omega}(\tilde{k}_x - \tilde{k}_{x0})^2/2 \gg \hbar\tilde{\omega}$ (within the channel of width W), while $|V_{XC}| < \hbar\tilde{\omega}$], the eigenvalue can be obtained using first-order perturbation theory as:

$$E_{0,k_x,1} = \varepsilon_{0,k_x,1} + \langle 0, k_x, 1|V_{XC}(y)|0, k_x, 1\rangle. \tag{4.39}$$

We now apply our theory to the experiment of Ref. [50] in GaAlAs/GaAs QWs. The parameters for sample 1 are $\hbar\Omega \approx 0.65meV$, $B \approx 10T$, $W \approx 0.30\mu m$; this gives $\tilde{k}_F \approx 15$, $\omega_c/\Omega \approx 25$. For sample 2, the estimated parameters are $\hbar\Omega = (0.46 \pm 0.2)meV$, $B \approx 7.3T$, $W \approx 0.33\mu m$, which lead to $\tilde{k}_F \approx 15$ and $\omega_c/\Omega \approx 32$. [Note, this number is very close to the average value ($\omega_c/\Omega = 33.8$) obtained from the measured data: $\hbar\Omega = (0.46 \pm 0.2)meV$, while in Ref.[35] this ratio was taken as $\omega_c/\Omega = 45$.] We plot our results for sample 1 and sample 2 in Figs. 3 and 4, respectively. Figure 3 shows that electronic correlations suppress the spin-splitting and therefore there is no $\nu = 1$ quantum Hall effect (QHE) state in sample 1. In Fig. 4, at the Fermi edge, there is an activation gap $\Delta E_{\downarrow F} \approx 0.013\hbar\omega_c$. Or the gap between the bottom of the empty ($n = 0, \sigma = -1$) LL (curve 1 represented by $E = \tilde{k}_x^2(\Omega/\omega_c)^2/2$) and the top of the occupied ($n = 0, \sigma = 1$) LL (curve 2) is around $1.5K$. This is very closed to the experimental results [50] $\Delta E_{\downarrow F} \approx 1K$. (Note that, in Figs. 4.6 and 4.7, the energy E does not include the zero point energy $\hbar\tilde{\omega}/2$ and the Zeeman energy, i.e., $E = E_{0,k_x,\sigma} - \hbar\tilde{\omega}/2 - g_0\mu_B\sigma B/2$.)

The single-particle group velocity at the Fermi level $v_g(k_x) = (1/\hbar)(\partial/\partial\tilde{k}_x)E_{0,k_x,1}$ can be calculated as

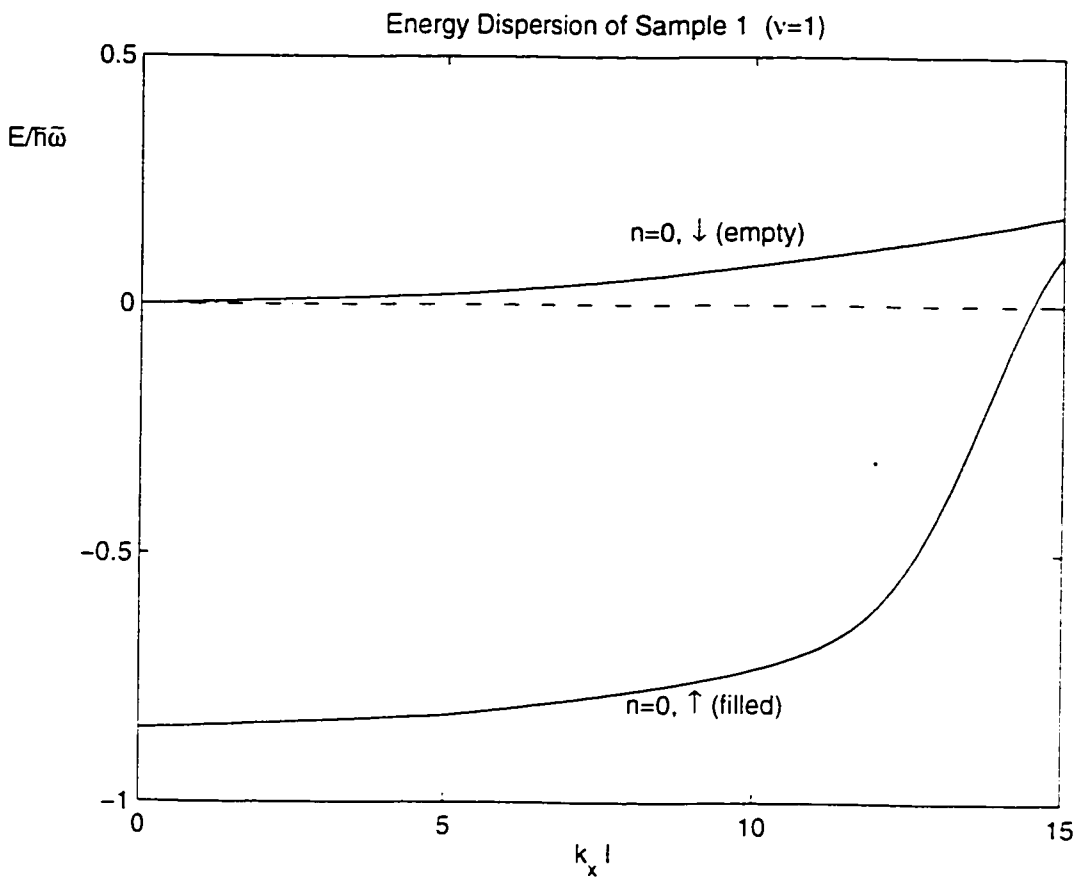

Figure 4.6: Single particle energies $E/(\hbar\tilde{\omega})$ for sample 1 of Ref. [50], with $\nu = 1$. The parameters are $\hbar\Omega \approx 0.65meV$, $B \approx 10T$, $W \approx 0.30\mu m$, $\tilde{k}_F \approx 15$, and $\omega_c/\Omega \approx 25$. Curve 1 shows $E/(\hbar\tilde{\omega}) = \varepsilon_{0,k_x,-1}/(\hbar\tilde{\omega}) - 1/2 = \tilde{k}_x^2(\Omega/\omega_c)^2/2$ for the empty spin down LL. Curve 2 gives total particle energy $E_{0,k_x,1}/(\hbar\tilde{\omega})$ obtained from Eqs. (3.12), (4.32), (4.33), and (4.39). Curve 3 is the quasi-Fermi level. There is no finite gap for a QHE state.

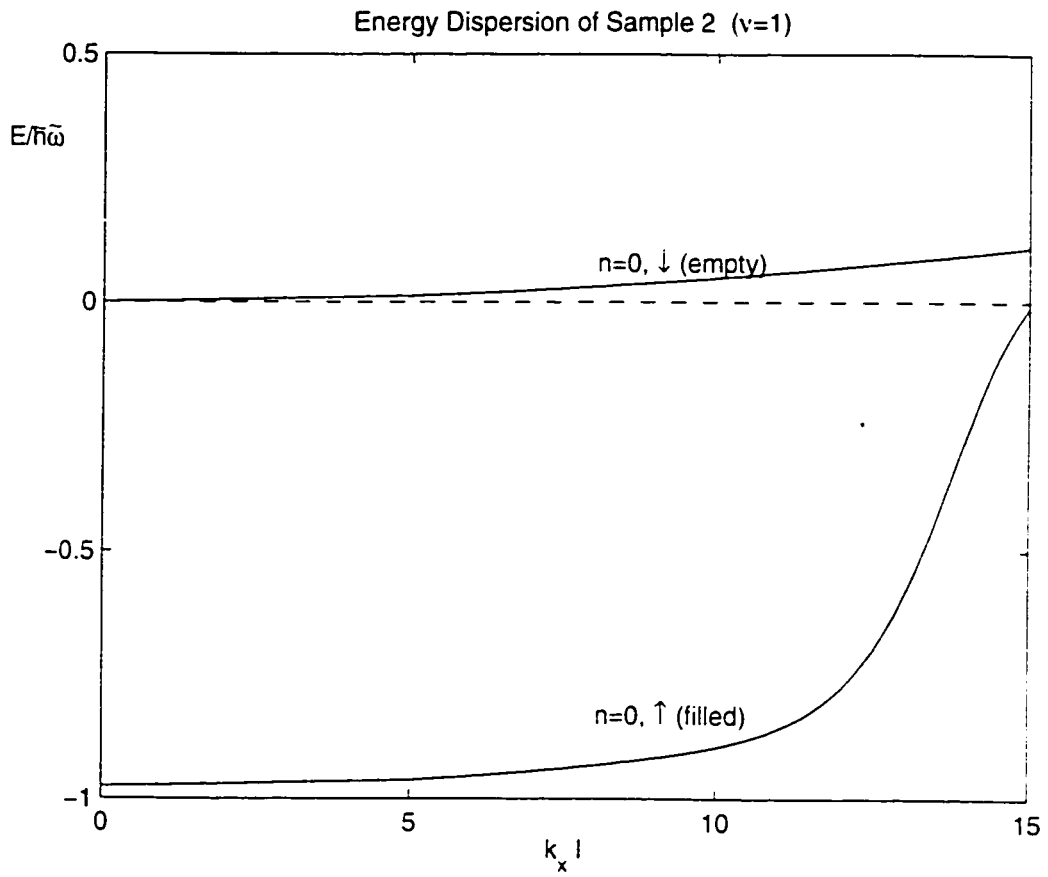

Figure 4.7: Same as in previous figure with the parameters of sample 2 of Ref. [50], i.e., $\hbar\Omega = (0.46 \pm 0.2)meV$, $B \approx 7.3T$, $W \approx 0.33\mu m$, $\tilde{k}_F \approx 15$, and $\omega_c/\Omega \approx 32$. In contrast with Sample 1, when exchange and correlations are taken into account a gap appears between the curves for the $\sigma = -1$ and $\sigma = 1$ LLs and leads to the $\nu = 1$ QHE state.

$$v_g(k_F) = v_g^H(k_F) + \frac{l}{\hbar}\frac{\partial}{\partial k_x}\langle 0, k_x, 1|\xi^{ec}_{0,k_z',1}|0, k_x, 1\rangle|_{k_x \to k_F} \tag{4.40}$$

A numerical calculation gives $v_g(k_F) = 6.9v_g^H$ and $v_g(k_F) \approx 11v_g^H$ for sample 1 and 2, respectively. These two are very close to those given in Ref. [35], where the results are $v_g(k_F) = 5v_g^H$ and $v_g(k_F) \approx 10v_g^H$ for sample 1 and 2. (In Ref. [35], the results for sample 1 and 2 have been interchanged by mistake. Later it was found by our suggestion, cf. the private communication with the related author[75].)

4.2 $\nu = 2$

4.2.1 Basic formulas

The exchange and correlation contribution to the single-particle energy, when the spin $\uparrow$ and $\downarrow$ states of the $n = 0$ LLs are fully occupied, can be calculated according to Eq.(3.46):

$$\varepsilon^{ec}_{0,k_x,\uparrow} \approx \sum_{k'_x} \langle 0, k_x, \uparrow | \langle 0, k'_x, \uparrow | V_2^s(R, R') | 0, k_x, \uparrow \rangle | 0, k'_x, \uparrow \rangle, \tag{4.41}$$

where $V_2^s(R, R')$ is the screened potential for $\nu = 2$ and is assumed to be independent of the spin operator s_z. Similarly, we have

$$\varepsilon^{ec}_{0,k_x,\downarrow} \approx \sum_{k'_x} \langle 0, k_x, \downarrow | \langle 0, k'_x, \downarrow | V_2^s(R, R') | 0, k_x, \downarrow \rangle | 0, k'_x, \downarrow \rangle \tag{4.42}$$

Neglecting the difference between the eigenstate $|0, k'_x, \sigma\rangle$ and the free electron eigenstate $|0, k'_x\rangle|\sigma\rangle$, we have

$$\begin{aligned} \varepsilon^{ec}_{0,k_x,\uparrow} \approx \varepsilon^{ec}_{0,k_x,\downarrow} &\approx \sum_{k'_x} \langle 0, k_x | \langle 0, k'_x | V_2^s(R, R') | 0, k_x \rangle | 0, k'_x \rangle \\ \approx & -\frac{1}{(2\pi)^3} \int dk'_x dq_y dq'_y V_2^s(k_x - k'_x, q_y, q'_y) (0k_x | e^{iq_y y} | 0k'_x) (0, k'_x | e^{iq'_y y} | 0, k_x). \end{aligned} \tag{4.43}$$

Equation (4.43) means that the exchange and correlation on the spin $\uparrow$ level is the same as that on the spin $\downarrow$ level. Note that this does not mean the calculated result would be the same as that in $\nu = 1$ case, for the screened potential has been

changed. The screened potential obeys

$$V_{c2}^{s}(q_x, q_y, q_y') = \frac{v_0\,\delta(q_y + q_y')}{q} + \frac{v_0}{8\pi^3 q}\int_{-\infty}^{\infty} dq_{y1}\, V_{c2}^{s}(q_x, q_{y1}, q_y')$$
$$\times \sum_{n_\alpha, n_\beta, \sigma} \int dk_{x\alpha} F_{\alpha,\beta}^{\sigma}(n_\alpha, k_{x\alpha}|e^{iq_{y1}y}|n_\beta, k_{x\alpha} - q_x)(n_\beta, k_{x\alpha} - q_x|e^{-iq_y y}|n_\alpha, k_{x\alpha}). \tag{4.44}$$

For $\nu = 2$, the nonzero $F_{\alpha,\beta}^{\sigma}$ are $F_{0,n}^{\pm 1}$ and $F_{n,0}^{\pm 1}$ ($n = 0, 1, 2, 3, \ldots$). In the following discussion, we will neglect the influence caused by the Zeeman Energy and take

$$F_{\alpha,\beta}^{\uparrow} \approx F_{\alpha,\beta}^{\downarrow} \approx F_{\alpha,\beta} = \frac{f_{n_\alpha,k_{x\alpha}} - f_{n_\beta,k_{x\beta}}}{\varepsilon_{n_\alpha,k_{x\alpha}} - \varepsilon_{n_\beta,k_{x\beta}}}. \tag{4.45}$$

with

$$f_{n,k_x} = \frac{1}{1 + e^{(\epsilon_{n,k_x} - E_{F2})/kT}} \tag{4.46}$$

and

$$\epsilon_{n,k_x} = \hbar\tilde{\omega}(n + 1/2) + \hbar^2 k_x^2/2\tilde{m}. \tag{4.47}$$

4.2.2 Solution of the integral equation for $\nu = 2$

Similar to the approach for the $\nu = 1$ case, we split V_2^s as $V_{c2}^s(q_x, q_y, q_y') = v_0\delta(q_y + q_y')/q + V_{c2}^s(q_x, q_y, q_y')(q = \sqrt{q_x^2 + q_y^2})$, with V_{c2}^s satisfying

$$
\begin{aligned}
& V_{c2}^s(q_x, q_y, q_y') \\
= & \frac{v_0^2}{8\pi^3 q q'} \sum_{n_\alpha, n_\beta} \int dk_{x\alpha} 2F_{\alpha,\beta}(n_\alpha, k_{x\alpha}|e^{-iq_y' y}|n_\beta, k_{x\alpha} - q_x)(n_\beta, k_{x\alpha} - q_x|e^{-iq_y y}|n_\alpha, k_{x\alpha}) \\
+ & \frac{v_0}{8\pi^3 q} \int_{-\infty}^{\infty} dq_{y1} V_{c2}^s(q_x, q_{y1}, q_y') \\
& \times \sum_{n_\alpha, n_\beta} \int dk_{x\alpha} 2F_{\alpha,\beta}(n_\alpha, k_{x\alpha}|e^{iq_{y1} y}|n_\beta, k_{x\alpha} - q_x)(n_\beta, k_{x\alpha} - q_x|e^{-iq_y y}|n_\alpha, k_{x\alpha}).
\end{aligned}
\tag{4.48}
$$

with $q' = \sqrt{q_x^2 + q_y'^2}$. As Eq. (4.48) can be obtained from Eq. (4.3) by changing $F_{\alpha,\beta}$ to $2F_{\alpha,\beta}$, we can predict that the form of the solution of Eq.(4.48) should be similar to that of the $\nu = 1$ case. Indeed, following the approach used for $\nu = 1$, we obtain

$$
\begin{aligned}
& V_{c2}^s(q_x, q_y, q_y') = v_0 \Phi(\tilde{q}_x, \tilde{q}_y)\Phi(\tilde{q}_x, \tilde{q}_y') \\
\times & \; [k_{c2} \cos \tilde{k}_{F2}\tilde{q}_y \cos \tilde{k}_{F2}\tilde{q}_y' + k_{s2} \sin \tilde{k}_{F2}\tilde{q}_y \sin \tilde{k}_{F2}\tilde{q}_y' + k_{sc2}(\tilde{q}_x^2 - \tilde{q}_y \tilde{q}'_y) sinc(\tilde{q}_y + \tilde{q}_y')].
\end{aligned}
\tag{4.49}
$$

where $\Phi(\tilde{q}_x, \tilde{q}_y)$ is given in Eq. (4.14) and ($\nu = 2$)

$$
\begin{aligned}
k_{i\nu}(\tilde{q}_x, \tilde{q}_y, \tilde{q}_y') &= -\frac{\pm\nu\alpha_0}{1 + \nu\alpha_0 \tilde{K}_{\pm,\nu}} \frac{1}{1 + \nu\frac{r_0}{2}\tilde{q}e^{-\tilde{q}^2/2}} \left[1 - \frac{\nu\frac{r_0}{2} X \tilde{q}' e^{-\tilde{q}'^2/2}}{1 + \nu r_0 \tilde{q}' e^{-\tilde{q}'^2/2}}\right] \\
&\equiv -\frac{\pm\alpha_0\nu}{1 + \nu\alpha_0 \tilde{K}_{\pm,\nu}} C_1^\nu(\tilde{q}_x, \tilde{q}_y) C_2^\nu(X, \tilde{q}_x, \tilde{q}'_y). \\
& (: i = c : +: \;\; i = s : -:)
\end{aligned}
\tag{4.50}
$$

and

$$\tilde{\kappa}_{sc\nu}(\tilde{q}_x, \tilde{q}_y, \tilde{q}_y') = \frac{-X\nu r_0/\pi}{1 + \nu r_0 \tilde{q} e^{-\tilde{q}^2/2}}, \tag{4.51}$$

where $X, K_{\pm,\nu}$ are given by Eq. (4.24) and Eq. (4.29), respectively. For $\nu = 1$, this expression leads to the screened fields given earlier.

Note that although the form of the above solution is very similar to that for $\nu = 1$, the parameters in this solution need to be modified according to

$$\tilde{k}_{F,\nu} = \frac{\tilde{k}_{F,1}}{\sqrt{\nu}} = \frac{\tilde{k}_F}{\sqrt{\nu}}, \tag{4.52}$$

$$(\frac{\tilde{\omega}}{\Omega})_\nu = \frac{1}{\nu}(\frac{\tilde{\omega}}{\Omega})_1, \tag{4.53}$$

$$r_{0,\nu} = \frac{r_{0,1}}{\sqrt{\nu}} = \frac{r_0}{\sqrt{\nu}}. \tag{4.54}$$

Compared with the numerical solution, screened fields given by (4.49) are confirmed to be very good approximations when $\tilde{q}_x \gg \tilde{k}_F$ and $\tilde{q}_x \ll \tilde{k}_F$. (This is similar to the case of $\nu = 1$.) When $\tilde{q}_x$ is around $\tilde{k}_F$, there are certain differences between the numerical solution and the analytic one. As shown in Figs. 4.8 to 4.9, the analytic approximations for $\nu = 2$ are not as accurate as that for $\nu = 1$ shown in Fig. 4.2, because the larger the value of $\tilde{k}_F$, the better is the approximations in Eqs. (4.20). For the case of $\nu = 3$, i.e., ($\tilde{k}_F = 8.6$), we can predict that the analytic approximations will be less accurate than those for $\nu = 2$, but not by much. This is because from $\nu = 2$ ($\tilde{k}_{F2} = 10.6$) to $\nu = 3$($\tilde{k}_{F3} = 8.6$), the change of $\tilde{k}_F$ is not large.

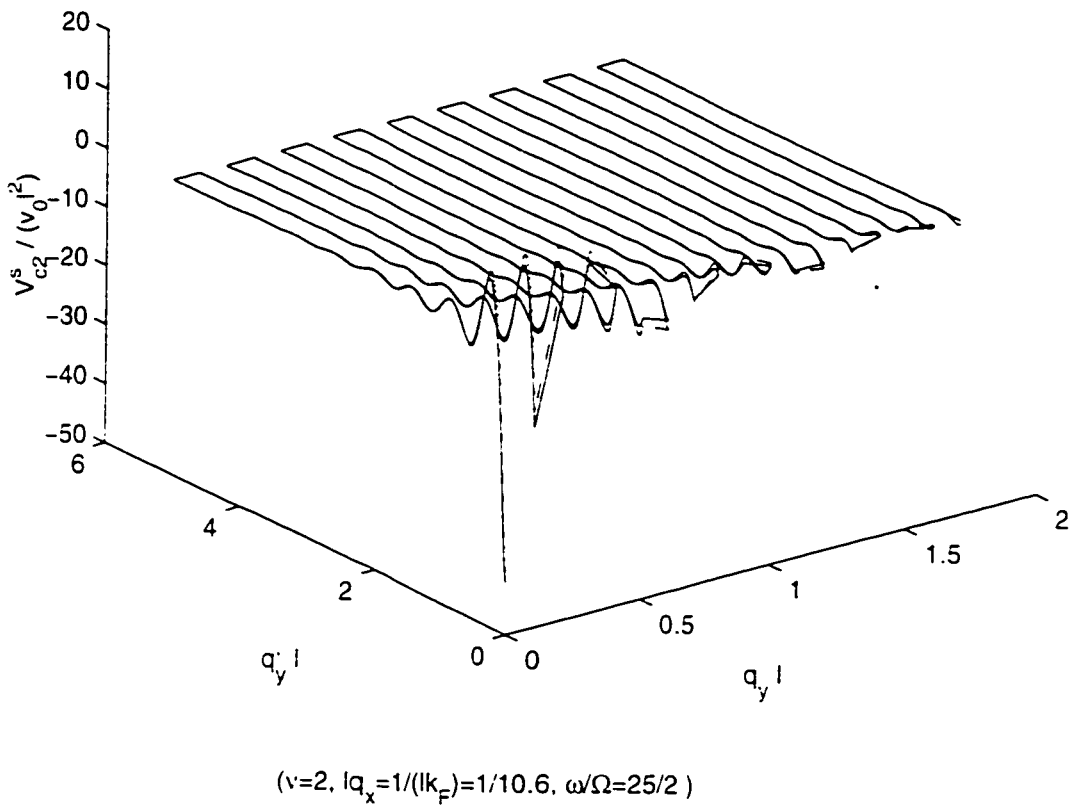

Figure 4.8: Solved correlation interactions in QW (Sample 1 of Ref. [50]) with $\nu = 2, \tilde{k}_{F2} = 10.6$, and $\Omega = \omega/12.5$. Dashed curve is the approximate analytic solution and the solid one shows the numerical calculation. For $\tilde{q}_x \sim 1/\tilde{k}_{F2} = 1/10.6$, there are certain differences between the numerical solution and the analytical one.

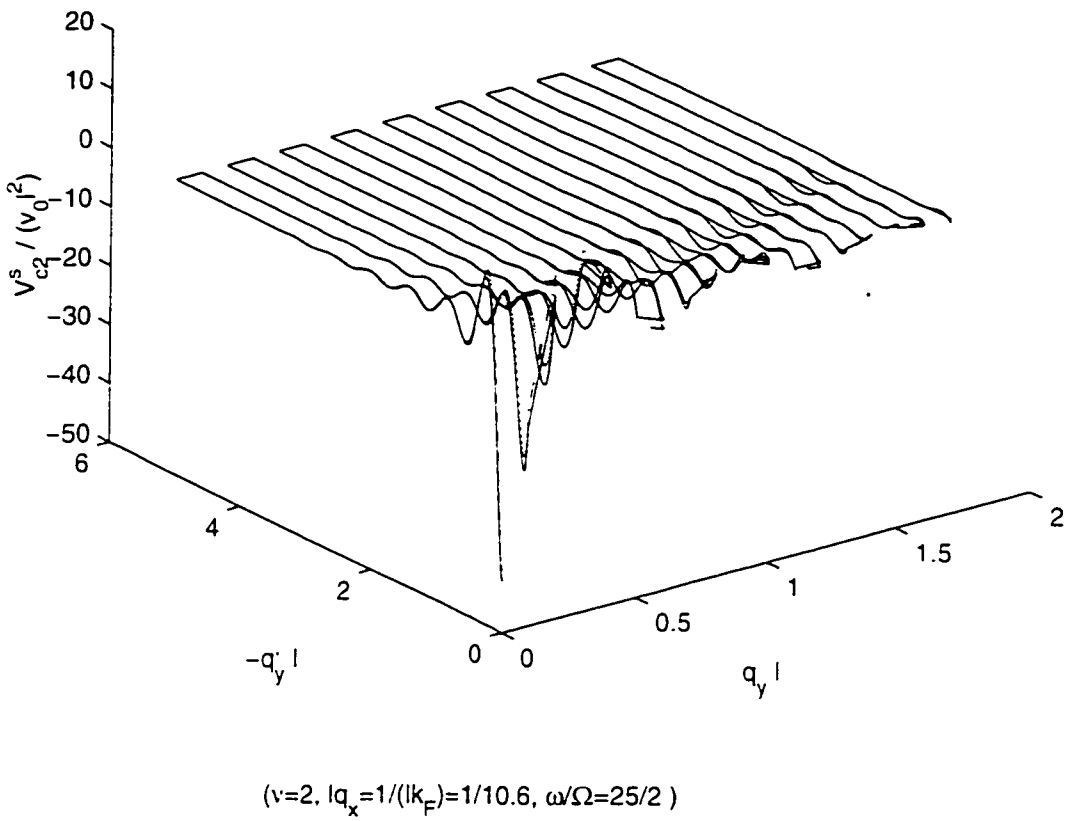

Figure 4.9: Solved correlation interactions in QW (Sample 1 of Ref. [50]) with $\nu = 2$, $\tilde{k}_{F2} = 10.6$, $\tilde{q}_x = 1/\tilde{k}_{F2}$ and $\Omega = \omega/12.5$. Dashed curve is the approximate analytic solution and the solid one shows the numerical calculation. In this figure $\tilde{q}_{y'} < 0$, while in the previous figure, $\tilde{q}_{y'} > 0$.

4.2.3 Exchange and correlation energies, group velocities near the Fermi edge

Based on the discussion in subsection 4.2.1 and with the help of Eqs. (3.48), (4.43), (4.45), (4.50), and (4.51), we have ($\tilde{k}_{F2} = \tilde{k}_F/\sqrt{2}$)

$$
\begin{aligned}
& \varepsilon^{co}_{0,k_x,1} \approx \varepsilon^{co}_{0,k_x,-1} \\
\approx \quad & -\frac{1}{(2\pi)^3}\int_{-k_{F2}}^{k_{F2}} dk'_x \int_{-\infty}^{\infty} dq_y dq'_y V^s_{c2}(k_x - k'_x, q_y, q'_y)(0k_x|e^{iq_y y}|0k'_x)(0k'_x|e^{iq'_y y}|0k_x) \\
= \quad & -\frac{1}{(2\pi)^3}\left(\int_0^{\tilde{k}_{F2}-\tilde{k}_x} - \int_0^{\tilde{k}_x-\tilde{k}_{F2}}\right)\frac{d\tilde{k}_-}{\tilde{l}}\int_{-\infty}^{\infty} dq_y dq'_y v_0 \tilde{l}^2 \frac{e^{-\tilde{q}_-^2/4-\tilde{q}'^2_-/4}}{\tilde{q}_-\tilde{q}'_-} \\
& \times [k_{c2}\cos\tilde{k}_{F2}\tilde{q}_y \cos\tilde{k}_{F2}\tilde{q}'_y + k_{s2}\sin\tilde{k}_{F2}\tilde{q}_y \sin\tilde{k}_{F2}\tilde{q}'_y \\
& + k_{sc2}(\tilde{q}_x^2 - \tilde{q}_y\tilde{q}'_y)sinc(\tilde{q}_y + \tilde{q}'_y)] \times e^{i\tilde{q}_y\tilde{k}_-/2-\tilde{q}_-^2/4} e^{i\tilde{q}'_y\tilde{k}_-/2-\tilde{q}'^2_-/4}.
\end{aligned}
\tag{4.55}
$$

and

$$
\varepsilon^{ex}_{0,k_x,1} \approx \varepsilon^{ex}_{0,k_x,-1} = -\frac{v_0}{(2\pi)^3}\left(\int_0^{\tilde{k}_F-\tilde{k}_x} + \int_0^{\tilde{k}_F-\tilde{k}_x}\right)\frac{d\tilde{k}_-}{\tilde{l}}\int d\tilde{q}_y \frac{e^{-\tilde{q}_-^2/2}}{\tilde{q}_-} \tag{4.56}
$$

We can see from Eqs. (4.55), (4.56) that the group velocity $v_g^{ec}(\tilde{k}_{F2})$ near Fermi edge does not diverge and its value is about half of the Fermi edge group velocity $v_g^{HA}(k_{F2})$ in the HA. This is shown below.

$$
\begin{aligned}
v_g^{ec}(k_{F2}) &= \frac{l}{\hbar}\frac{\partial}{\partial \tilde{k}_x}\varepsilon^{ec}_{0,k_x,\sigma}|_{k_x\to k_{F2}} \\
&= \frac{l\tilde{\omega}r_0}{2\pi}\left[K_0(\frac{\tilde{k}_0^2}{4}) - \frac{2a_0\tilde{K}_+(\tilde{k}_0)\tilde{K}_+(\tilde{k}_0)}{1+2a_0\tilde{K}_-(\tilde{k}_0)} - \frac{2a_0\tilde{K}_-(\tilde{k}_0)\tilde{K}_-(\tilde{k}_0)}{1+2a_0\tilde{K}_-(\tilde{k}_0)}\right]|_{\tilde{k}_0\to 0}.
\end{aligned}
\tag{4.57}
$$

or

$$v_g^{ec}(k_{F2}) = \frac{l\tilde{\omega}r_0}{2\pi}\left[K_0(\frac{\tilde{k}_0^2}{4}) - (1 - \frac{1}{1+2a_0\tilde{K}_-})K_- - (1 - \frac{1}{1+2a_0\tilde{K}_-})K_-\right]|_{\tilde{k}_0\to 0}$$

$$\approx l\Omega(\frac{\Omega}{\tilde{\omega}}\tilde{k}_{F2})\left[\frac{K_-}{\tilde{K}_-} + \frac{K_-}{\tilde{K}_-} - \frac{K_-}{2a_0\tilde{K}_-^2}\right]/(2\nu)|_{\tilde{k}_0=0} \tag{4.58}$$

which is smaller than the value given by Eq.(4.35). Similar to the calculation in Eq.4.36, we have, in strong magnetic field,

$$v_g^{ec}(k_{F2}) \approx v_g^{HA}(k_{F2})/2. \tag{4.59}$$

Note that $v_g^{HA}(k_{F1}) \neq v_g^{HA}(k_{F2})$. The factor 1/2 in Eq.(4.59) is due to the fact that the total screened interaction comes from the two lowest occupied LLs. It is also necessary to point out that Eq. (4.36) and Eq. (4.59) do not mean that the Fermi-edge slopes of the energy correction are not affected by the parameters of QW samples. Actually, they are not so sensitive to the QW parameters. In the later sections, we will see that, for $\nu = 3$, the results are much more complicated and they are effected by the parameter a_0.

4.2.4 Single particle energies for $\nu = 2$ QHE states

The single-particle energy for the case of $\nu = 2$ can be calculated in the manner described in subsection 4.1.4. We have

$$E_{0,k_z,\sigma}|_{\nu=2} = \varepsilon_{0,k_z,\sigma} + \langle |V_{XC}(y)| \rangle \quad (\sigma = \pm 1) \tag{4.60}$$

with

$$\langle |V_{XC}(y)| \rangle = \int_{-\tilde{k}_F}^{\tilde{k}_F} d\tilde{k}'_z \varepsilon^{ec}_{0,k'_z,\sigma} \frac{e^{-(\tilde{k}'_z - \tilde{k}_z)^2}}{\sqrt{\pi}} \tag{4.61}$$

and $\varepsilon^{ec}_{0,k'_z,\pm 1}$ is the sum of Eq. (4.55) and Eq. (4.56).

Figs. 4.10 and 4.11 show the energy dispersion curves for sample 1 and 2 for $\nu = 2$. As can be seen, both samples have obvious gaps between the bottom of the empty $(n = 1, \sigma = 1)$ LL and the top of the occupied $(n = 0, \sigma = \pm 1)$LL's. This is consistent with the experimentally observed results[50]. The main reason is that the energy difference $(\hbar\omega_c)$ between $n = 0$ and $n = 1$ LLs is much larger than the total exchange and correlation corrections. Therefore, for $\nu = 2$, it is very hard to let the correlations be strong enough to destroy the QHE state. Also, near the Fermi edge, the slope of the total single-particle energy is smaller than for $\nu = 1$. For sample 1 (2), we have $v_g(\tilde{k}_{F2}) \approx 3(4) v_g^{HA}(\tilde{k}_{F2})$. In spite of this, we still can conclude that the overall exchange-correlation corrections in these samples have no effect on the flattening of edge states discussed in Ref. [51].

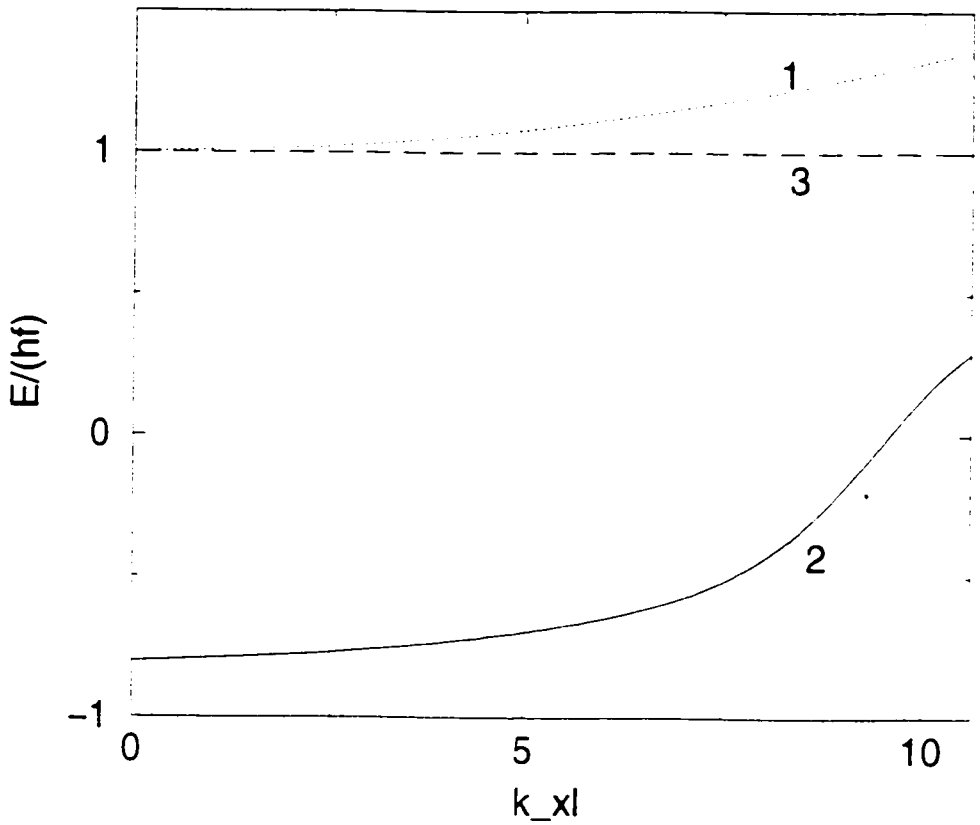

Figure 4.10: Single particle energies as functions of $\tilde{k}_x$, for sample 1 of Ref. [50], with $\nu = 2$. The parameters are $\hbar\Omega \approx 0.65meV$, $B \approx 5T$, $W \approx 0.30\mu m$, $\tilde{k}_{F2} \approx 10.6$, and $\omega_c/\Omega \approx 12.5$. Curve 1 shows $E/(\hbar\omega_c) = (\varepsilon_{1,k_x,1}/(\hbar\omega_c) - 1/2 = \tilde{k}_x^2(\Omega/\omega_c)^2/2$ of the empty ($n = 1, \sigma = 1$) LL. Curve 2, obtained from Eq.(4.60), is the single-particle energy $E_{0,k_x,\pm 1}/(\hbar\omega_c) - 1/2$ of the occupied ($n = 0, \sigma = \pm 1$) LL. The Zeeman energy splitting has been neglected. Curve 3 is the Fermi level. There is an obvious energy gap for the $\nu = 2$ QHE state.

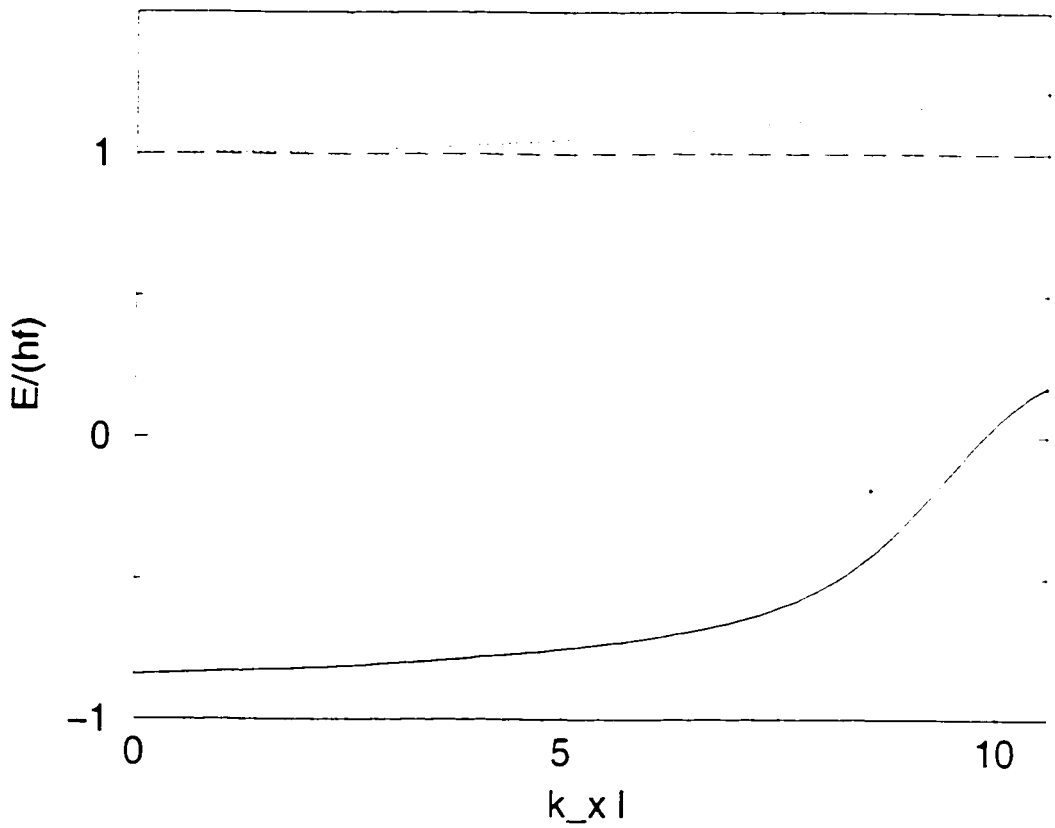

Figure 4.11: Same as in previous figure with the parameters of sample 2 of Ref. [50], i.e., $\hbar\Omega = (0.46 \pm 0.2)meV$, $B \approx 3.65T$, $W \approx 0.33\mu m$, $\tilde{k}_{F2} \approx 10.6$, and $\omega_c/\Omega \approx 16$. The Zeeman splitting between the two lowest LLs is very small ($\Delta E_{Zeeman} \approx 0.013\hbar\omega$) and has been neglected. Curve 3 is the Fermi level. The finite gap between the empty ($n = 1, \sigma = 1$) LL and the occupied ($n = 0, \sigma = \pm 1$) LLs means that the $\nu = 2$ QHE state is a thermodynamically allowed equilibrium state.

4.3 $\nu = 3$

The discussion for $\nu = 3$ is similar to that for $\nu = 1, 2$. But the relevant calculations are much more complicated. This is mainly because, taking into account up to adjacent-level screening, there are many nonzero coupling coefficients $F^{\sigma}_{\alpha,\beta}$ in the simplified Poisson-PRA equation for $\nu = 3$. To show the related calculation clearly, lets start from the matrix elements related to the nonzero coefficients $F^{\sigma}_{\alpha,\beta}$.

4.3.1 Integral equation for $\nu = 3$

According to the discussion given in subsection 3.2.7, the nonzero $F^{\sigma}_{\alpha,\beta}$ that need to be considered, within the adajecent-level approximation, are $F^{\pm 1}_{(0,0)}$, $F^{\pm 1}_{(1,0)}$, $F^{\pm 1}_{(0,1)}$, $F^{1}_{(1,1)}$, $F^{1}_{(2,1)}$, and $F^{1}_{(1,2)}$.

With the help of Eq. (3.14) and the approximation (3.52), the relevant terms in the integral equation (3.49) can be calculated. For example:

$$\begin{aligned} P_{0,0} &= \int_{-\infty}^{\infty} dk_{x\alpha} F_{0,0}(0, k_x|e^{-iq_{y'}y}|0, k_{x\alpha} - q_x)(0, k_{x\alpha} - q_x|e^{-iq_y y}|0, k_x) \\ &= v_1 e^{-\tilde{q}^2/4} e^{-\tilde{q}'^2/4} 2\cos(\tilde{q}_y + \tilde{q}'_y)\tilde{k}_F \end{aligned} \tag{4.62}$$

$$\begin{aligned} P_{1,1} &= \int_{-\infty}^{\infty} dk_{x\alpha} F_{1,1}(1, k_x|e^{-iq_{y'}y}|1, k_{x\alpha} - q_x)(1, k_{x\alpha} - q_x|e^{-iq_y y}|1, k_x) \\ &= v_1 e^{-\tilde{q}^2/4} e^{-\tilde{q}'^2/4} 2\cos(\tilde{q}_y + \tilde{q}'_y)\tilde{k}_F(1 - \tilde{q}^2/2)(1 - \tilde{q}'^2/2) \end{aligned} \tag{4.63}$$

$$P_{0,1} = \int_{-\infty}^{\infty} dk_{x\alpha} F_{0,1}(0, k_x|e^{-iq_{y'}y}|1, k_{x\alpha} - q_x)(1, k_{x\alpha} - q_x|e^{-iq_y y}|0, k_x)$$

$$\approx \frac{1}{\hbar\tilde{\omega}\tilde{l}} e^{-\tilde{q}^2/4} e^{-\tilde{q}'^2/4} [\tilde{q}_x^2 - i(\tilde{q}_y + \tilde{q}'_y)\tilde{q}_x - \tilde{q}_y\tilde{q}'_y] sinc(\tilde{q}_y + \tilde{q}'_y) \tag{4.64}$$

$$P_{1.0} = \int_{-\infty}^{\infty} dk_{x\alpha} F_{1.0}(1, k_x | e^{-iq_{y'}y} | 0, k_{x\alpha} - q_x)(0, k_{x\alpha} - q_x | e^{-iq_y y} | 1, k_x)$$
$$\approx \frac{1}{\hbar\tilde{\omega}\tilde{l}} e^{-\tilde{q}^2/4} e^{-\tilde{q}'^2/4} [\tilde{q}_x^2 + i(\tilde{q}_y + \tilde{q}'_y)\tilde{q}_x - \tilde{q}_y\tilde{q}'_y] sinc(\tilde{q}_y + \tilde{q}'_y) \tag{4.65}$$

$$P_{1.2} = \int_{-\infty}^{\infty} dk_{x\alpha} F_{1.2}(1, k_x | e^{iq_{y'}y} | 2, k_{x\alpha} - q_x)(2, k_{x\alpha} - q_x | e^{-iq_y y} | 1, k_x)$$
$$\approx \frac{-2}{\hbar\tilde{\omega}\tilde{l}} sinc(\tilde{q}_y + \tilde{q}'_y) e^{-\tilde{q}^2/4} e^{-\tilde{q}'^2/4} \frac{(\tilde{q}_x - i\tilde{q}_y)(\tilde{q}_x - i\tilde{q}'_y)}{4} (2 - \tilde{q}^2/2)(2 - \tilde{q}'^2/2) \tag{4.66}$$

$$P_{2.1} = \int_{-\infty}^{\infty} dk_{x\alpha} F_{2.1}(2, k_x | e^{iq_{y'}y} | 1, k_{x\alpha} - q_x)(1, k_{x\alpha} - q_x | e^{-iq_y y} | 2, k_x)$$
$$\approx \frac{-2}{\hbar\tilde{\omega}\tilde{l}} sinc(\tilde{q}_y - \tilde{q}'_y) e^{-\tilde{q}^2/4} e^{-\tilde{q}'^2/4} \frac{(\tilde{q}_x + i\tilde{q}_y)(\tilde{q}_x + i\tilde{q}'_y)}{4} (2 - \tilde{q}^2/2)(2 - \tilde{q}'^2/2) \tag{4.67}$$

From Eq. (4.65) to Eq. (4.67), $e^{\pm i(\tilde{q}_y - \tilde{q}'_y)\tilde{q}_x/2} \approx 1$ has been used because of the factor $sinc(\tilde{q}_y + \tilde{q}'_y)$.

Substituting Eqs. (4.62)-(4.67), into the integral equation (3.49) and splitting V_{c3}^s, in an exchange and a correlation, i.e., $V_{c3}^s = v_o\delta(q_y + q'_y)/q + V_3^c(q_x, q_y, q'_y)$, the correlation integral equation for $\nu = 3$ takes the form

$$\begin{aligned} V_{c3}^s(q_x, q_y, q'_y) &= \frac{2v_0 v_1 \tilde{l}^2}{8\pi^3} v_0 \frac{e^{-\tilde{q}^2/4}}{\tilde{q}} \frac{e^{-\tilde{q}'^2/4}}{\tilde{q}'} \\ &\times [2\cos\tilde{k}_{F3}(\tilde{q}_y + \tilde{q}'_y) - \frac{2}{\hbar\tilde{l}v_1}(\tilde{q}_x^2 - \tilde{q}_y\tilde{q}'_y) sinc(\tilde{q}_y + \tilde{q}'_y) \end{aligned}$$

$$+(1-\tilde{q}^2/2)(1-\tilde{q}'^2/2)\cos\tilde{k}_{F3}(\tilde{q}_y+\tilde{q}'_y)$$

$$-\frac{2}{\tilde{\omega}\hbar\tilde{l}v_1}(1-\tilde{q}^2/4)(1-\tilde{q}'^2/4)(\tilde{q}_x^2-\tilde{q}_y\tilde{q}'_y)sinc(\tilde{q}_y+\tilde{q}'_y)]$$

$$+\quad \frac{2v_0v_1}{8\pi^3}\frac{e^{-\tilde{q}^2/4}}{\tilde{q}}\int d\tilde{q}_{y1}V^s_{c3}(q_x,q_{y1},q'_y)e^{-\tilde{q}_1^2/4}$$

$$\times\quad [2\cos\tilde{k}_{F3}(\tilde{q}_y-\tilde{q}_{y1})-\frac{2}{\tilde{\omega}\hbar\tilde{l}v_1}(\tilde{q}_x^2+\tilde{q}_y\tilde{q}_{y1})sinc(\tilde{q}_{y1}-\tilde{q}_y)$$

$$+(1-\tilde{q}_1^2/2)(1-\tilde{q}^2/2)\cos\tilde{k}_{F3}(\tilde{q}_{y1}-\tilde{q}_y)$$

$$-\frac{2}{\tilde{\omega}\hbar\tilde{l}v_1}(1-\tilde{q}_1^2/4)(1-\tilde{q}^2/4)(\tilde{q}_x^2+\tilde{q}_{y1}\tilde{q}_y)sinc(\tilde{q}_{y1}-\tilde{q}_y)]$$

(4.68)

Note that in Eq. (4.68) the terms associated with $2\cos\tilde{k}_{F3}(\tilde{q}_y-\tilde{q}'_y)$ come from the induced charge of the occupied $(n=0,\sigma=1)$ LL, while those with $(1-\tilde{q}^2/2)(1-\tilde{q}'^2/2)\cos\tilde{k}_{F3}(\tilde{q}_y+\tilde{q}'_y)$ come from those at the occupied $(n=1,\sigma=1)$ LL. They all belong to intra-level screening. The rest terms are related to the inter-level screening. For example, the $(\tilde{q}_x^2-\tilde{q}_y\tilde{q}'_y)sinc(\tilde{q}_y+\tilde{q}'_y)$ one comes from the transition between $(n=0,\sigma=1)$ and $(n=1,\sigma=1)$ LLs and the $(1-\tilde{q}^2/4)(1-\tilde{q}'^2/4)(\tilde{q}_x^2-\tilde{q}_y\tilde{q}'_y)sinc(\tilde{q}_y+\tilde{q}'_y)$ one is that between $(n=2,\sigma=1)$ and $(n=1,\sigma=1)$ LLs.

4.3.2 Screened fields in QWs ($\nu=3$)

The solution of the Eq. (4.68) can be sought in the form

$$V^s_{c3}(q_x,q_y,q'_y)=v_0\Phi(\tilde{q}_x,\tilde{q}_y)\Phi(\tilde{q}_x,\tilde{q}'_y)$$

$$\times \quad [K_c(\tilde{q}_x, \tilde{q}_y, \tilde{q'}_y)\cos\tilde{k}_{F3}\tilde{q}_y\cos\tilde{k}_{F3}\tilde{q}'_y + K_s(\tilde{q}_x, \tilde{q}_y, \tilde{q'}_y)\sin\tilde{k}_{F3}\tilde{q}_y\sin\tilde{k}_{F3}\tilde{q}'_y$$

$$+K_{sc}(\tilde{q}_x, \tilde{q}_y, \tilde{q'}_y)(\tilde{q}_x^2 - \tilde{q}_y\tilde{q'}_y)sinc(\tilde{q}_y + \tilde{q}'_y)], \tag{4.69}$$

where $\Phi(\tilde{q}_x, \tilde{q}_y) = \tilde{l}e^{-\tilde{q}^2/4}/\tilde{q}$, as before. K_c, K_s, and K_{sc} can be assumed to have the following forms

$$K_c = 2k_c + k_{cy}(1 - \frac{\tilde{q}^2}{2}) + k_{cy'}(1 - \frac{\tilde{q'}^2}{2}) + k_{cyy'}(1 - \frac{\tilde{q}^2}{2})(1 - \frac{\tilde{q'}^2}{2}),$$

$$K_s = 2k_s + k_{sy}(1 - \frac{\tilde{q}^2}{2}) + k_{sy'}(1 - \frac{\tilde{q'}^2}{2}) + k_{syy'}(1 - \frac{\tilde{q}^2}{2})(1 - \frac{\tilde{q'}^2}{2}),$$

$$K_{cs} = k_{cs}[\,1 + (1 - \frac{\tilde{q}^2}{4})(1 - \frac{\tilde{q'}^2}{4})\,]. \tag{4.70}$$

where $k_c(\tilde{q}_x, \tilde{q}_y, \tilde{q'}_y)$, $k_{cy}(\tilde{q}_x, \tilde{q}_y, \tilde{q'}_y)$, $k_{cy'}(\tilde{q}_x, \tilde{q}_y, \tilde{q'}_y)$, and $k_{cyy'}(\tilde{q}_x, \tilde{q}_y, \tilde{q'}_y)$ are the coefficients of the constant term as well as those of the $(1 - \frac{\tilde{q}^2}{2})$, $(1 - \frac{\tilde{q'}^2}{2})$, and $(1 - \frac{\tilde{q}^2}{2})(1 - \frac{\tilde{q'}^2}{2})$ terms in (4.70), respectively. They can be determined by applying the quasi mode-matching technique. Substituting (4.69), $1/(v_1\hbar\tilde{\omega}\tilde{l}) = -\tilde{k}_{F3}(\frac{\tilde{\Omega}}{\tilde{v}})^2$, and $2v_0v_1/(8\pi^3) = -\frac{r_0}{\pi}(\frac{\tilde{v}}{\tilde{\Omega}})^2/\tilde{k}_{F3} = -\alpha_0$ into Eq.(4.68), we obtain a long integral equation. To treat it in a clearer way, we use $K_c(\tilde{q}_x, \tilde{q}_y, \tilde{q'}_y)cc'$ to denote $K_c(\tilde{q}_x, \tilde{q}_y, \tilde{q'}_y)\cos\tilde{k}_{F3}\tilde{q}_y\cos\tilde{k}_{F3}\tilde{q'}_y$, etc. and have

$$K_c(\tilde{q}_x, \tilde{q}_y, \tilde{q'}_y)cc' + K_s(\tilde{q}_x, \tilde{q}_y, \tilde{q'}_y)ss' + K_{sc}(\tilde{q}_x, \tilde{q}_y, \tilde{q'}_y)(\tilde{q}_x^2 - \tilde{q}_y\tilde{q'}_y)sinc(\tilde{q}_y + \tilde{q'}_y)$$

$$= \quad -\frac{r_0\alpha}{\pi}\{I(\tilde{q}_x, \tilde{q}_y, \tilde{q'}_y)(cc' - ss') + \frac{2}{\alpha}II(\tilde{q}_x, \tilde{q}_y, \tilde{q'}_y)(\tilde{q}_x^2 - \tilde{q}_y\tilde{q'}_y)sinc(\tilde{q}_y + \tilde{q'}_y)$$

$$+ \int \frac{d\tilde{q}_{y1} e^{-\tilde{q}_1^2/2}}{\tilde{q}_1} \times [K_c(\tilde{q}_x, \tilde{q}_{y1}, \tilde{q'}_y) c_1 c'$$

$$+ K_s(\tilde{q}_x, \tilde{q}_{y1}, \tilde{q'}_y) s_1 s' + K_{sc}(\tilde{q}_x, \tilde{q}_{y1}, \tilde{q'}_y)(\tilde{q}_x^2 - \tilde{q}_{y1}\tilde{q'}_y) sinc(\tilde{q}_{y1} + \tilde{q'}_y)]$$

$$\times \quad [I(\tilde{q}_x, \tilde{q}_y, \tilde{q}_{y1})(cc_1 + ss_1) + \frac{2}{\alpha} II(\tilde{q}_x, \tilde{q}_y, \tilde{q}_{y1})(\tilde{q}_x^2 + \tilde{q}_y \tilde{q}_{y1}) sinc(\tilde{q}_y - \tilde{q}_{y1})]\} \quad (4.71)$$

with

$$I(\tilde{q}_x, \tilde{q}_y, \tilde{q'}_y) = 2 + (1 - \frac{\tilde{q}^2}{2})(1 - \frac{\tilde{q'}^2}{2})$$

$$II(\tilde{q}_x, \tilde{q}_y, \tilde{q'}_y) = 1 + (1 - \frac{\tilde{q}^2}{4})(1 - \frac{\tilde{q'}^2}{4}) \quad (4.72)$$

As for $\nu = 1$ and $\nu = 2$, we equate the coefficients of the $\cos \tilde{k}_{F3}\tilde{q}_y \cos \tilde{k}_{F3}\tilde{q}'_y$, $\sin \tilde{k}_{F3}\tilde{q}_y \sin \tilde{k}_{F3}\tilde{q}'_y$, and $(\tilde{q}_x^2 - \tilde{q}_y \tilde{q'}_y) sinc(\tilde{q}_y + \tilde{q}'_y)$ terms on both sides of Eq. (4.71) and obtain following three equations ($\tilde{q}^2 = \tilde{q}_x^2 + \tilde{q}_y^2$, $\tilde{q'}^2 = \tilde{q}_x^2 + \tilde{q'}_y^2$, and $\tilde{q}_1^2 = \tilde{q}_x^2 + \tilde{q}_{y1}^2$)

$$K_c = -\frac{r_0 \alpha}{\pi} \quad \{ \quad I(\tilde{q}_x, \tilde{q}_y, \tilde{q'}_y) + \int \frac{d\tilde{q}_{y1} e^{-\tilde{q}_1^2/2}}{\tilde{q}_1} K_c(\tilde{q}_x, \tilde{q}_{y1}, \tilde{q'}_y) I(\tilde{q}_x, \tilde{q}_y, \tilde{q}_{y1}) c_1^2$$

$$+ \frac{\pi}{2} K_{cs}(\tilde{q}_x, -\tilde{q'}_y, \tilde{q'}_y) I(\tilde{q}_x, \tilde{q}_y, -\tilde{q'}_y) \tilde{q'} e^{-\tilde{q'}^2/2}$$

$$+ \frac{2}{\alpha} \frac{\pi}{2} K_c(\tilde{q}_x, \tilde{q}_y, \tilde{q'}_y) II(\tilde{q}_x, \tilde{q}_y, \tilde{q}_y) \tilde{q} e^{-\tilde{q}^2/2} \quad \}. \quad (4.73)$$

$$K_s = -\frac{r_0 \alpha}{\pi} \quad \{ \quad -I(\tilde{q}_x, \tilde{q}_y, \tilde{q'}_y) + \int \frac{d\tilde{q}_{y1} e^{-\tilde{q}_1^2/2}}{\tilde{q}_1} K_s(\tilde{q}_x, \tilde{q}_{y1}, \tilde{q'}_y) I(\tilde{q}_x, \tilde{q}_y, \tilde{q}_{y1}) s_1^2$$

$$- \frac{\pi}{2} K_{cs}(\tilde{q}_x, -\tilde{q'}_y, \tilde{q'}_y) I(\tilde{q}_x, \tilde{q}_y, -\tilde{q'}_y) \tilde{q'} e^{-\tilde{q'}^2/2}$$

$$+ \frac{2}{\alpha} \frac{\pi}{2} K_s(\tilde{q}_x, \tilde{q}_y, \tilde{q'}_y) II(\tilde{q}_x, \tilde{q}_y, \tilde{q}_y) \tilde{q} e^{-\tilde{q}^2/2} \quad \}. \quad (4.74)$$

and

$$K_{cs} = k_{cs} II(\tilde{q}_x, \tilde{q}_y, \tilde{q'}_y)$$

$$= \frac{-r_0\alpha}{\pi}\{\frac{2}{\alpha}II(\tilde{q}_x, \tilde{q}_y, \tilde{q'}_y) + \frac{2}{\alpha}\pi K_{cs}(\tilde{q}_x, \tilde{q}_y, \tilde{q'}_y)II(\tilde{q}_x, \tilde{q}_y, \tilde{q}_y)\tilde{q}e^{-\tilde{q}^2/2}\} \tag{4.75}$$

From Eq.(4.75), we immediately obtain

$$k_{cs} = \frac{-2r_0/\pi}{1 + 2r_0[1 + (1 - \frac{\tilde{q}^2}{4})^2]\tilde{q}e^{-\tilde{q}^2/2}}. \tag{4.76}$$

As for $\nu = 1$ and 2, we modify k_{cs} as

$$k_{cs} = \frac{-X_3\frac{2r_0}{\pi}}{1 + 2r_0[1 + (1 - \frac{\tilde{q}^2}{4})^2]\tilde{q}e^{-\tilde{q}^2/2}}, \tag{4.77}$$

where

$$X_3 = 1 - e^{-\tilde{q}_x^2}. \tag{4.78}$$

This definition simply gives more accurate analytic approximations, cf. Eq.(4.24). Substituting Eq. (4.70) into Eq. (4.73), we find that $k_c, k_{cy}, k_{cy'}$, and $k_{cyy'}$ are related by following equation.

$$\begin{aligned}
& 2k_c + k_{cy}(1 - \frac{\tilde{q}^2}{2}) + k_{cy'}(1 - \frac{\tilde{q'}^2}{2}) + k_{cyy'}(1 - \frac{\tilde{q}^2}{2})(1 - \frac{\tilde{q'}^2}{2}) \\
= - & \frac{r_0\alpha}{\pi}[2 + (1 - \frac{\tilde{q}^2}{2})(1 - \frac{\tilde{q'}^2}{2})] \\
- & \frac{r_0\alpha}{\pi}\int d\tilde{q}_{y1}\frac{e^{-\tilde{q}_1^2/2}c_1^2}{\tilde{q}_1}[2 + (1 - \frac{\tilde{q}^2}{2})(1 - \frac{\tilde{q}_1^2}{2})] \\
& \times[2k_c + k_{cy1}(1 - \frac{\tilde{q}_1^2}{2}) + k_{cy'}(1 - \frac{\tilde{q'}^2}{2}) + k_{cy1y'}(1 - \frac{\tilde{q}_1^2}{2})(1 - \frac{\tilde{q'}^2}{2})] \\
- & \frac{r_0\alpha}{\pi}\frac{\pi}{2}k_{cs}(\tilde{q}_x, -\tilde{q'}_y, \tilde{q'}_y)[1 + (1 - \frac{\tilde{q'}^2}{4})^2][2 + (1 - \frac{\tilde{q}^2}{2})(1 - \frac{\tilde{q'}^2}{2})]\tilde{q'}e^{-\tilde{q'}^2/2} \\
- & \frac{r_0\alpha}{\pi}\frac{\pi}{2}\frac{2}{\alpha}[1 + (1 - \frac{\tilde{q}^2}{4})^2]\tilde{q}e^{-\tilde{q}^2/2} \\
& \times[2k_c + k_{cy}(1 - \frac{\tilde{q}^2}{2}) + k_{cy'}(1 - \frac{\tilde{q'}^2}{2}) + k_{cyy'}(1 - \frac{\tilde{q}^2}{2})(1 - \frac{\tilde{q'}^2}{2})]
\end{aligned} \tag{4.79}$$

Further, equating the coeficients of the constant term as well as those of the $(1-\frac{\tilde{q}^2}{2})$, $(1-\frac{\tilde{q}'^2}{2})$, and $(1-\frac{\tilde{q}^2}{2})(1-\frac{\tilde{q}'^2}{2})$ terms, we get the following four equations:

$$
\begin{aligned}
2k_c = \quad & -2\frac{r_0\alpha}{\pi} - \frac{r_0\alpha}{\pi}[4k_c(\tilde{q}_x, \tilde{q}'_y)\kappa_+ + 2k_{cy}(\tilde{q}_x, \tilde{q}'_y)(\kappa_+ - \Delta_{c1})] \\
& -r_0\alpha\frac{\frac{-X_3 2r_0}{\pi}[1+(1-\frac{\tilde{q}'^2}{4})^2]\tilde{q}'e^{-\tilde{q}'^2/2}}{1+2r_0[1+(1-\frac{\tilde{q}'^2}{4})^2]\tilde{q}'e^{-\tilde{q}'^2/2}} - r_0 2k_c[1+(1-\frac{\tilde{q}^2}{4})^2]\tilde{q}e^{-\tilde{q}^2/2}
\end{aligned}
\tag{4.80}
$$

$$
\begin{aligned}
k_{cy} = \quad & -r_0 k_{cy}[1+(1-\frac{\tilde{q}^2}{4})^2]\tilde{q}e^{-\tilde{q}^2/2} \\
& -\frac{r_0\alpha}{\pi}[2k_c(\tilde{q}_x, \tilde{q}'_y)(\kappa_+ - \Delta_{c1}) + k_{cy}(\tilde{q}_x, \tilde{q}'_y)(\kappa'_+ - 2\Delta'_{c1} + \Delta'_{c2})]
\end{aligned}
\tag{4.81}
$$

$$
\begin{aligned}
k_{cy'} = \quad & -r_0 k_{cy'}[1+(1-\frac{\tilde{q}^2}{4})^2]\tilde{q}e^{-\tilde{q}^2/2} \\
& -\frac{r_0\alpha}{\pi}[2k_{cy'}(\tilde{q}_x, \tilde{q}'_y)\kappa''_+ + 2k_{cyy'}(\tilde{q}_x, \tilde{q}'_y)(\kappa'''_+ - \Delta'''_{c1})]
\end{aligned}
\tag{4.82}
$$

$$
\begin{aligned}
k_{cyy'} \quad = \quad & \\
& -\frac{r_0\alpha}{\pi} - \frac{r_0\alpha}{\pi}[k_{cy'}(\tilde{q}_x, \tilde{q}'_y)(\kappa''_+ - \Delta''_{c1}) + k_{cyy'}(\tilde{q}_x, \tilde{q}'_y)(\kappa'''_+ - 2\Delta'''_{c1} + \Delta'''_{c2})] \\
& -\frac{r_0\alpha}{2}\frac{\frac{-X_3 2r_0}{\pi}[1+(1-\frac{\tilde{q}'^2}{4})^2]\tilde{q}'e^{-\tilde{q}'^2/2}}{1+2r_0[1+(1-\frac{\tilde{q}'^2}{4})^2]\tilde{q}'e^{-\tilde{q}'^2/2}} - r_0 k_{cyy'}[1+(1-\frac{\tilde{q}^2}{4})^2]\tilde{q}e^{-\tilde{q}^2/2}
\end{aligned}
\tag{4.83}
$$

The solutions are

$$
\begin{aligned}
k_c = \quad & \frac{-r_0\alpha/\pi}{1+\frac{r_0\alpha}{\pi}[2\kappa_+ + \kappa_c(\kappa_+ - \Delta_{c1})]} \\
& \times\frac{1}{1+r_0[1+(1-\frac{\tilde{q}^2}{4})^2]\tilde{q}e^{-\tilde{q}^2/2}}[1-\frac{X_3 r_0[1+(1-\frac{\tilde{q}'^2}{4})^2]\tilde{q}'e^{-\tilde{q}'^2/2}}{1+2r_0[1+(1-\frac{\tilde{q}'^2}{4})^2]\tilde{q}'e^{-\tilde{q}'^2/2}}]
\end{aligned}
$$

$$\equiv \quad \frac{-\alpha_0 D_1(\tilde{q}_x, \tilde{q}_y) D_2(X_3, \tilde{q}_x, \tilde{q}'_y)}{1 + \alpha_0[2\kappa_+ + \lambda_c(\kappa_+ - \Delta_{c1})]} \tag{4.84}$$

$$k_{cy} = \quad \frac{-2\alpha_0(\kappa_+ - \Delta_{c1})}{1 + \alpha_0(\kappa_+ - 2\Delta_{c1} + \Delta_{c2})} k_c \equiv \lambda_c k_c. \tag{4.85}$$

$$k_{cyy'} = \quad \frac{-\alpha_0 D_1(\tilde{q}_x, \tilde{q}_y) D_2(X_3, \tilde{q}_x, \tilde{q}'_y)}{1 + \alpha_0[\lambda_c(\kappa_+ - \Delta_{c1}) + \kappa_+ - 2\Delta_{c1} + \Delta_{c2}]}. \tag{4.86}$$

and

$$k_{cy'} = \quad \frac{-2\alpha_0(\kappa_+ - \Delta_{c1})}{1 + 2\alpha_0\kappa_+} k_{cyy'} \equiv \lambda_c k_{cyy'}. \tag{4.87}$$

Here we have

$$\kappa_\pm(\tilde{q}_x) = \int_{-\infty}^{\infty} \frac{d\tilde{q}_y e^{-\tilde{q}^2/2}(1 \pm \cos 2\tilde{k}_{F3}\tilde{q}_y)/2}{\tilde{q}} D_1(\tilde{q}_x, \tilde{q}_y) \tag{4.88}$$

and

$$\Delta_{i1}(\tilde{q}_x) = \int_{-\infty}^{\infty} d\tilde{q}_y \frac{\tilde{q}}{2} e^{-\tilde{q}^2/2} D_1(\tilde{q}_x, \tilde{q}_y)(1 \pm \cos 2\tilde{k}_{F3}\tilde{q}_y)/2 \quad (i = c : +;\ i = s : -;) \tag{4.89}$$

$$\Delta_{i2}(\tilde{q}_x) = \int_{-\infty}^{\infty} d\tilde{q}_y \frac{\tilde{q}^3}{4} e^{-\tilde{q}^2/2} D_1(\tilde{q}_x, \tilde{q}_y)(1 \pm \cos 2\tilde{k}_{F3}\tilde{q}_y)/2 \quad (i = c : +;\ i = s : -;) \tag{4.90}$$

K_s in (4.69) can also be solved by substituting (4.70) into Eq.(4.74) and then getting the expressions of $k_s, k_{sy}, k_{sy'}$, and $k_{syy'}$ by equating the coefficients of

same type terms. The results are

$$k_s = \frac{\alpha_0 D_1(\tilde{q}_x, \tilde{q}_y) D_2(X_3, \tilde{q}_x, \tilde{q'}_y)}{1 + \alpha_0[2\kappa_- + \lambda_s(\kappa_- - \Delta_{s1})]}, \tag{4.91}$$

$$k_{sy} = \frac{-2\alpha_0(\kappa_- - \Delta_{s1})}{1 + \alpha_0(\kappa_- - 2\Delta_{s1} + \Delta_{s2})} k_s \equiv \lambda_s k_s. \tag{4.92}$$

$$k_{syy'} = \frac{\alpha_0 D_1(\tilde{q}_x, \tilde{q}_y) D_2(X_3, \tilde{q}_x, \tilde{q'}_y)}{1 + \alpha_0[\lambda_s(\kappa_- - \Delta_{s1}) + \kappa_- - 2\Delta_{s1} + \Delta_{s2}]}. \tag{4.93}$$

$$\tag{4.94}$$

and

$$k_{sy'} = \frac{-2\alpha_0(\kappa_- - \Delta_{s1})}{1 + 2\alpha_0\kappa_-} k_{syy'} \equiv \lambda_s k_{syy'}. \tag{4.95}$$

Figures 4.12-4.14 show that the approximate analytic solutions obtained in this subsection agree well with the numerical solutions, from small $\tilde{q}_x$ (e.g., $0.1/\tilde{k}_F = 1/86$), to large $\tilde{q}_x$ (e.g., $\tilde{q}_x = 2$). Similar to the cases of $\nu = 1$ and $\nu = 2$, the analytic approximations are not very accurate when $\tilde{q}_x$ is close to $1/\tilde{k}_F$. Also, the accuracy of the analytic approximation is nearly not affected by the ratio of ω/Ω, at least within the range $25/3 \leq \frac{\omega}{\Omega} \leq 45/3$.

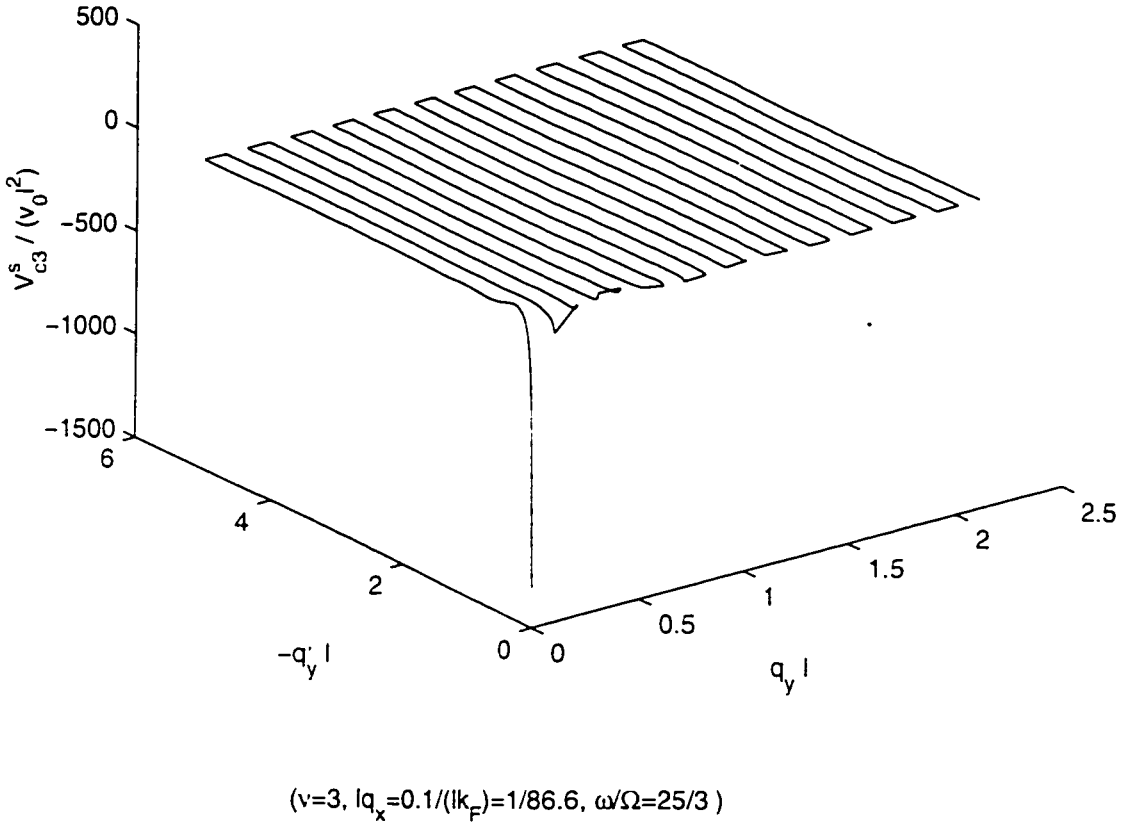

Figure 4.12: Solved correlation interactions in QW (Sample 1 of Ref. [50]) with $\nu = 3, \tilde{k}_{F3} = 8.66$. Dashed curve is the approximate analytic solution and the solid one shows the numerical calculation. The confinement potential is defined by $\Omega = \omega/(25/3)$. In the long wavelength limit, screened fields tend to diverge and the two curves almost coincide with each other.

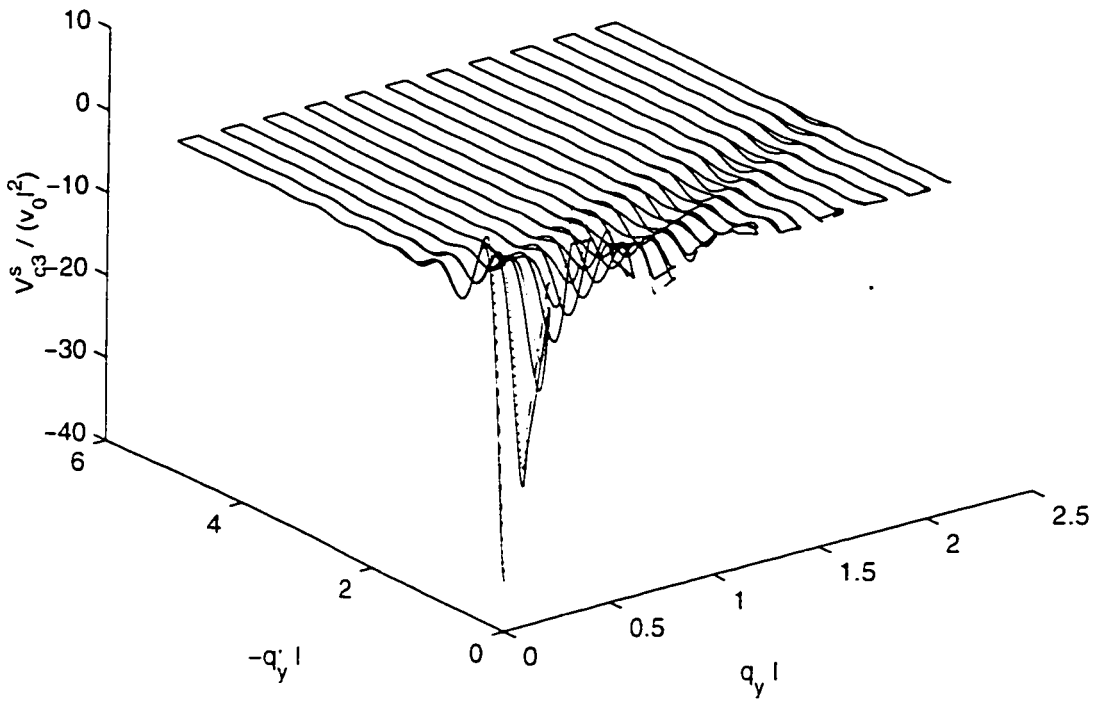

(ν=3, lq_x=1/(lk_F)=1/8.66, ω/Ω=25/3)

Figure 4.13: Solved correlation interactions in QW (Sample 1 of Ref. [50])with $\nu = 3$, $\tilde{k}_{F3} = 8.66$, $\Omega = \omega/(25/3)$. Dashed curve is the approximate analytic solution and the solid one shows the numerical calculation. For $\tilde{q}_x \sim 1/\tilde{k}_F = 1/8.66$, there are certain differences between the two curves.

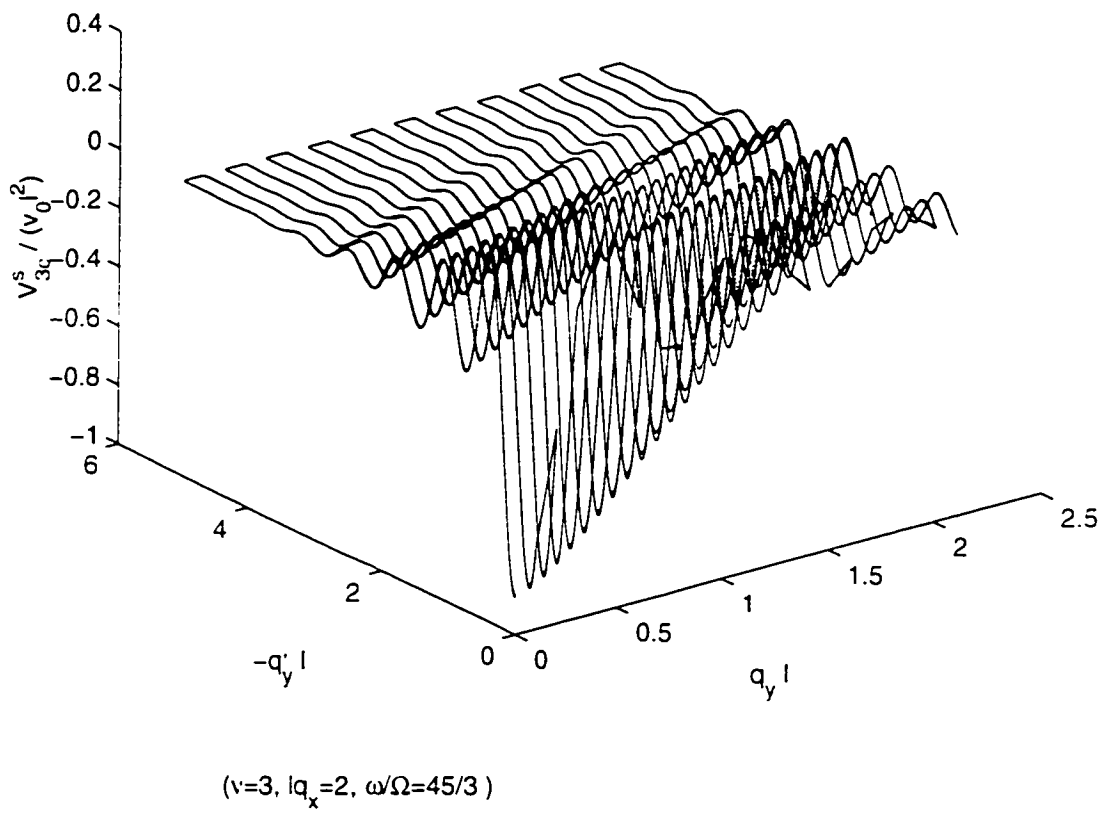

Figure 4.14: Same as Fig.4.12, except for $\tilde{q}_x = 2$, and $\Omega = \omega/(45/3)$. (Sample 2 of Ref. [50])

4.3.3 Exchange and correlation corrections

To consider the many-body effects on the $\nu = 3$ QHE state, we calculate the exchange-correlation correction to the subband structure of the occupied $(n = 1, \sigma = 1)$ LL. According to Eq. (3.48), it can be calculated as

$$
\begin{aligned}
&\varepsilon^{ec}_{1,k_x,1} \\
&\approx -\frac{1}{(2\pi)^3}\int dk'_x dq_y dq'_y V^s_3(k_x - k'_x, q_y, q'_y)(1, k_x|e^{iq_y y}|1k'_x)(1, k'_x|e^{iq'_y y}|1, k_x) \\
&\quad -\frac{1}{(2\pi)^3}\int dk'_x dq_y dq'_y V^s_3(k_x - k'_x, q_y, q'_y)(1, k_x|e^{iq_y y}|0k'_x)(0, k'_x|e^{iq'_y y}|1, k_x) \\
&\equiv \varepsilon^{ec1}_{1,k_x,1} + \varepsilon^{ec2}_{1,k_x,1},
\end{aligned}
\tag{4.96}
$$

where $\varepsilon^{ec1}_{1,k_x,1}$ refers to the exchange and correlations contributed from the same $(n = 1)$ LL and the $\varepsilon^{ec2}_{1,k_x,1}$ from the lower adjacent $(n = 0)$ LL. No corrections are contributed from other LLs, because the LLs above the $(n = 1, \sigma = 1)$ one are empty and there is no electron to exchange with those at the $(n = 1, \sigma = 1)$ LL. Also electrons at the $(n = 0, \sigma = -1)$ LL cannot be exchanged with those at the $(n = 1, \sigma = 1)$ LL, for they belong to different spin states. Substituting $V^s_3 = v_0\delta(q_y + q'_y)/q + V^s_{c3}$ and the screened potential given by Eq. (4.69) into Eq. (4.96), we express $\varepsilon^{ec}_{1,k_x,1}$ as the summation of 4 parts:

$$
\begin{aligned}
\varepsilon^{col}_{1,k_x,1} &= -\frac{v_0}{(2\pi)^3}\left(\int_0^{\tilde{k}_F - \tilde{k}_x} + \int_{\tilde{k}_x - \tilde{k}_F}^0\right)\frac{d\tilde{k}_-}{\tilde{l}}\int_{-\infty}^{\infty} d\tilde{q}_y d\tilde{q}'_y \frac{e^{\tilde{q}_-^2/2}}{\tilde{q}_-}\frac{e^{\tilde{q}'^2_-/2}}{\tilde{q}'_-} \\
&\quad \times \left[K_c cc + K_s ss + K_{sc} sinc(\tilde{q}_y + \tilde{q}'_y)(\tilde{q}_x^2 - \tilde{q}'_y\tilde{q}_y)\right] \\
&\quad \times e^{i(\tilde{q}_y + \tilde{q}'_y)(\tilde{k}_x - \tilde{k}'_x)/2}\left(1 - \frac{\tilde{q}_-^2}{2}\right)\left(1 - \frac{\tilde{q}'^2_-}{2}\right),
\end{aligned}
\tag{4.97}
$$

$$\varepsilon^{ex1}_{1,k_x,1} = -\frac{v_0}{(2\pi)^3}\left(\int_0^{\tilde{k}_F-\tilde{k}_x} + \int_0^{\tilde{k}_F-\tilde{k}_x}\right)\frac{d\tilde{k}_-}{\tilde{l}}\int_{-\infty}^{\infty} d\tilde{q}_y \frac{e^{-\tilde{q}_-^2/2}}{\tilde{q}_-}\left(1-\frac{\tilde{q}_-^2}{2}\right)^2. \tag{4.98}$$

$$\begin{aligned}\varepsilon^{co2}_{1,k_x,1} &= -\frac{v_0}{(2\pi)^3}\left(\int_0^{\tilde{k}_F-\tilde{k}_x} + \int_{\tilde{k}_x-\tilde{k}_F}^{0}\right)\frac{d\tilde{k}_-}{\tilde{l}}\int_{-\infty}^{\infty} d\tilde{q}_y d\tilde{q}_y \frac{e^{-\tilde{q}_-^2/2}}{\tilde{q}_-}\frac{e^{-\tilde{q}'^2_-/2}}{\tilde{q}'_-} \\ &\times \quad [K_c cc + K_s ss + K_{sc} sinc(\tilde{q}_y + \tilde{q}'_y)(\tilde{q}_x^2 - \tilde{q}'_y\tilde{q}_y)] \\ &\times \quad \frac{(\tilde{k}'_x - \tilde{k}_x) + i\tilde{q}_y}{\sqrt{2}}\frac{(\tilde{k}'_x - \tilde{k}_x) + i\tilde{q}'_y}{\sqrt{2}} e^{i(\tilde{q}_y+\tilde{q}'_y)(\tilde{k}_x-\tilde{k}'_x)/2}\end{aligned} \tag{4.99}$$

and

$$\varepsilon^{ex2}_{1,k_x,1} = -\frac{v_0}{(2\pi)^3}\left(\int_0^{\tilde{k}_F-\tilde{k}_x} + \int_0^{\tilde{k}_F-\tilde{k}_x}\right)\frac{d\tilde{k}_-}{\tilde{l}}\int_{-\infty}^{\infty} d\tilde{q}_y e^{-\tilde{q}_-^2/2}\frac{\tilde{q}_-}{2} \tag{4.100}$$

The calculated exchange-correlation correction vs. $\tilde{k}_x$, for sample 1 of Ref. [50] is shown in Fig. 4.15.

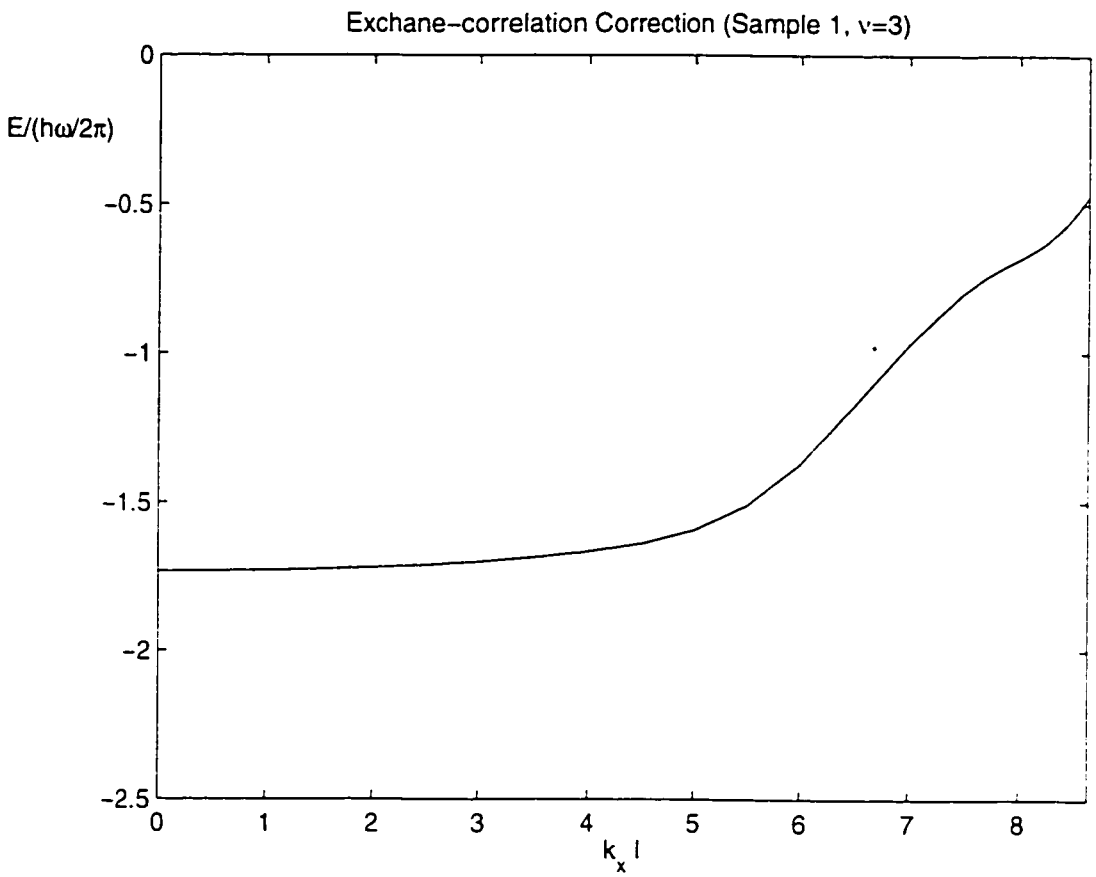

Figure 4.15: The exchange-correlation correction $\varepsilon^{ec}_{1,\tilde{k}_x,1}/(\hbar\tilde{\omega})$ vs. $\tilde{k}_x$ curve for sample 1 of Ref. [50] with $\nu = 3$. For $\tilde{k}_x \to \tilde{k}_F = 8.66$, this curve has negative slope.

4.3.4 v_g^{ec} at Fermi edge: $\nu = 3$

For $\nu = 1$ and 2, we have shown that the derivatives, with respect to the wave vector, of the exchange-correlation energy at Fermi level are nonsingular. It is natural to ask, what happens to this derivative when $\nu = 3$? Below, it will be shown that there exist logarithm singularities in $\varepsilon^{col}_{1,k_F,1}$ and $\varepsilon^{ex1}_{1,k_F,1}$, but they cancel each other EXACTLY, as in the $\nu = 1$ and $\nu = 2$ cases. Here are the details.

With the help of relations (4.70), (4.84)-(4.87), (4.91)-(4.95), and following approximations ($i = c : +;\ \ i = s : -;$)

$$\lambda_i(\tilde{k}_- \to 0) = -2[1 - \frac{\Delta_{i1} - \Delta_{i2} - \frac{1}{\alpha_0}}{\kappa_\pm - 2\Delta_{i1} + \Delta_{i2} + 1/\alpha_0}],$$

$$\lambda_i(\tilde{k}_- \to 0) \approx -1 + \frac{\Delta_{i1} + 1/(2\alpha_0)}{\kappa_\pm + 1/(2\alpha_0)}], \tag{4.101}$$

$$k_i(\tilde{k}_- \to 0) \approx k_{iyy'}(\tilde{k}_- \to 0)/2 \approx -\frac{\pm 1/2}{\Delta_{i2} + \frac{3}{2\alpha_0}}, \tag{4.102}$$

$$\frac{2+\lambda_i}{2}(\kappa_\pm - 2\Delta_{i2} + \Delta_{i1}) + \Delta_{i1} - \Delta_{i2} = \frac{1}{\alpha_0} - \frac{1}{\alpha_0}\frac{2+\lambda_i}{2} \tag{4.103}$$

$$(\lambda_i + 1)(\kappa_\pm - \Delta_{i1}) - \Delta_{i1} + \Delta_{i2} = \frac{1}{2\alpha_0} + \Delta_{i2} - (\frac{1}{2\alpha_0} + \Delta_{i1})(\lambda_i + 1) \tag{4.104}$$

we have, to order κ_i^0,

$$v_g^{col}(k_x \to k_{F3}) = \frac{\tilde{l}}{\hbar}\frac{\partial}{\partial \tilde{k}_x}\varepsilon^{col}_{1,k_x,1}|_{\tilde{k}_x \to \tilde{k}_{F3}}$$

$$\approx \frac{-r_0\tilde{l}\tilde{\omega}}{2\pi}\frac{\partial}{\partial \tilde{k}_x}|_{\tilde{k}_x \to \tilde{k}_{F3}}\int_0^{\tilde{k}_{F3}-\tilde{k}_x} d\tilde{k}_- e^{-\tilde{k}_-^2}\int_{-\infty}^{\infty} d\tilde{q}_y d\tilde{q}'_y \frac{e^{-\tilde{q}_y^2/2}}{\tilde{q}_-}\frac{e^{-\tilde{q}'^2_y/2}}{\tilde{q}'_-}$$

$$\times e^{i\tilde{q}_y(\tilde{k}_x - \tilde{k}'_x)/2} e^{i\tilde{q}'_y(\tilde{k}_x - \tilde{k}'_x)/2}(1 - \frac{\tilde{q}_-^2}{2})(1 - \frac{\tilde{q}'^2_-}{2})[K_c cc + K_s ss]$$

$$= \frac{r_0\tilde{l}\tilde{\omega}}{2\pi}\sum_{i=c,s} \pm 4\{$$

$$\int_0^\infty d\tilde{q}_y \frac{e^{-\tilde{q}_-^2/2}(1 \pm \cos 2\tilde{q}_y \tilde{k}_{F3})/2}{\tilde{q}_-} k_\iota(\tilde{k}_-) \left[2 + \gamma_\iota - \tilde{q}_-^2(1+\gamma_\iota) + \gamma_\iota \frac{\tilde{q}_-^4}{4}\right] D_1|_{\tilde{k}_- \to 0}$$
$$\times \int_0^\infty d\tilde{q}'_y \frac{e^{-\tilde{q}'^2_-/2}(1 \pm \cos 2\tilde{q}'_y \tilde{k}_{F3})/2}{\tilde{q}'_-}(1 - \frac{\tilde{q}'^2_-}{2})$$
$$\int_0^\infty d\tilde{q}_y \frac{e^{-\tilde{q}_-^2/2}(1 \pm \cos 2\tilde{q}_y \tilde{k}_{F3})/2}{\tilde{q}_-} k_{\iota yy'}(\tilde{k}_-) \left[\lambda_\iota + 1 - \frac{\tilde{q}_-^2}{2}(\lambda_\iota + 2) + \frac{\tilde{q}_-^4}{4}\right] D_1|_{\tilde{k}_- \to 0}$$
$$\times \int_0^\infty d\tilde{q}'_y \frac{e^{-\tilde{q}'^2_-/2}(1 \pm \cos 2\tilde{q}'_y \tilde{k}_{F3})/2}{\tilde{q}'_-}(1 - \frac{\tilde{q}'^2_-}{2})^2\}$$
$$(c: +;\ s: -)$$

$$= \frac{r_0 \tilde{l}\tilde{\omega}}{2\pi} \sum_{\iota=c,s} \pm\{4k_\iota(0)\left[(2+\gamma_\iota)\frac{\kappa_\pm}{2} - \Delta_{\iota 1}(1+\gamma_\iota) + \gamma_\iota \frac{\Delta_{\iota 2}}{2}\right] \frac{K_\pm + \Gamma_{\pm 1}}{2}$$
$$-4k_{\iota yy'}(0)\left[(\lambda_\iota + 1)\kappa_\pm - \Delta_{\iota 1}(\lambda_\iota + 2) - \Delta_{\iota 2}\right] \frac{K_\pm + 2\Gamma_{\pm 1} + \Gamma_{\pm 2}}{2}\} \tag{4.105}$$
$$\approx \frac{v_g^{HA}(k_{F3})}{2}\left[-(K_+ + K_- - 1)\alpha_0 + \sum_{\iota=c,s} \frac{\zeta_\iota}{\Delta_{\iota 2} + 3/(2\alpha_0)} \frac{K_\pm}{\kappa_\pm}\right]|_{\tilde{k}_0 \to 0}. \tag{4.106}$$

where

$$\Gamma_{\pm 1} \equiv -\frac{1}{2}\int_{-\infty}^{\infty} d\tilde{q}_y |\tilde{q}_y| e^{\frac{-\tilde{q}_y^2}{2}} \frac{1 \pm \cos 2\tilde{k}_F \tilde{q}_y}{2} \approx -0.5.$$
$$\Gamma_{\pm 2} \equiv \frac{1}{4}\int_{-\infty}^{\infty} d\tilde{q}_y |\tilde{q}_y^3| e^{\frac{-\tilde{q}_y^2}{2}} \frac{1 \pm \cos 2\tilde{k}_F \tilde{q}_y}{2} \approx 0.5 \tag{4.107}$$

and $\zeta_\iota = \Delta_{\iota 2} - \Delta_{\iota 1} + \frac{1}{\alpha_0} + \alpha_0(\Delta_{\iota 1} + \frac{1}{2\alpha_0})^2$. Due to the fact that X_3 becomes zero when $\tilde{k}_- \to 0$, we neglect the inter-level coupling term in $v_g^{co1}(k_x \to k_{F3})$ and take $D_2(X_3, \tilde{k}_-, \tilde{q}'_y) = 1$ in the above derivation. The Fermi edge group velocity $v_g^{co2}(k_x \to k_{F3})$ can be calculated, from Eq. (4.99), as

$$v_g^{co2}(k_x \to k_{F3}) = \frac{\tilde{l}}{\hbar}\frac{\partial}{\partial \tilde{k}_x} \varepsilon^{co2}_{1,k_x,1}|_{\tilde{k}_x \to \tilde{k}_{F3}}$$
$$\approx \frac{-r_0 \tilde{l}\tilde{\omega}}{2\pi}\frac{\partial}{\partial \tilde{k}_x}|_{\tilde{k}_x \to \tilde{k}_{F3}} \int_{\tilde{k}_x - \tilde{k}_{F3}}^0 d\tilde{k}_- e^{-\tilde{k}_-^2} \int_{-\infty}^{\infty} d\tilde{q}_y d\tilde{q}'_y \frac{e^{-\tilde{q}_y^2/2}}{|\tilde{q}_y|}\frac{e^{-\tilde{q}'^2_y/2}}{|\tilde{q}'_y|}$$

$$\times e^{i(\tilde{q}_y-\tilde{q}'_y)\tilde{k}_F}\frac{-\tilde{q}_y\tilde{q}'_y}{2}[K_c cc + K_s ss]$$

$$= \frac{r_0\tilde{l}\tilde{\omega}}{2\pi}\int_0^\infty d\tilde{q}_y d\tilde{q}'_y e^{-\tilde{q}_y^2/2}e^{-\tilde{q}'^2_y/2}\frac{1}{2}[-K_c + K_s]\sin 2\tilde{k}_{F3}\tilde{q}_y \sin 2\tilde{k}_{F3}\tilde{q}'_y$$

$$\approx 0. \tag{4.108}$$

where the integrations[74]

$$\int_0^\infty e^{-ax^2}\cos bx dx = \frac{\sqrt{\pi}}{2a}e^{-b^2/(4a^2)} \tag{4.109}$$

have been used. Eqs. (4.98) and (4.98) give exchange contribution to the group velocity

$$v_g^{ex}(k_x \to k_{F3}) = \frac{\tilde{l}}{\hbar}\frac{\partial}{\partial \tilde{k}_x}(\tilde{\varepsilon}^{ex1}_{1,k_x,1} - \tilde{\varepsilon}^{ex2}_{1,k_x,1})|_{\tilde{k}_x\to\tilde{k}_{F3}}$$

$$= \frac{r_0\tilde{l}\tilde{\omega}}{2\pi}[K_0 - 2\int_0^\infty d\tilde{q}_y e^{-\frac{\tilde{q}_y^2}{2}}(-\frac{\tilde{q}_y}{2} + \frac{\tilde{q}_y^3}{4})] = \frac{r_0\tilde{l}\tilde{\omega}}{2\pi}K_0. \tag{4.110}$$

Therefore the total group velocity $v_g^{ex}(k_x \to k_{F3})$ gives

$$v_g^{ec}(k_x \to k_{F3}) \approx \frac{v_g^{HA}(k_{F3})}{2}\left[\alpha_0 + \sum_{i=c,s}\frac{S_i}{\Delta_{i2} + 3/(2\alpha_0)}\frac{K_\pm}{K_\mp}\right]|_{\tilde{k}_0\to 0}. \tag{4.111}$$

Above results show that the group velocity $v_g^{co2}(\tilde{k}_{F3})$ associated with the charge exchange within the $(n = 0, \sigma = 1)$ LL have no contribution to the Fermi edge slope of the many-body correction for the $(n = 1, \sigma = 1)$ LL, while that due to the exchange within the $(n = 1, \sigma 1)$ LL, $v_g^{co1}(\tilde{k}_{F3})$, is negative and nearly logarithmically divergent. Its sigularity part is exactly cancelled by the velocity $v_g^{ex}(\tilde{k}_{F3})$ caused by the exchange between elecctrons in the $(n = 0, \sigma = 1)$ and $(n = 1, \sigma = 1)$ LLs.

For sample 1 in Ref. [50], with $R_0 = 1.47$ and $\alpha_0 = 3.76$, the velocity $v_g^{ec}(\bar{k}_F)$ thus obtained is about $3.2v_g^{HA}(\bar{k}_{F3})$, which is very closed to the value of $3.6v_g^{HA}(\bar{k}_{F3})$ obtained from the numerical result given in Fig 4.15.

4.3.5 Ground state energies ($\nu = 3$)

As discussed before, the ground state energy can be calculated by

$$E_{1,k_x,1} = \varepsilon_{1,k_x,1} + \langle 1, \tilde{k}_x, 1 | V_{XC}(y) | 1, \tilde{k}_x, 1 \rangle \tag{4.112}$$

with

$$\langle 1, \tilde{k}_x, 1 | V_{XC}(y) | 1, \tilde{k}_x, 1 \rangle = \int_{-\tilde{k}_F}^{\tilde{k}_F} d\tilde{k}'_x \varepsilon^{ec}_{1,k'_x,1} 2(\tilde{k}'_x - \tilde{k}_x)^2 e^{-(\tilde{k}'_x - \tilde{k}_x)^2} / \sqrt{\pi}. \tag{4.113}$$

Here, $\varepsilon^{ec}_{1,k_x,1}$ in Eq.(4.113) is given by Eq. (4.96) and $\varepsilon_{1,k_x,1}$ in Eq.(4.96) by Eq. (3.12), which is

$$\varepsilon_{1,k_x,1} = \hbar\tilde{\omega}[\frac{3}{2} - \frac{1}{2}\tilde{k}_x^2(\frac{\Omega}{\tilde{\omega}})^2]. \tag{4.114}$$

The factor $2(\tilde{k}'_x - \tilde{k}_x)^2/\sqrt{\pi}$ in Eq. (4.113) comes from the Harmonic function $\Phi_1(y) = \frac{1}{\pi^{1/4}}\sqrt{\frac{2}{l}}\frac{y}{l}e^{-\frac{y^2}{2l^2}}$.

The dispersion curve for sample 1 is plotted in Figs. 4.16. In this figure we can see that the top of the modified ($n = 1, \sigma = 1$) LL is larger than the bottom of the empty ($n = 1, \sigma = -1$) LL, which means the correlation correction strongly suppress the spin-splitting pertinent to the $\nu = 3$ QHE state and destruct this state. This is consistent with the experimentally observed result [50]. Also the Fermi edge single-particle group velocity, calculated from this figure, is $v_g \approx 2.2 v_g^{HA}(\tilde{k}_{F3})$.

4.4 Exchange-correlation enhanced g^* factor

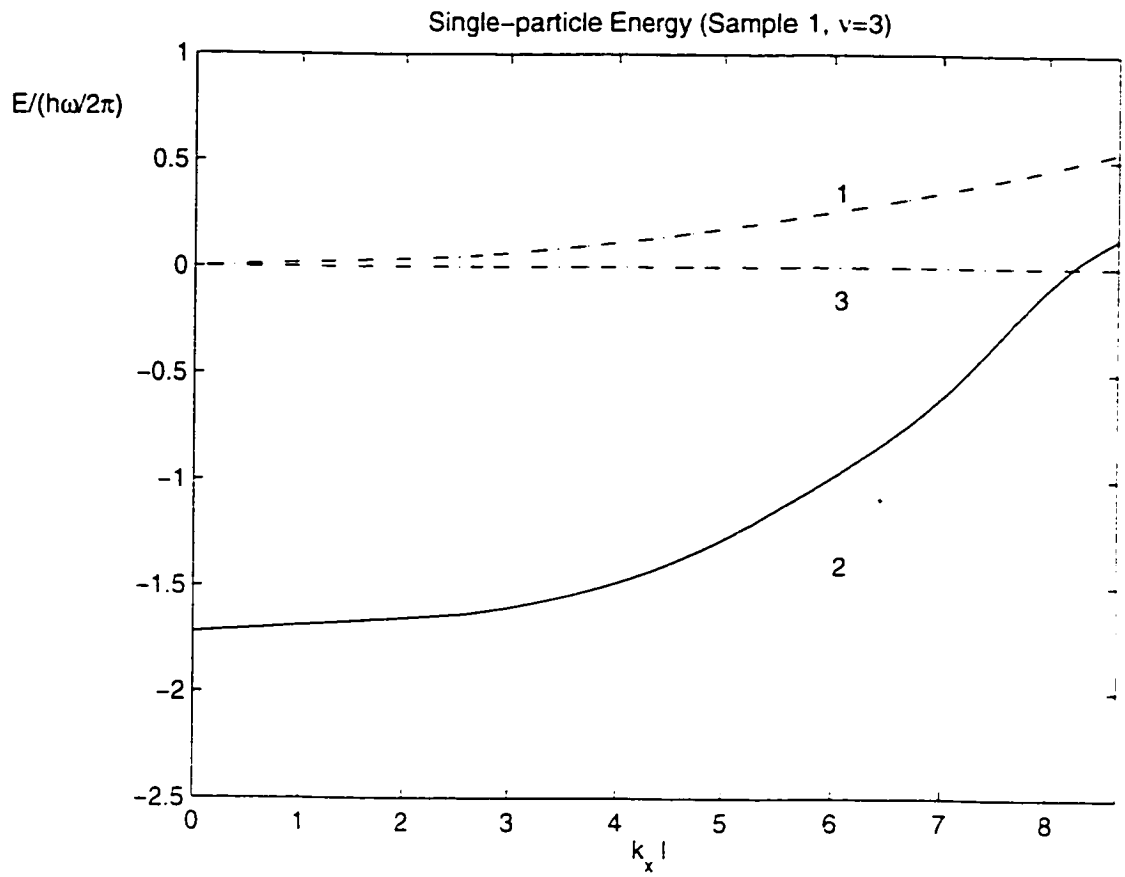

Figure 4.16: Single-particle energies as functions of $\tilde{k}_x$ for sample 1 of Ref. [50], with $\nu = 3$. The parameters are $\hbar\Omega \approx 0.65 meV$, $B \approx 3.3T$, $W \approx 0.30\mu m$, $\tilde{k}_{F3} \approx 8.66$, and $\omega_c/\Omega \approx 25/3$. Curve 1 shows $E/(\hbar\tilde{\omega}) = \varepsilon_{1,k_x,-1}/(\hbar\tilde{\omega}) - 3/2 = \tilde{k}_x^2(\Omega/\omega_c)^2/2$ for the empty $(n = 1, \sigma = -1)$ LL. Curve 2, calculated from Eq.(4.112), is the total energy $E_{1,k_x,1}/(\hbar\tilde{\omega})$ of single electron occupying the $(n = 1, \sigma = 1)$ LL. Curve 3 is the quasi-Fermi level. Notice that there is no gap that would lead to the $\nu = 3$ QHE state.

As is well known from studies of the effective g^* factor of the two-dimensional electron gas (2DEG) [76]-[80], the screening properties change substantially when a Landau level (LL) is partially or fully occupied. Thus, it is of interest to assess the influence of the screening on the filling factor in quantum wires, because the later is more close to the experimental measurements.

In this section we deal with the effective exchange-correlation enhanced g^* factor. It is part of the total enhanced effective g^* factor. We calculate it as

$$g^*_{op} = (E_{n,k_z,-1} - E_{n,k_z,1})/\mu_B B, \tag{4.115}$$

which was used in many papers: it is different from that deduced from the activated behavior of the conductance [50]. It is called *optical* g^* factor because it is related to the spin splitting between states having the same center coordinate $y(k_x)$. Note that in Eq. [4.115] the effect of the Zeeman energy on the $E_{n,k_z,\sigma}$ should not be neglected, for the exchange-correlation spin splitting may be small near the channel edges. Generally, g^*_{op} is inhomogeneous in $y(k_x)$, because the screening in QWs is inhomogeneous in the transverse direction. However, based on our discussion in previous sections, Eq. [4.115] will give $g^*_{op} = |g_0|$ with filling factor $\nu = 2, 4, \ldots$, where g_0 is the bare g factor. For AlGaAs/GaAs, the experimental measurement gave $g_0 = -0.44$, cf. Ref. [83]. For $\nu = 1, 3, \ldots$, Eq. [4.115] can be expressed as

$$g^*_{op} = \langle \varepsilon^{ec}_{n,k_z,1} \rangle / \mu_B B + |g_0| \quad . \tag{4.116}$$

In Fig. [4.17] we plot $g^*_{op}(n = 0)$, given by Eq. [4.116], as a function of $\tilde{k}_x$, in sample

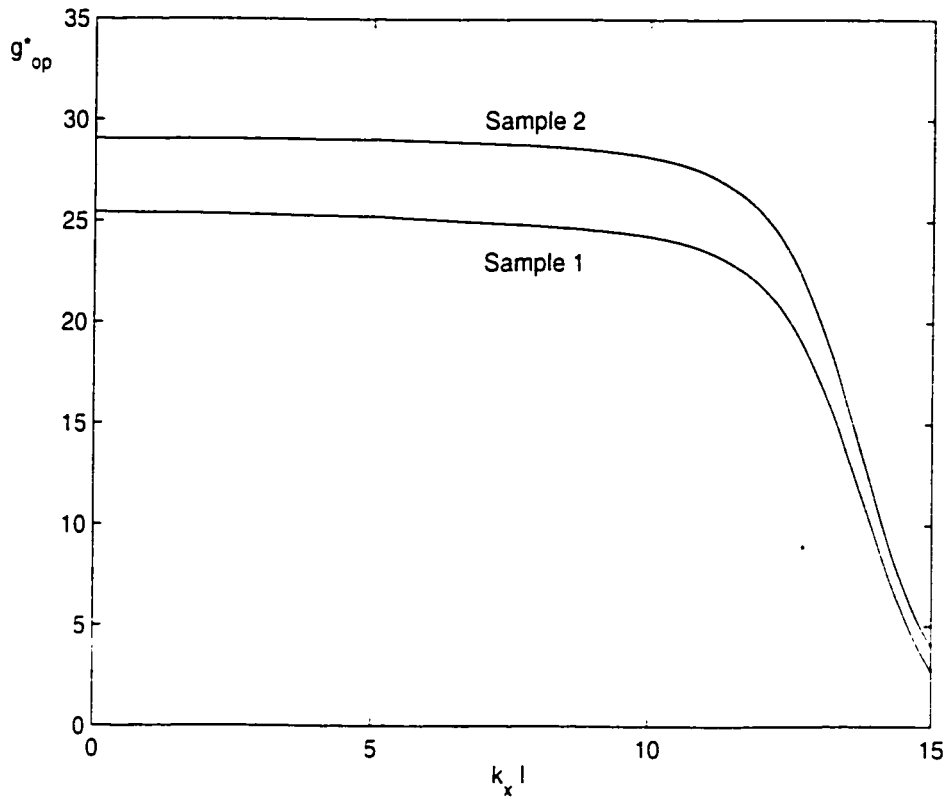

Figure 4.17: The effective g factor $g^*_{op} = \varepsilon^{ec}_{n,k_x,1}/\mu_B B + g_0$ as a function of $\tilde{k}_x$, in sample 1 and 2 of [50] for filling factor $\nu = 1$.

1 and 2 of Ref. [50] with $\nu = 1$. The calculated g^*_{op} is in the range $5 \sim 30$, with resonable approximation $1/\tau \to 0$. Figure [4.18] gives the calculated $g^*_{op}(n = 1)$ in sample 1 for $\nu = 3$. It should be mentioned that the spin splitting for $\nu = 3$ is larger than that for $\nu = 1$, because when $\nu = 3$ the inverse number $N_{inv} = N_+ - N_-$ is only 1/3 of the total electron number, the N_{inv} of $\nu = 1$. Acturally, a similar result was obtained in a 2DEG system: the exchange-correlation induced spin splitting increases with the decrease of the inverse number N_{inv}, cf. Ref. [76].

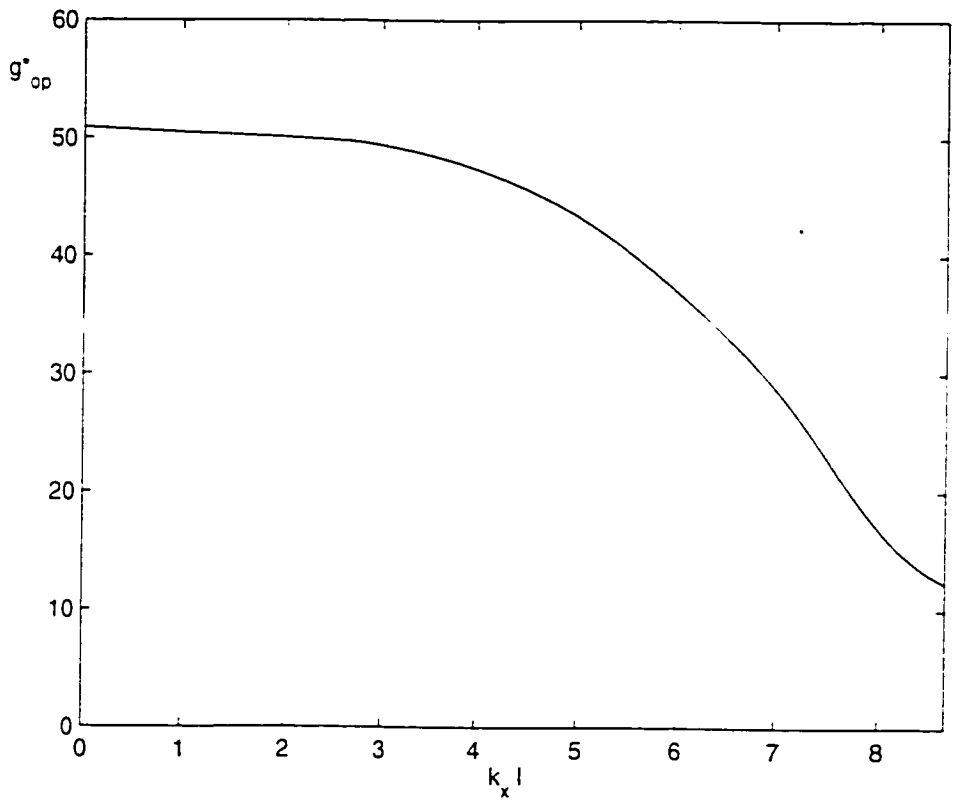

Figure 4.18: Same as in Fig. [4.17] in sample 1 for $\nu = 3$.

Chapter 5

Screen fields & correlation energies in QWs: B || QW

5.1 Channel characteristics without many-body effects

In chapter 4, we considered the screening properties when the magnetic field is perpendicular to the (x, y) plane. One important feature of the electron motion in the QW is that its component in the transverse direction is "displaced" by its motion in the longitudinal direction of the QW. Classically, this is caused by the Lorentz interaction in the (x, y) plane. For QWs in parallel magnetic fields, as there is no such action in the (x, y) plane, we can expect that there is no coupling

between the motions in these two directions. This is shown below.

We still consider the same QW discussed in chapter 3 and 4, i.e., a 2DEG confined in a narrow channel in the (x, y) plane of width W and length L. The confining potential along the y direction is taken as $V_y = m^*\Omega^2 y^2/2$. We choose the gauge for the vector potential $\mathbf{A} = (0, 0, By)$, which gives a magnetic field in the x direction. In the absence of the exchange and correlation effects, the one-electron Hamiltonian h^0 is given by

$$\begin{aligned} h^0 &= \frac{p_x^2 + p_y^2}{2m^*} + \frac{(p_z - \frac{eBy}{c})^2}{2m^*} + m^*\Omega^2 y^2/2 + g_0\mu_B s_z B/2 \\ &= \frac{p_x^2}{2m^*} + \frac{p_y^2}{2m^*} + m^*\tilde{\omega}^2 y^2/2 + g_0\mu_B s_z B/2, \end{aligned} \tag{5.1}$$

where $p_z|\alpha\rangle = 0|\alpha\rangle$ and $\tilde{\omega}^2 = \omega_c^2 + \Omega^2$ $[\omega_c^2 = |e|B/(m^*c)]$ have been used. Its eigenvalues $\varepsilon_{n,k_x,\sigma}$ and eigenstates $|\alpha\rangle$ are given by

$$\varepsilon_{n,k_x,\sigma} = \hbar\tilde{\omega}(n + 1/2) + \hbar^2 k_x^2/(2m^*) + g_0\mu_B\sigma B/2. \tag{5.2}$$

$$\langle x, y|\alpha\rangle \equiv \langle x, y|nk_x\rangle|\sigma\rangle = e^{ik_x x}\Phi_n(y))|\sigma\rangle/\sqrt{L}. \tag{5.3}$$

Compared to the states in QWs in perpendicular magnetic fields, the above eigenstate is simpler than that given by Eq. (3.13), i.e., the electron motion in the y direction is no longer displaced by the wavenumber k_x. As a result, the one-electron group velocity in Hartree Approximation

$$u_g^{HA}(k_x) = \frac{\hbar k_x}{m^*} = \tilde{l}^2\tilde{\omega}k_x \tag{5.4}$$

is $(\omega_c/\Omega)^2$ times larger than the group velocity $v_g^{HA}(k_x)$ given by Eq. (3.18). (To distinguish from v_g in previous chapters, we use u_g to represent the group velocity when the magnetic field is parallel to the magnetic field.) Besides, the matrix elements, which are used to calculating the screened fields and relevant energies, can also be simplified as

$$\begin{aligned}
\langle n'k_x'|e^{i\mathbf{q}\cdot\mathbf{r}}|nk_x\rangle &= \int d\mathbf{r} e^{-ik_x'x}\Phi_{n'}^*(y)\Phi_n(y)e^{ik_x x}e^{i\mathbf{q}\cdot\mathbf{r}}/L(L\to\infty) \\
&\equiv \delta_{q_x-k_-,0}\langle n'|e^{iq_y y}|n\rangle \\
&= \delta_{q_x-k_-,0}\left(\frac{n'!}{n!}\right)^{1/2}\left(\frac{iq_y}{\sqrt{2}/\tilde{l}}\right)^{n-n'}e^{-u/2}L_{n'}^{n-n'}(u) \quad (n>n') \\
&= \delta_{q_x-k_-,0}\left(\frac{n!}{n'!}\right)^{1/2}\left(\frac{iq_y}{\sqrt{2}/\tilde{l}}\right)^{n'-n}e^{-u/2}L_{n}^{n'-n}(u), \quad (n'>n).
\end{aligned} \tag{5.5}$$

where $u = \tilde{q}_y^2/2$, $\tilde{q}_y = q_y\sqrt{\hbar/(m^*\tilde{\omega})}$. Equation (5.5) can be obtained from Eq. (3.14) by setting $k_- = k_x - k_x' = 0$. In this case, the transition matrix elements can be further factorized as the pure x space part and the pure y space part. It would appear that the screening properties in the current case are a special case of those discussed previously. Unfortunately, this is not true. This can be seen by considering the electrons centered in the middle of the channel ($y = 0$). In the case of a perpendicular magnetic field, such electrons have $k_x \to 0$, cf. Fig. 5.1. However, when magnetic field is parallel to the QW, electrons having the same index of Landau level, say $n = 0$, are all "located" near the middle of the channel, where they can have various values of k_x that has no upper limit, cf. Fig 5.2. For

a QW with fixed linear charge density, its Fermi level is a constant. When the magnetic field **B** is increased so that $\hbar\tilde{\omega} \gg (\hbar k_F)^2/(2m^*)$, or $k_F\tilde{l} \ll (1/2)$, then all electrons are occupied at the $(n = 0, \sigma = 1)$ LL and are centered in the middle of the channel.(In the next section we will show that the spin splitting due to the strong exchange and correlation correction can result in the obvious separation between the occupied $(n = 0, \sigma = 1)$ LL and the empty $(n = 0, \sigma = -1)$ LL). On the other hand, if we fix the intensity of the magnetic field and keep increase the linear electron density, then the $n \geq 1$ LLs will be populated gradually. In this chapter, we will consider two cases: 1) the lowest $(n = 1, \sigma = 1)$ LL is occupied; and 2) the $(n = 1, \sigma = \pm 1)$ LLs are fully occupied.

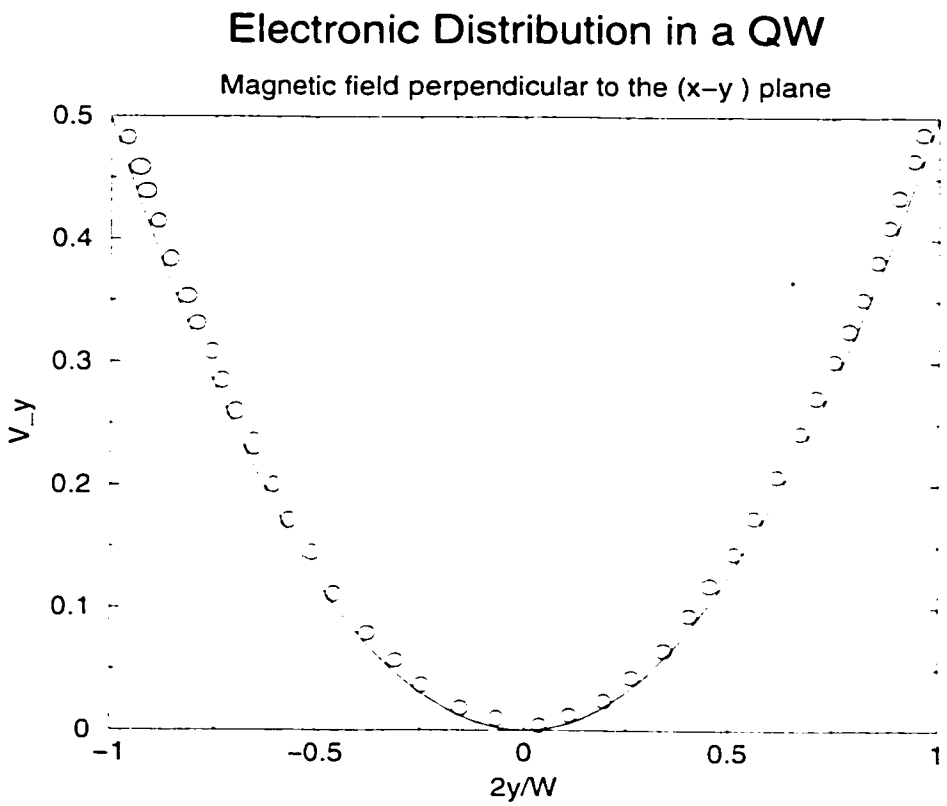

Figure 5.1: Electron ditribution in a QW when the magnetic field is perpendicular to the $x - y$ plane. The electrons are displaced by $y_0(k_x) = \hbar k_x \omega_c/(m^* \omega^2)$.

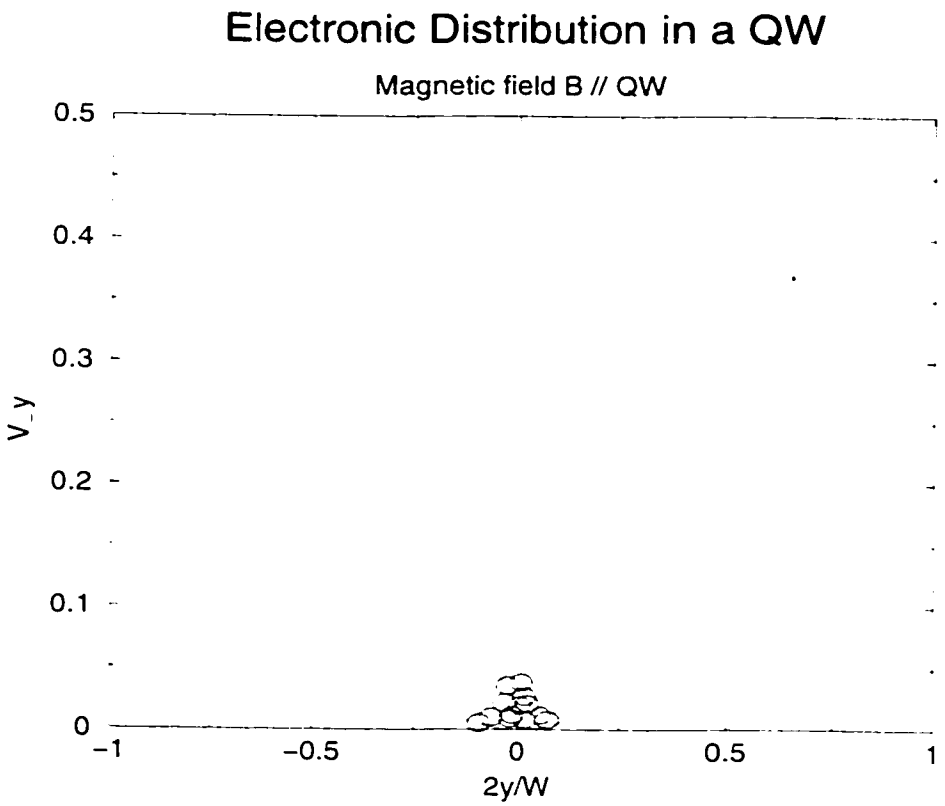

Figure 5.2: Electron ditribution in a QW when the magnetic field is parallel to the QW. All electrons are located around $y = 0$ and they have different values of k_x.

5.2 Exchange and correlation: formulation

In chapter 3, we presented the formalism of SFHA for electrons in narrow QWs subject to perpendicular magnetic fields. This formalism can also be applied to QWs that are parallel to the magnetic field, provided that we make the corresponding modifications. Actually, similar to Eq. (3.33), with the $n = 0$ LL being occupied, the exchange and correlation energy can be calculated as

$$\begin{aligned}
&\xi^{ec}_{0,k_x,\pm 1} \\
&\approx -\frac{1}{(2\pi)^3}\int_{-\infty}^{\infty} dq_x dq_y dq'_y U^s(q_x, q_y, q'_y) \sum_{k'_x} \langle 0k_x|\langle 0k'_x|e^{i\mathbf{q}\cdot\mathbf{r}-i\mathbf{q}'\cdot\mathbf{r}'}|0k_x\rangle|0k'_x\rangle|_{q'_x=-q_x} \\
&= -\frac{1}{(2\pi)^3}\int dk'_x dq_y dq'_y U^s(k_x - k'_x, q_y, q'_y)\langle 0|e^{iq_y y}|0\rangle\langle 0|e^{iq'_y y}|0\rangle. \qquad (5.6)
\end{aligned}$$

where U^s is the screened potential in the QW when the magnetic field $\mathbf{B}$ is in x direction. It is described by the modified Poisson-RPA integral equation

$$\begin{aligned}
U^s(q_x, q_y, q'_y) = \quad & \frac{v_0\,\delta(q_y + q'_y)}{q} + \frac{v_0}{8\pi^3 q}\int_{-\infty}^{\infty} dq_{y1} U^s(q_x, q_{y1}, q'_y) \\
& \times \sum_{n_\alpha, n_\beta}\int dk_{x\alpha} F_{\alpha,\beta}\langle n_\alpha|e^{iq_{y1}y}|n_\beta\rangle\langle n_\beta|e^{-iq_y y}|n_\alpha\rangle.
\end{aligned} \qquad (5.7)$$

where $F_{\alpha,\beta} = (f_{n_\alpha,k_{x\alpha}} - f_{n_\beta,k_{x\alpha}-q_x})/(\xi_{n_\alpha,k_{x\alpha}} - \xi_{n_\beta,k_{x\alpha}-q_x})$ and $f_{n,k_x} = 1/(1+e^{(\xi_{n,k_x}-E_F)/kT})$. Also, we split the screened potential in the exchange and the correlation parts, $U^s = v_0\delta(q_y + q'_y)/q + U^c(q_x, q_y, q'_y)$. Then Eq. (5.7) can be written as

$$U^c_1(q_x, q_y, q'_y) = \frac{v_0^2}{8\pi^3 q q'}\sum_{n_\alpha, n_\beta}\int dk_{x\alpha} F_{\alpha,\beta}\langle n_\alpha|e^{-iq'_y y}|n_\beta\rangle\langle n_\beta|e^{-iq_y y}|n_\alpha\rangle$$

$$+ \quad \frac{v_0}{8\pi^3 q}\int_{-\infty}^{\infty} dq_{y1} U_1^c(q_x, q_{y1}, q_y')$$

$$\times \quad \sum_{n_\alpha, n_\beta} \int dk_{x\alpha} F_{\alpha,\beta} \langle n_\alpha | e^{iq_{y1}y} | n_\beta \rangle \langle n_\beta | e^{-iq_y y} | n_\alpha \rangle. \tag{5.8}$$

which leads to same formalism given by Eq.(3.44). But it will give a different integral equation. because of the new channel properties.

5.3 Spin-splitting between filled $(n = 0, \sigma = 1)$ LL and empty $(n = 0, \sigma = -1)$ LL

5.3.1 Simplification of the integral equation and its analytic solution

Similar to the discussion in the previous chapters, we first consider the case when only the lowest LL $(n = 0, \sigma = 1)$ is occupied, which means there are only $F_{0,n}$ and $F_{n,0}$ terms in the Eq. (5.8). Further, we reduce this integral equation by neglecting the screening from the $n \geq 2$ LLs. Therefore, at $T = 0K$, the Poisson-RPA equation is simplified as

$$\begin{aligned} U_1^c(q_x, q_y, q_y') &= \frac{v_0^2}{8\pi^3 q q'} \int dk_{x\alpha} [F_{0,0} \langle 0|e^{-iq_y y}|0\rangle \langle 0|e^{-iq_y' y}|0\rangle \\ &\quad + F_{0,1} \langle 0|e^{-iq_y y}|1\rangle \langle 1|e^{-iq_y' y}|0\rangle + F_{1,0} \langle 1|e^{-iq_y y}|0\rangle \langle 0|e^{-iq_y' y}|1\rangle] \\ &+ \frac{v_0}{8\pi^3 q} \int_{-\infty}^{\infty} dq_{y1} U_1^c(q_x, q_{y1}, q_y') [F_{0,0} \langle 0|e^{-iq_{y1} y}|0\rangle \langle 0|e^{-iq_y' y}|0\rangle \\ &\quad + F_{0,1} \langle 0|e^{-iq_{y1} y}|1\rangle \langle 1|e^{-iq_y' y}|0\rangle + F_{1,0} \langle 1|e^{-iq_{y1} y}|0\rangle \langle 0|e^{-iq_y' y}|1\rangle] \end{aligned} \tag{5.9}$$

Note that, due to different channel characteristics, integration of the coupling coefficient $F_{\alpha,\beta}$ gives results different from those in subsection 4.1.1, e.g.,

$$\int F_{0,0} dk_{x\alpha} = \int_{-\infty}^{\infty} dk_{x\alpha} \frac{f_{0,k_{x\alpha}-q_x} - f_{0,k_{x\alpha}}}{\frac{\hbar^2}{2m^*}[(k_{x\alpha} - q_x)^2 - k_{x\alpha}^2]}$$

$$\approx -\frac{\tau_0(\tilde{q}_x)}{\hbar u_g^{HA}(k_F)} \tag{5.10}$$

where $\tau_0(\tilde{q}_x) = (2\tilde{k}_F/\tilde{q}_x)\ln|[1+\tilde{q}_x/(2\tilde{k}_F)]/[1-\tilde{q}_x/(2\tilde{k}_F)]|$. Also

$$\int F_{0,1}dk_{x\alpha} = \int_{-\infty}^{\infty} dk_{x\alpha}\frac{f_{0,k_{x\alpha}} - f_{1,k_{x\alpha}-q_x}}{\frac{\hbar^2}{2m^*}k_{x\alpha}^2 - [\frac{\hbar^2}{2m^*}(k_{x\alpha}-q_x)^2 + \hbar\tilde{\omega}]} \approx -\frac{2\tilde{k}_F}{\hbar\tilde{\omega}\tilde{l}}. \tag{5.11}$$

and

$$\int F_{1,0}dk_{x\alpha} = \int_{-\infty}^{\infty} dk_{x\alpha}\frac{f_{1,k_{x\alpha}} - f_{0,k_{x\alpha}-q_x}}{[\hbar\tilde{\omega} + \frac{\hbar^2}{2m^*}k_{x\alpha}^2] - \frac{\hbar^2}{2m^*}(k_{x\alpha}-q_x)^2} \approx -\frac{2\tilde{k}_F}{\hbar\tilde{\omega}\tilde{l}}. \tag{5.12}$$

With these relations and

$$\begin{aligned}
\langle 0|e^{iq_y y}|0\rangle &= e^{-q_y^2/4}, \\
\langle n|e^{iq_y y}|0\rangle &= \langle 0|e^{iq_y y}|n\rangle = (\frac{iq_y}{\sqrt{2}})^n \frac{1}{\sqrt{n!}} e^{-q_y^2/4}.
\end{aligned} \tag{5.13}$$

Eq. (5.8) can be rewritten as as

$$\begin{aligned}
U_1^c(\tilde{q}_x, \tilde{q}_y, \tilde{q}'_y) = & -\frac{v_0 a_0}{2}\frac{e^{-(\tilde{q}_y^2+\tilde{q}'^2_y)^2/4}}{qq'}[\tau_0(\tilde{q}_x) - 2\tilde{k}_F^2\tilde{q}_y\tilde{q}'_y] \\
& -\frac{v_0 a_0}{2}\frac{e^{-\tilde{q}_y^2/4}}{q}\int d\tilde{q}_{y1}e^{-\tilde{q}_{y1}^2/4}U_1^c(\tilde{q}_x, \tilde{q}_{y1}, \tilde{q}'_y)\left[\tau_0(\tilde{q}_x) + 2\tilde{k}_F^2\tilde{q}_{y1}\tilde{q}'_y\right].
\end{aligned} \tag{5.14}$$

with $a_0 = 2v_0/(8\pi^3\hbar u_g^{HA}(k_F))$ and $u_g^{HA}(k_F)$ given by Eq. (5.4). The analytic solution of Eq. (5.14) is attempted in the form

$$U_1^c(\tilde{q}_x, \tilde{q}_y, \tilde{q}'_y) = \frac{v_0}{qq'}e^{-(\tilde{q}_y^2+\tilde{q}'^2_y)^2/4}\left[\mu_1(\tilde{q}_x) + \mu_2(\tilde{q}_x)\tilde{q}_y\tilde{q}'_y\right]. \tag{5.15}$$

where $\mu_1(\tilde{q}_x)$ [$\mu_2(\tilde{q}_x)$] can be obtained by substituting Eq. (5.15) into Eq. (5.14) and equating the coefficients of the intra-level [adjacent-level] terms on both sides of Eq. (5.14). respectively. The results are

$$\begin{aligned}\mu_1(\tilde{q}_x) &= \frac{-a_0\tau_0/2}{1+\frac{a_0\tau_0}{2}K_0(\frac{\tilde{q}_x^2}{4})e^{\tilde{q}_x^2/4}} \\ &\approx -\frac{1}{K_0(\frac{\tilde{q}_x^2}{4})e^{\tilde{q}_x^2/4}}\left[1-\frac{1}{\frac{a_0\tau_0}{2}K_0(\frac{\tilde{q}_x^2}{4})e^{\tilde{q}_x^2/4}}\right] \qquad (5.16)\end{aligned}$$

$$\mu_2(\tilde{q}_x) = \frac{a_0\tilde{k}_F^2}{1+a_0\tilde{k}_F^2\left[\mathcal{D}(\tilde{q}_x)-\tilde{q}_x^2K_0(\frac{\tilde{q}_x^2}{4})e^{\tilde{q}_x^2/4}\right]}. \qquad (5.17)$$

Here $\mathcal{D}$ is defined by

$$\mathcal{D}(\tilde{q}_x) = \int_{-\infty}^{\infty} d\tilde{q}_y e^{-\tilde{q}_y^2/2}\tilde{q} \qquad (5.18)$$

and

$$K_0(\frac{\tilde{q}_x^2}{4})e^{\tilde{q}_x^2/4} = \int_{-\infty}^{\infty} d\tilde{q}_y \frac{e^{-\tilde{q}_y^2/2}}{\tilde{q}}. \qquad (5.19)$$

One important difference between the screened potential obtained in chapter 4 and the one given by Eq. (5.15) is that the former always oscillates in the $(\tilde{q}_y, \tilde{q'}_y)$ space. while the later does not. This is because. in chapter 4. such oscillations are cause by the phase factor in Eq. (3.14) or the transition between different displaced Fock states: but now the electron motion in the x and y directions are independent of each other and there is no phase shift in the transition between the non-displaced Fock states. This screened field feature will lead to very strong spin splitting between the occupied $(n = 0, \sigma = 1)$ LL and the empty $(n = 0, \sigma = -1)$ LL. We will discuss this in the next subsection.

5.3.2 Exchange-correlation correction to the lowest LL

The exchange and correlation energies of electrons occupying the $(n = 0, \sigma = 1)$ LL can be calculated by substituting Eqs. (5.15) and (5.5) into Eq. (5.6). We have

$$\begin{aligned}
\varepsilon^{ex}_{0,k_x,1} &= -\frac{v_0}{(2\pi)^3}\int_{-k_F}^{k_F} dk'_x \int_{-\infty}^{\infty} dq_y \frac{e^{-\tilde{q}_y^2/2}}{q} \\
&= -\frac{v_0}{(2\pi)^3 \tilde{l}}\int_{\tilde{k}_x-\tilde{k}_F}^{\tilde{k}_x+\tilde{k}_F} d\tilde{k}_- K_0(\frac{\tilde{k}_-^2}{4}) e^{-\frac{\tilde{k}_-^2}{4}}
\end{aligned} \tag{5.20}$$

and

$$\begin{aligned}
\varepsilon^{co}_{0,k_x,1} &= -\frac{v_0}{(2\pi)^3 \tilde{l}}\int_{-\tilde{k}_F}^{\tilde{k}_F} d\tilde{k}'_x \int_{-\infty}^{\infty} d\tilde{q}_y d\tilde{q}'_y (\mu_1 + \mu_2 \tilde{q}_y \tilde{q}'_y) \frac{e^{-\frac{\tilde{q}_y^2}{2}} e^{-\frac{\tilde{q}'^2_y}{2}}}{\tilde{q}_y \tilde{q}'_y} \\
&= \frac{v_0}{(2\pi)^3 \tilde{l}}\int_{\tilde{k}_x-\tilde{k}_F}^{\tilde{k}_x+\tilde{k}_F} d\tilde{k}_- K_0(\frac{\tilde{k}_-^2}{4}) e^{-\frac{\tilde{k}_-^2}{4}} \left[1 - \frac{1}{\frac{a_0\tau_0}{2} K_0(\frac{\tilde{k}_-^2}{4}) e^{\tilde{k}_-^2/4}}\right].
\end{aligned} \tag{5.21}$$

In the above calculation, the correlation contributed from the adjacent LL is zero because the second term in the square brackets in Eq. (5.21) is an odd function of $\tilde{q}_y$ and $\tilde{q}'_y$. The total exchange and correlation correction is

$$\begin{aligned}
\varepsilon^{ec}_{0,k_x,1} &= \varepsilon^{ex}_{0,k_x,1} + \varepsilon^{co}_{0,k_x,1} \\
&= -\frac{v_0}{(2\pi)^3 \tilde{l}}\int_{\tilde{k}_x-\tilde{k}_F}^{\tilde{k}_x+\tilde{k}_F} d\tilde{k}_- \left[\frac{1}{a_0\tau_0(\tilde{k}_-)/2} + \mathcal{O}(\frac{1}{K_0(\frac{\tilde{k}_-^2}{4}) e^{\tilde{k}_-^2/4}})\right] \\
&= -\frac{\hbar u_g^{HA}(k_F)}{\tilde{l}}\left[\int_0^{\tilde{k}_x-\tilde{k}_F} + \int_0^{\tilde{k}_x-\tilde{k}_F}\right] \frac{d\tilde{k}_-}{\tau_0(\tilde{k}_-)}
\end{aligned} \tag{5.22}$$

Figure 5.3 gives the distribution of the exchange-correlation energy $\varepsilon^{ec}_{0,k_x,1}/(\hbar\tilde{k}_F^2)$ over the normalized wavenumber k_x/k_F. From this figure we can see that the spin-splitting due to the exchange-correlation correction is much stronger than the

kinetic energy in the x direction. Therefore, if the electron density in the QW is increased gradually, the $(n = 0, \sigma = 1)$ LL will be populated first, followed by the $n = 0, \sigma = -1$ LL and so on. Figure 5.3 shows that the spin-splitting due to exchange-correlation correction is stronger than that when the magnetic field is perpendicular to the (x,y) plane, cf. Fig. 4.5. This is reasonable for now there is no oscillation of the screened field.

Based on Eq. (5.22), we can show the non-singularity of the Fermi-level group velocity $u_g^{ec}(k_F)$ as follows.

$$\begin{aligned} u_g^{ec}(k_F) &= \frac{\tilde{l}}{\hbar}\frac{\partial}{\partial \tilde{k}_x}\varepsilon^{ec}_{0,k_z,1,k_x\to k_F} \\ &= -u_g^{HA}\left[\frac{\partial}{\partial(\tilde{k}_F+\tilde{k}_z)}\int_0^{\tilde{k}_F+\tilde{k}_z} - \frac{\partial}{\partial(\tilde{k}_F-\tilde{k}_z)}\int_0^{\tilde{k}_F-\tilde{k}_z}\right]\frac{d\tilde{k}_-}{\tau_0}|_{k_x\to k_F} \\ &= u_g^{HA}(k_F)/2. \end{aligned} \tag{5.23}$$

which is a constant. Note that, because all electrons are centered near the $y = 0$ axis, both integration $\int_0^{\tilde{k}_F+\tilde{k}_z} d\tilde{k}_-...$ and $\int_0^{\tilde{k}_F-\tilde{k}_z} d\tilde{k}_-...$ have non-negligible contributions to the Fermi level group velocity. This is different from the case when $B\perp QW$, where the Fermi edge group velocity is basically contributed from the corresponding edge and that from the opposite edge is very small.

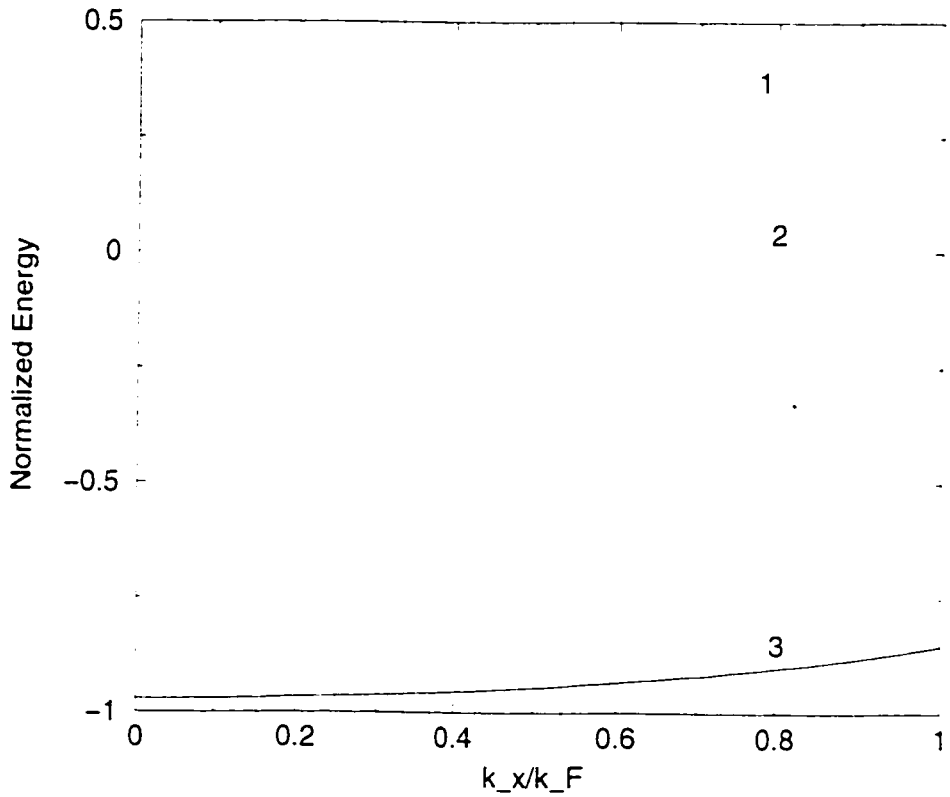

Figure 5.3: Energy dependence on the wavenumber when the QW is parallel to the magnetic field and the ($n = 0, \sigma = 1$) LL is populated. Curve 1 shows the normalized kinetic energy without many-body interactions, i.e., $(\varepsilon_{0,k_x,1} - \hbar\tilde{\omega}/2 - g_0\mu_B s_z B/2)/(\hbar\tilde{\omega}\tilde{k}_F^2)$. Curve 3 is the normalized exchange-correlation energy $\varepsilon^{ec}_{0,k_x,1}/(\hbar\tilde{\omega}\tilde{k}_F^2)$. The x axis is the normalized wavenumber k_x/k_F.

5.4 Many-body effects on the $(n = 0, \sigma = -1)$ LL

In this section, we assume the two LLs ($n = 0, \sigma = \pm 1$) are fully occupied and the other LLs are empty. Based on the discussion given in chapter 4 for $\nu = 2$ and the approach used in the previous section, we have $U_2^s(q_x, q_y, q_y') = v_0\delta(q_y + q_y')/q + U_2^c(q_x, q_y, q_y')$ and

$$\begin{aligned} U_2^c(q_x, q_y, q_y') &= \frac{2v_0^2}{8\pi^3 qq'}\int dk_{x0}[F_{0,0}\langle 0|e^{-iq_y y}|0\rangle\langle 0|e^{-iq_y' y}|0\rangle \\ &\quad + F_{0,1}\langle 0|e^{-iq_y y}|1\rangle\langle 1|e^{-iq_y' y}|0\rangle + F_{1,0}\langle 1|e^{-iq_y y}|0\rangle\langle 0|e^{-iq_y' y}|1\rangle] \\ &+ \frac{2v_0}{8\pi^3 q}\int_{-\infty}^{\infty} dq_{y1} U_1^c(q_x, q_{y1}, q_y')[F_{0,0}\langle 0|e^{-iq_{y1} y}|0\rangle\langle 0|e^{-iq_y' y}|0\rangle \\ &\quad + F_{0,1}\langle 0|e^{-iq_{y1} y}|1\rangle\langle 1|e^{-iq_y' y}|0\rangle + F_{1,0}\langle 1|e^{-iq_{y1} y}|0\rangle\langle 0|e^{-iq_y' y}|1\rangle]. \end{aligned} \tag{5.24}$$

Obviously, the solution of the above equation is

$$U_2^c(\tilde{q}_x, \tilde{q}_y, \tilde{q}_y') = \frac{v_0}{qq'} e^{-(\tilde{q}_y^2 + \tilde{q}_y'^2)/4}\left[\tilde{\mu}_1(\tilde{q}_x) + \tilde{\mu}_2(\tilde{q}_x)\tilde{q}_y\tilde{q}_y'\right]. \tag{5.25}$$

with ($\nu = 2$)

$$\tilde{\mu}_1(\tilde{q}_x) = \frac{-a_0\tau_0(\nu/2)}{1 + a_0\tau_0\frac{\nu}{2}K_0(\frac{\tilde{q}_x^2}{4})e^{\tilde{q}_x^2/4}} \approx -\frac{1}{K_0(\frac{\tilde{q}_x^2}{4})e^{\tilde{q}_x^2/4}}\left[1 - \frac{1}{a_0\tau_0\frac{\nu}{2}K_0(\frac{\tilde{q}_x^2}{4})e^{\tilde{q}_x^2/4}}\right]. \tag{5.26}$$

$$\tilde{\mu}_2(\tilde{q}_x) = \frac{a_0\tilde{k}_F^2\nu}{1 + a_0\tilde{k}_F^2\nu\left[\mathcal{D}(\tilde{q}_x) - \tilde{q}_x^2 K_0(\frac{\tilde{q}_x^2}{4})e^{\tilde{q}_x^2/4}\right]}. \tag{5.27}$$

and $\mathcal{D}$ being given by Eq. (5.18). When $\nu = 1$, Eqs. (5.26) and (5.27) reduce to Eqs. (5.16) and (5.17), respectively.

Similarly, when we neglect the Zeeman energy difference, the exchange and correlation are ($\sigma = \pm 1, \nu = 2$)

$$\varepsilon^{ex}_{0,k_z,\sigma} = -\frac{v_0}{(2\pi)^3 \bar{l}} \int_{\bar{k}_z - \bar{k}_{F2}}^{\bar{k}_z + \bar{k}_{F2}} d\bar{k}_- K_0(\frac{\bar{k}_-^2}{4}) e^{-\frac{\bar{k}_-^2}{4}}. \tag{5.28}$$

and

$$\varepsilon^{co}_{0,k_z,\sigma} = \frac{v_0}{(2\pi)^3 \bar{l}} \int_{\bar{k}_z - \bar{k}_{F2}}^{\bar{k}_z + \bar{k}_{F2}} d\bar{k}_- K_0(\frac{\bar{k}_-^2}{4}) e^{-\frac{\bar{q}_-^2}{4}} \left[1 - \frac{1}{a_0 \tau_0 \frac{\nu}{2} K_0(\frac{\bar{k}_-^2}{4}) e^{\bar{k}_-^2/4}} \right]. \tag{5.29}$$

The total exchange-correlation energy for electrons occupying the ($n = 0, \sigma = 1$) or ($n = 0, \sigma = -1$) LL is

$$\varepsilon^{ec}_{0,k_z,\sigma} = -\frac{\hbar u_g^{HA}(k_{F2})}{2\bar{l}} \left[\int_0^{\bar{k}_z - \bar{k}_{F2}} + \int_0^{\bar{k}_z - \bar{k}_F} \right] d\bar{k}_- \frac{\bar{k}_-/2\bar{k}_{F2}}{\ln \left| \frac{1 - \bar{k}_-/2\bar{k}_{F2}}{1 - \bar{k}_-/2\bar{k}_{F2}} \right|} \tag{5.30}$$

Note that, for a given QW with fixed linear charge density, when the magnetic field B is decreased so that the ($n = 0, \sigma = \pm 1$) LLs are occupied, the dimensionless Fermi wavelength will decrease from $\bar{k}_F \equiv \bar{k}_F$ to $\bar{k}_{F2} = \bar{k}_{F1}/2$. Also, we have the Fermi-level group velocity for

$$u_g^{ec}(k_{F2}) = 0.5(u_g^{HA}(k_{F2})/2), \tag{5.31}$$

which is a constant. The factor 0.5 in Eq. (5.31) is due to the screened field is the contribution from both ($n = 1, \sigma = \pm 1$) LLs, while the exchange-correlation only related with those charges having same spin.

5.5 Eigenvalue and eigenstate in a tilted magnetic field

The previous discussion dealt with two special cases: 1) magnetic field in the z direction or $B\perp$ the $(x-y)$ plane; 2) magnetic field in the x direction or $B//$ the x axis. For a tilted field B having components both in the x and z directions, the one-electron Hamiltonian h^0, in the gauge $\mathbf{A} = (-B_\perp y, 0, B_\parallel y)$, is given by

$$\begin{aligned} h^0 &= \frac{(p_x + eB_\perp y/c)^2}{2m^*} + \frac{p_y^2}{2m^*} + \frac{(p_z - eB_\parallel y/c)^2}{2m^*} + m^*\Omega^2 y^2/2 + g_0\mu_B s_z B/2 \\ &= \frac{p_y^2}{2m^*} - \frac{m^*}{2}\tilde{\omega}^2(y-y_0)^2 + \frac{p_x^2}{2m^*} - \frac{\omega_{c\_}^2 p_x^2}{2m^*\tilde{\omega}^2} + g_0\mu_B s_z B/2. \end{aligned} \tag{5.32}$$

where $p_z|\alpha\rangle = 0|\alpha\rangle$ has been used and $\tilde{\omega}^2 = \omega_c^2 + \Omega^2$, $\omega_c^2 = \omega_{c\_}^2 + \omega_{c\parallel}^2$, $\omega_{c\_}^2 = |e|B_\perp/(m^*c)$, $\omega_{c\parallel}^2 = |e|B_\parallel/(m^*c)$, and $y_0 = p_x\omega_{c\_}/(m^*\tilde{\omega}^2)$. The eigenvalue and eigenstate of Eq. (5.32) are

$$\varepsilon_{n,k_x,\sigma} = \hbar\tilde{\omega}(n+1/2) + \hbar^2 k_x^2/(2\tilde{m}) + g_0\mu_B\sigma B/2. \tag{5.33}$$

$$\langle x, y|\alpha\rangle \equiv \langle x, y|nk_x\rangle|\sigma\rangle = e^{ik_x x}\Phi_n(y-y_0))|\sigma\rangle/\sqrt{L}. \tag{5.34}$$

with $\tilde{m} = \tilde{\omega}^2/(\omega_{c\parallel}^2 + \Omega^2)$. Therefore, the may-body problem in this case is very similar to that when the magnetic field B is perpendicular to the $x-y$ plane, if we make some changes for the related constants, such as $\tilde{\omega}$, y_0 and $\tilde{m}$.

In principle, when a magnetic ñeld B lies in a plane formed by any two axes, the corresponding many-body problems can be considered by making use of our

previous work, provide that we choose a suitable gauge. However, if the tilted magnetic field B has components along the x, y, and z directions, the eigenvalue and eigenstate of the one-electron Hamiltonian h^0 becomes be much more complicated. We do not consider such case in this work.

Chapter 6

Summary

In this work, the screened fields, the exchange-correlation corrections, and the single-particle energies in narrow QWs subjected to strong magnetic fields have been explored within the SHFA. As a basis of this work, the general principle of the SHFA, its formalism, and its characteristics have been discussed, after an overview of related classical many-body techniques used in 3DEG systems.

In the SHFA the key point is how to correctly find the screened Coulomb interactions described by the semi-classical Poisson-RPA scheme. In this work a new approach has been proposed to solve this integral equation. The first step of this approach is to simplify the integral equation by taking into account only the intra-level and adjacent-level screening. Furthermore, the total screened field is decomposed into different independent modes (not necessarily orthogonal) and the integral equation can be solved by using the generalized mode-matching technique.

One important feature of this approach is that it does not need the limitation $r_0 < 1$, which is often required in the perturbative studies of electron-electron interactions in QWs. With some extra work it can be applied to situations described by $\nu \geq 4$ provided the magnetic field is strong enough and the dimensionless Fermi wavenumber $\tilde{k}_{F\nu}$ large enough.

For QWs in perpendicular magnetic fields we used this approach to get the analytical approximations of the screened potentials for the $\nu = 1, 2, 3$ QHE states, while, the approximation used in Ref. [35] only dealt with the $\nu = 1$ QHE state. The main characteristic of the solved screened potentials is that they diverge in the long wavelength limit and are distributed in the form of damped sinusoidal oscillations, due to the fact that electron states in the parallel direction are "entangled" with those in the perpendicular direction and there is a phase shift related with the centers of the displaced Fock states.

To confirm the results obtained with the new approach, we also solved the Poisson-RPA integral equation numerically. Note that we cannot use the traditional iterative method directly, because the integral kernel in the equation becomes very large in the long-range Coulomb limit. To avoid the divergent result in repeat iterations, a new method, named "weighted iterative method", has been proposed. The cost of this method is that the convergence to the real solution is slow. The larger the integral kernel, the slower the convergence and the higher the accuracy requirement on the initial value. For the Poisson-RPA integral equa-

tion, the analytic approximations can also be used as initial values and we can get the numerical solution with any accuracy, provided the number of iterations is large enough. The numerical solutions obtained agree very well with the analytic solution of the integral equation. This also confirms that the generalized mode-matching technique used in this work is reliable.

Based on the analytic approximations of the screened potentials, we calculated the exchange and correlation energy dispersion and the group velocities near the Fermi edges. The obtained exchange-correlations are symmetrical to k_x, i.e., $\varepsilon^{ec}_{n,k_x,\pm 1} = \varepsilon^{ec}_{n,-k_x,\pm 1}$. This property is determined by the fact that the solved screened fields are even functions of the wavenumber in the x direction. Actually, this is a reasonable conclusion, considering the geometric symmetry of the QWs. We have also shown that, near the Fermi edge, the logarithmic divergence in the exchange energy is cancelled exactly by that in the correlation energy. The overall Fermi-edge group velocity, $v_g^{ec}(\tilde{k}_{F\nu})$, is caused by the nonsinglar part of the correlation contribution that corresponds to the intra-level screened potential. For QWs in strong enough magnetic fields, e.g., $B \sim 10T$, with filling factor $\nu = 1, 2$, the group velocities $v_g^{ec}(k_{Fi})(i = 1, 2)$ are not so sensitive to the sample parameters and are basically determined by the group velocities in the Hartree approximation $v_g^{HA}(k_{Fi})(i = 1, 2)$. However, for $\nu = 3$, the group velocity $v_g^{xc}(k_F 3)$ is more sensitive to the QW parameters. This is because the solved screened fields are more sensitive to the sample parameters such as r_0 and Ω/Σ. Actually, for $\nu = 3$, the

correlation due to the intra-level screened field, i.e., $\varepsilon^{co}_{1,k_z,1}$, can be further decomposed into two parts: the one corresponding to the charge exchange within the same LL ($n = 1, \sigma = 1$) and the one due to the exchange within the adjacent LL ($n = 0, \sigma = 1$). The latter is relatively small and it has zero slope at the Fermi edge. The many-body effects on the $n = 1, \sigma = 1$ LL of sample 2 of Ref. [50] is not investigated in this work. This is because in this QW sample the effective confining potential $m^*\omega^2[y - y_0(p_x)]^2/2$ around $1.5\hbar\omega$ is complicated and it goes beyond the assumptions used in this work.

The dispersion of the sigle-particle energies for filling factor $\nu = 1, 2, 3$ have been calculated within the LDA. The results thus obtained agree well with those of experiment and can help explain the experimentally observed [50], [59] destruction of the $\nu = 1$ and $\nu = 3$ QHE states in sample 1 of Ref. [50] and the existence of the $\nu = 1$ QHE states in sample 2 as well as $\nu = 2$ states in both samples. The Fermi-edge group velocity is an important parameter related to the edge properties of QWs. We have obtained it from numerically calculated single-particle energy.

The effective g factor is related to the single electron energy by $g^*_{op} = (E_{n,k_z,-1} - E_{n,k_z,1})/\mu_B B$. For $\nu = 2, 4, \ldots$ this formula give $g^*_{op} = |g_0| = 0.44$. For $\nu = 1, 3$, we obtained a spatially inhomogeneous g factor in the transverse direction.

For QWs in strong parallel magnetic fields, one important feature is that the electron states in the transverse and longitudinal directions are independent of each other, which is fundamentally different from those states discussed previously. As

a primary exploration, we considered two cases: 1)the lowest LL ($n = 0, \sigma = 1$) is half occupied and 2) the lowest LL ($n = 0, \sigma = +/-1$) is fully occupied. The simplified Poisson-RPA integral equation can be solved analytically. The screened fields obtained still diverge in the long wavelength limit, but have no oscillations in the wavenumber space. Based on the analytical solution of the simplified Poisson-RPA, the spin-splitting caused by exchange and correlations and the group velocities near the Fermi level have been calculated. Because all electrons are centered in the middle of the channel and the screened fields have no oscillation in the wavenumber space, the energy corrections due to exchange and correlation are stronger than those in the $\nu = 1, 2$ QHE states. Also the group velocities $u_g^{ec}(k_F)$ are proportional to the group velocity $u_g^{HA}(k_F)$, which has no relation to the channel parameters.

With the exception of the $\nu = 1$ case for perpendicular magnetic fields, where our results are similar for those of Refs. [35] and [36], the results for $\nu = 2, 3$ and those for parallel fields are, to our knowledge, new. We hope they will be useful as a reference and in experimental studies.

One limitation of this work is that we only considered the screened interaction between electrons confined in a potential having hard boundaries at the edges of the QW. In real samples, the actual confining potential increases quickly near the channel edge. For very steep confining potentials, we can neglect the flattening of the edge states and consider the screening effects as in previous chapters. However,

for a QW with $W > 1\mu m$, usually the confining potential is rather flat near the channel edge, e.g. when the gate voltage is less than $\sim 1V$ in the split gate technique. In this case we need to take into account the effects of edge flattening. Accordingly, the SHFA-RPA we used should be modified to properly investigate the screening problems in such QWs.

Another limitation is the rather specific orientations of the magnetic fields. They were so chosen to simplify the numerical and analytical work. For a general orientation of the field, it appears that one has to resort to a numerical work. We expect to remove this limitation as well as the most important one mentioned above in further studies.

Bibliography

[1] R. H. Landau. *Quantum Mechanics II*. John Wiley & Sons. New York. Chichester. Brisbane. Toronto. Singapore (1996).

[2] O. Madelung. *Introduction to Solid-State Theory*. Springer-Verlag. Berlin and New York (1978).

[3] N. W. Ashcroft and N. D. Mermin *Solid State Physics*. Saunders College Publishing. New York.Toronto. Montreal. London. Sydney (1976).

[4] K. V. Klitzing. G. Dora. and M. Pepper. Phys. Rev. Lett. **45**. 494(1980).

[5] D. C. Tsui. H. L. Stormer. and A. C. Gossard. Phys. Rev. Lett.**48**. 1559 (1982).

[6] G. D. Mahan. *Many-Particle Physics*. Plenum. New York and Landon (1990).

[7] G. D. Mahan. *Many-Particle Physics*. Plenum. New York and Landon (1990). P.73.

[8] S. Fujita. *Introduction to Non-Equilibrium Quantum Statistical Mechanics.* W. B. Saunders. London (1966).

[9] D. Pine *Elementary Excitations in Solids.* W. A. Benjamin. New York (1963).

[10] W. Kohn and P. Vashishta. *Theory of The Inhomogeneous Electron Gas.* Plenum. New York (1983).

[11] A. W. Overhauser. *Simplified Theory of Electron Correlations in Metals.* Phys. Rev. B **3**. 1888 (1971).

[12] F. Stern. Phys. Rev. Lett. **30** 278 (1973).

[13] A. K. Rajagopal and J. C. Kimball. Phys. Rev. B **15** 2819 (1977).

[14] A. Isihara and T. Toyoda. Ann. Phys. (N.Y.) **106** 394 (1977).

[15] A. Isihara and L. C. Ioriatti. Phys. Rev. B **22** 214 (1980).

[16] T. Ando. A. B. Fowler. and F. Stern. Rev. Mod. Phys. **54** 437-672 (1982).

[17] John H. Davies *The Physics of Low-Dimentional Semiconductors.* Cambridge University Press (1997)

[18] Ulrich Wulf. Vidar Gudmundsson. and Rolf R. Gerhardts. Phys. Rev. B **38**. 4218 (1988).

[19] D. Weiss, K. v. Klitzing, and V. Mosser, in *Two-Dimensional in Solid-State Sciences*, edited by G. Bauer, F. Kuchar, and H. Heinrich (Springer, Berlin, 1986), p.204.

[20] T. P. Smith, B. B. Goldberg, P. J. Stiles, and M. Heiblum, Phys. Rev. B **32**, 2696 (1985).

[21] V. Mosser, D. Weiss, K. v. Klitzing, K. Ploog, and G. Weimann, Solid State Commun. **58**, 5 (1985)

[22] D. Weiss and K. v. Klitzing, in *High Magnetic Fields in Semi-conductor Physics*, Ref. 1, p.57.

[23] B. Tausendfreund and K. v. Klitzing, Surf. Sci. **142**, 220 (1984).

[24] E. Stahl, D. Weiss, G. Weimann, K. v. Klitzing, and K. Ploog, J. Phys. C **18** L 783 (1985).

[25] R. T. Zeller, F. F. Fang, B. B. Goldberg, S. L. Wright, and P. J. Stiles, Phys. Rev. B **33**, 1529 (1986).

[26] D. Weiss, V. Mosser, V. Gudmundsson, R. R. Gerhardts, and K. v. Klitzing, Solid State Commun. **62**, 89 (1987).

[27] E. Gornik, R. Lassnig, H. L. Strormer, A. C. Gosard, and W. Wiegmann, Phys. Rev. Lett. **54**, 1820 (1985)

[28] T. Ando and Y. Uemura. J. Phys. soc. Jpn. **37**. 1044 (1974).

[29] R. J. Nicholas. R. J. Haug. K. von Klizing and G. Weimann. Phys. Rev. B **37**. 1294 (1988) and references therein.

[30] C. Kallin and B. I. Haperin. Phys. Rev. B **30**. 5655 (1984).

[31] M. M. Fogler and B. I. Shklovskii. Phys. Rev. B **52**. 17366 (1995).

[32] W. Xu. P. Vasilopoulos. M. P. Das. and F. M. Peeters. J. Phys. Condens. Matter. **7**. 4419 (1995).

[33] D. R. Leadlay. R. J. Nicholas. J. J. Harris. and C. T. Foxon. Phys. Rev. B **58**. 13036 (1998).

[34] I. L. Drichko. A. M. D'yakonov. I. Y. Smirnov. V. V. Preobrazhenskii. and A. I. Toropov. Semiconductor **33**. 892 (1999).

[35] O. G. Balev and P.Vasilopoulos. Phys. Rev. B **56** 6798 (1997).

[36] O. G. Balev and N. Studart. Phys. Rev. B **64** 115309 (2001).

[37] O. G. Balev and P.Vasilopoulos. Phys. Rev. B **50** 8727 (1994).

[38] S. Chaturvedi. G. J. Milburn. and Zhongxi Zhang Phys. Rev. A **57** 1529 (1998): G. S. Agarwal and K. Tara. Phys. Rev. A **43** 492(1991): and references therein.

[39] T. Ando *etal*. *Mesoscopic Physics and Electronics*. Springer-verlag Berlin Heideberg. 1998;

[40] B. I. Halperin. Phys. Rev. B **25** 2185 (1982); M. Buttiker. Phys. Rev. Lett. **57** 1761 (1990); B. W. Alphenarr *et al.* Phys. Rev. Lett. **64** 677 (1990).

[41] See. e.g.. C. W. J. Beenakker and H. van Houten. in *Solid State Physics*. edited by H. Ehrenreich and D. Turnbull (Academic. New York. 1991). Vol. 44. p.1 and references therein.

[42] D. B. Chklovskii. B. I. Shklovskii. and L. I. Glazman. Phys. Rev. B **46** 4026 (1992);

[43] C. W. J. Beenakker. Phys. Rev. Lett. **64** 216 (1990); A. H. MacDonald. Phys. Rev. Lett. **64** 220 (1990).

[44] B. Y. Gelfand. B. I. Halperin. Phys. Rev. B **49** 1862 (1994).

[45] G. Muller. D. Weiss. A. V. Khaectskii. K. von. Klitzing. S. Koch. H. Nickel. W. Schlapp. and R. Losh. Phys. Rev. B **45** 3932 (1992).

[46] L. Brey. J. J. Palacios. and C. Tejedor. Phys. Rev. B **47** 13884 (1993).

[47] J. Labbe. Phys. Rev. B **35** 1373 (1987).

[48] J. M. Kinaret and P. A. Lee. Phys. Rev. B **42** 11768 (1990).

[49] T. Suzuki and T. Ando. J. Phys. Soc. Jpn. **62** 2986 (1993).

[50] J. Wrobel, F. Kuchar, K. Y. Lee, H. Nickel, W. Schlapp, G. Grobecki, and T. Dietl, Surf. Sci.**305**, 615 (1994).

[51] J. Dempsey, B. Y. Gelfand, and B. I. Halperin, Phys. Rev. Lett. **70** 3639 (1993); Surf. Sci.**305** 166 (1994).

[52] See for example, R. Kubo, S. J. Miyake, and N. Hashitsume: *Solid State Physics*, ed F. Seitz and D. turnbull (Academic Press, New York, 1965)Vol. 17, p. 269. **70** 3639 (1993); Surf. Sci.**305** 166 (1994).

[53] Zhongxi Zhang and P.Vasilopoulos, J. Phys.: Condens Matter **13** 1539 (2001).

[54] R. Mottahedeh *et al.* Solid State Commun.**72** 1065 (1989).

[55] A. Bratass, A. G. Malshukov, V. Gudmundsson, and K. A. Chao, J. Phys: Condens Matter **8** 6798 (1996).

[56] L. Calmels and A. Gold, Phys. Rev. B **52** 10841 (1995).

[57] A. Gold and L. Calmels, Phys. Rev. B **58** 3497 (1998).

[58] A. B. Fowler, A. Hartstein, and R. A. Webb, Physica B+C **117+118B**, 661 (1983).

[59] M. A. Kasterner *et al.* Phys. Rev. Lett.**60**, 2535, (1988)

[60] H. Wu. D. W. Sprung. J. Martorell. and S. Klarsfeld. Phys. Rev. B**44**. 6351 (1991).

[61] S. K. Ma and K. Brueckner. Phys. Rev. **165** 18 (1968).

[62] D. J. W. Geldart and M. Rasolt. Phys. Rev. B **13** 1477 (1976).

[63] O. Gunnarsson and B. I. Lundgvist. Phys. Rev. B **13** 4274 (1976).

[64] T. Ando. A.B. Fowler. and F. Stern Rev. Mod. Phys.**54** 437 (1982).

[65] A. C. Tselis and J. J. Quinn. Phys. Rev. B **29** 3318 (1984).

[66] A. Brataas. A.G. Mal'shukov. V. Gudmundsson and K. A. Chao. J. Phys.: Condens Matter **8** L325 (1996).

[67] J. F. Weisz and K. -F. Berggren. Phys. Rev B **40** 1325 (1989).

[68] S. E. Laux and D. J. Frank. and F. Stern. Surf. Sci. **196** 110 (1988).

[69] H. Akera and T. Ando. Phys. Rev B **43** 11676 (1991).

[70] T. J. Thornton. M. Pepper. H. Ahmed. D. Andrew and G.J. Davies. Phys. Rev. Lett. **56** 1198 (1986).

[71] H. Z. Zheng. H. P. Wei. D. C. Tsui and Weimann: Phys. Rev. B **34** 5635 (1986).

[72] W. Hansen, in *Physics of Nanostructures, Proceeding of the 38 Scottish University Summer school in physics*, Ed. J. H. Davies and A. R. long P. 257(1991).

[73] H. van Houten, B. J. van Wees, M. G. J. Heijman, and J. P. Andre, Appl. Phys. Lett. **49**1781 (1986).

[74] G. Gradshteyn and I. M. Ryzhik, *Table of Integrals, Series, and Products* (Academic, New York, 1965).

[75] This was confirmed by the private communication with Dr. O. G. Balev, cf. Ref. [35].

[76] T. Ando and Y. Uemura, J. Phys. Soc. Jpn **37** 1044 (1974).

[77] C. Kallin and B. I. Halperin, Phys. Rev. B **30**, 5655 (1984); M. M. Fogler and B. I. Shklovskii, *ibid* **52**, 1736 (1995).

[78] R. J. Nicholas, R. J. Haug, K. Von Klitzing, and G. Weimann, Phys. Rev. B **37**, 1294 (1988);

[79] A. P. Smith, A. H. MacDonald, G. Gumbs Phys. Rev. B **45** 8829 (1992).

[80] W. Xu, P.Vasilopoulos, M. P. Das, and F. M. Peeters, J. Phys.: Conens. Matter **7**, 4419 (1995).

[81] D. R. Leadley, R. J. Nicholas, J. J. Harris, and C. T. Foxon, Phys. Rev. B **58** 13036 (1998).

[82] S. Brosig, K. Ensslin, A. G. Jasen, C. Nguyen, B. Brar, M. Thomas, and H. Kroemer, Phys. Rev. B **61** 13045 (2000).

[83] C. Hermann and C. Weisbuch, Phys. Rev. B **15** 823 (1977).

[84] J. Hu and A. H. MacDonald, Phys. Rev. B **46** 12 554 (1992).

[85] J.H. Oh, Phys. Rev. B **48** 15 441 (1993).